Preparation of highly-oriented hydrogels of supergiant cyanobacterial polysaccharides

KITTIMA AMORNWACHIRABODEE

Japan Advanced Institute of Science and Technology

Doctoral Dissertation

Preparation of highly-oriented hydrogels of supergiant cyanobacterial polysaccharides

KITTIMA AMORNWACHIRABODEE

Supervisor: Associate Professor Tatsuo Kaneko

School of Materials Science

Japan Advanced Institute of Science and Technology

March 2016

Referee-in-chief: Associate Professor Dr. Tatsuo Kaneko
Japan Advanced Institute of Science and Technology

Referees: Professor Dr. Masayuki Yamaguchi
Japan Advanced Institute of Science and Technology

Associate Professor Dr. Kazuaki Matsumura
Japan Advanced Institute of Science and Technology

Associate Professor Dr. Toshiaki Taniike
Japan Advanced Institute of Science and Technology

Associate Professor Dr. Supason Wanichwecharungruang
Chulalongkorn University

Abstract

Oriented hydrogels have been widely studied in fields of soft-biomaterials due to their anisotropic properties possibly applicable in biomedics, optics, and electronics. According to the literatures, network structures of the hydrogels were oriented by various factors such as self-assembly under flow, mechanical elongation, solvent-cast, etc. However, no report on one-directional swelling of the hydrogels has been available in spite of ultimate targets for the anisotropic hydrogels. Molecularly-oriented hydrogels of sacran, which is a supergiant liquid crystalline polysaccharide extracted from *Aphanothece sacrum* biomaterials, showing ultra-high anisotropy of swelling is successfully prepared by two-step chemical cross-linking. Divinylsulfone (DVS) works as a chemical cross-linker of sacran chains in a dilute aqueous solution to form hydrogels, but some of the added DVS remains in the hydrogel without cross-linking. The remaining DVS cross-links further with the pre-formed networks of sacran chains in liquid crystalline state during slow drying to produce in-plane oriented xerogels. The xerogels show heterogeneous anisotropy in the successive swellings steps; the linear swelling ratio in the thickness direction is 10,000-40,000 fold higher than that in the width direction, due to the molecular orientation of the sacran hydrogels. X-ray diffraction imaging of the hydrogels reveal not only the orientation of the xerogel films but also the unusual orientation of water molecules binding to sacran networks in the hydrogel state. The oriented hydrogels show various anisotropies such as mechanical properties and stimuli-responsiveness.

Keywords: anisotropy, hydrogels, polysaccharide, liquid crystals, in-plane orientation

CONTENTS

This dissertation was prepared according to the curriculum for the Collaborative Education Program organized by Japan Advanced Institute of Science and Technology and Chulalongkorn University.

Chapter 1

General introduction

1.1 Hydrogels

The hydrophilic polymer can dissolve in water due to their special functional groups along the chains such as –COOH, –OH, –$CONH_2$, –CONH–, and –SO_3H. Hydrogels are three-dimensional (3D) networks of hydrophilic polymer with the ability to absorb large amount of water or biological fluid. The hydrogels can swell in aqueous media while their shape are maintained due to the presence of chemical cross-links or physical cross-links. These networks are allow to hydration in an aqueous environment because there exhibit a thermodynamic compatibility with water [1-5].

1.1.1 Classifications of hydrogels

Hydrogels have been classified in many different ways such as ionic charges, physical properties, source, preparation methods, rate of biodegradation and the nature of cross-linking (Figure 1.1) [6-9]. However, the types of cross-linking play an important role for the stability of hydrogels network in swollen state. In physical cross-linked hydrogels, the physical interaction are achieved by chain aggregation, complexation, association, crystallization and hydrogen bonding [10]. The physical hydrogels are reversible because these physical interaction are temporary cross-linking. In contrast, the chemical hydrogels are formed by covalently cross-linking. These gels are irreversible, the bonds do not break at elevated temperatures and hence do not reform at lower temperatures.

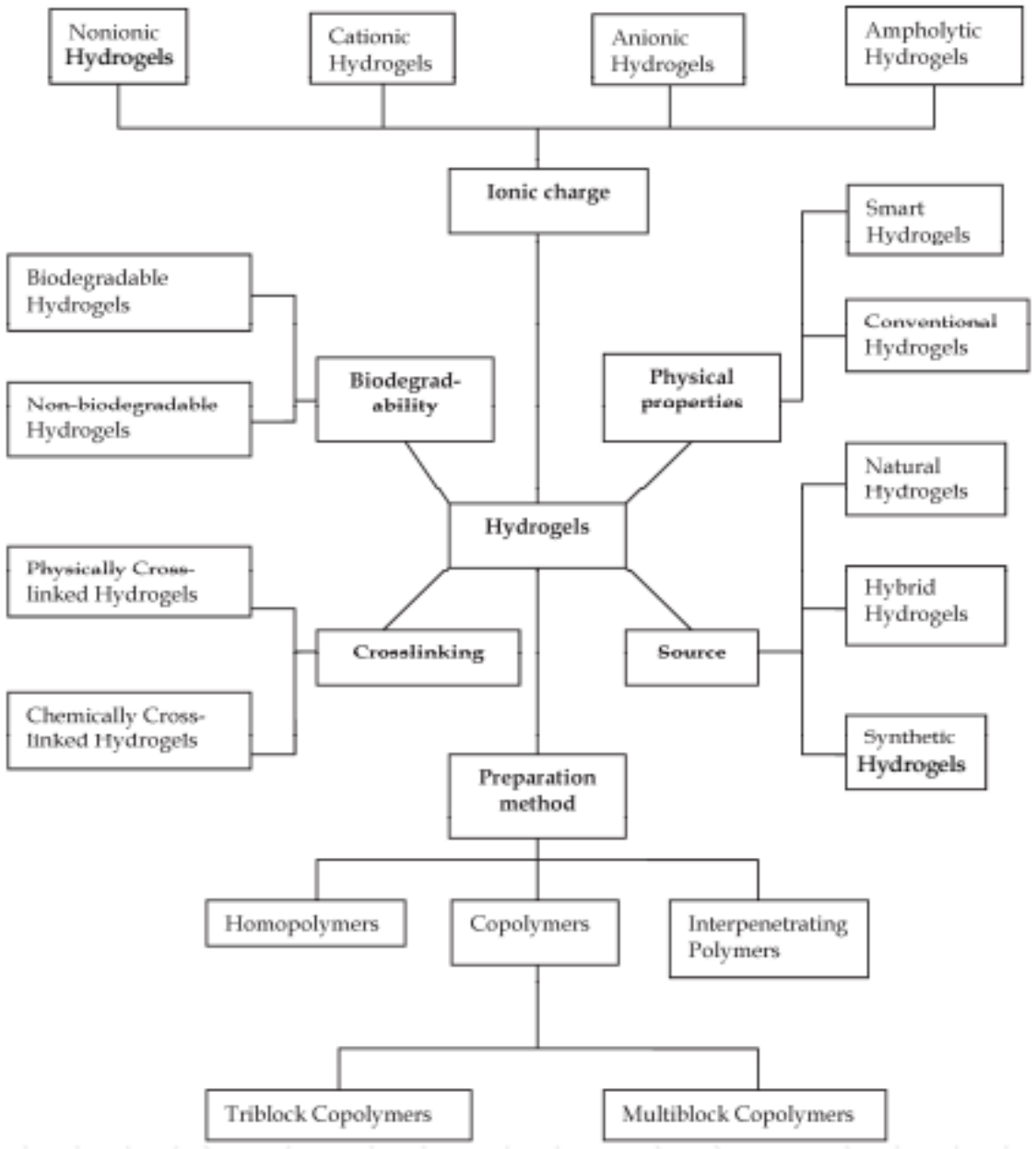

Figure 1.1 Classification of hydrogels [9].

1.1.2 Methods to preparation of hydrogels

Physical cross-linking

The networks of physical gels or reversible hydrogels are formed without cross-linking agents. Thus, the purification processes are not required, its can use in application directly. There are some of methods that widely used to prepare physical hydrogels.

- Ionic interaction

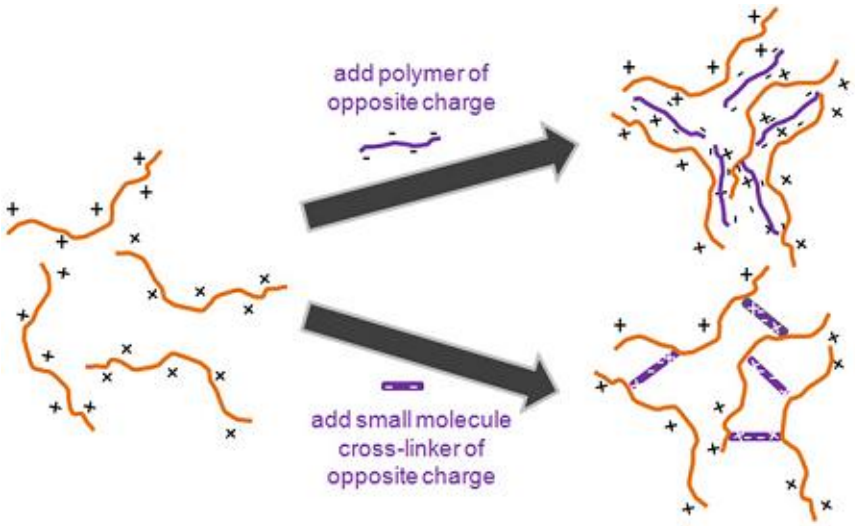

Figure 1.2 Mechanisms of *in situ* physical gelation based on charge interactions with an oppositely-charged polymer or an oppositely-charged small molecule cross-linker [11].

The ionic interaction can use to cross-link anionic or cationic polymer by forming ionic bridges between polymeric chains (Figure 1.2) [11]. Alginate is a polysaccharide that consist of β-D-mannuronic acid (M) and α-L-guluronic acid (G) residues and can be cross-linked by calcium ions (Figure 1.3) [12]. Some other polymer that can cross-linked by this method are chitosan and dextran based hydrogels [13-15].

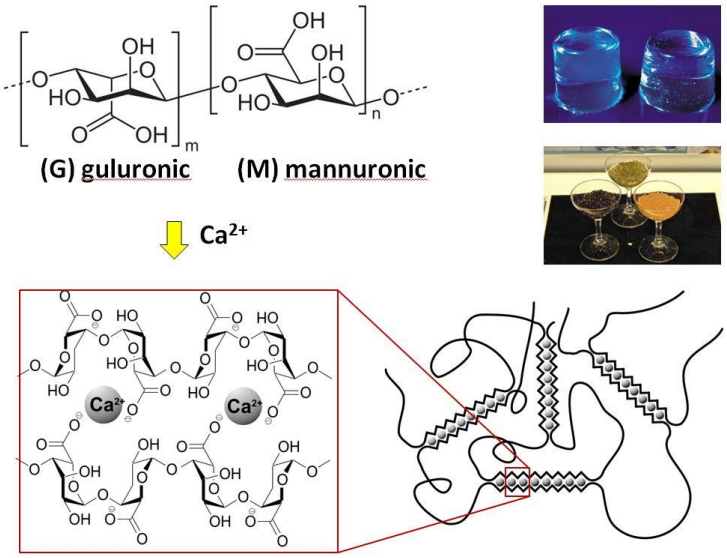

Figure 1.3 Alginate hydrogel cross-linked by divalent metal ions.

Moreover, polyanion also can from complex with polycation to be gels. The polymer with opposite charges can stick together and from soluble insoluble complexes depending on the concentration and pH of the polymer solution. For example is polyanionic xanthan gum and polycationic chitosan [16-17].

- Hydrogen bonding

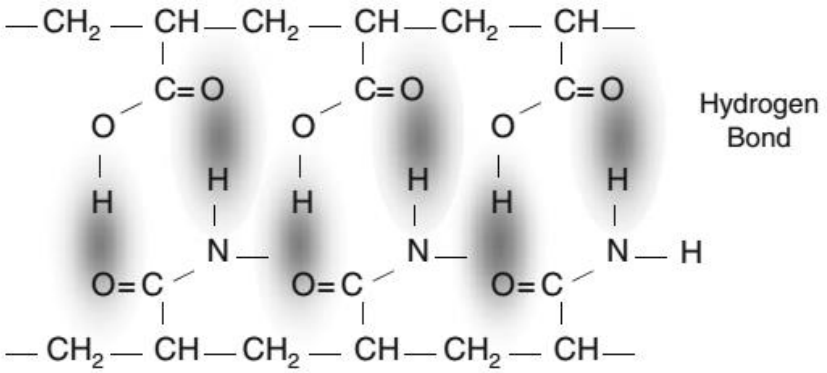

Figure 1.4 Gelation by intermolecular H-bonding.

The injectable cross-linking hydrogels can be produce *via* blends of two or more natural polymer. In mixing of polymer, the higher viscoelastic properties are induced by H-bonding. For examples, the blend hydrogels are prepared by mixing of gelatin-κ-carrageenan, gelatin-agar, and κ-carrageenan-agar [18]. In recently report, the hydrogen bonding can be used to prepare hydrogel by freeze-thawing method [19].

- Hydrophobic interaction

The amphiphilic polymer are soluble in water at low temperature. When temperature are increased, the aggregation of hydrophobic segments along polymer chains can be occur (Figure 1.5). This method can be used to prepare physical hydrogels known as 'sol-gel' chemistry. The gelation temperature can control by adjust the concentration of polymer, the ratio between hydrophobic and hydrophilic segments, and the chemical structure of polymer. Recently, the amphiphilic block copolymer are synthesized and cross-linked to be hydrogels. For examples, triblock copolymers of poly(ethylene oxide)-poly(propylene oxide)-poly(ethylene oxide) (PEO-PPO-PEO) are most widely used to prepare thermal gelation [20-22].

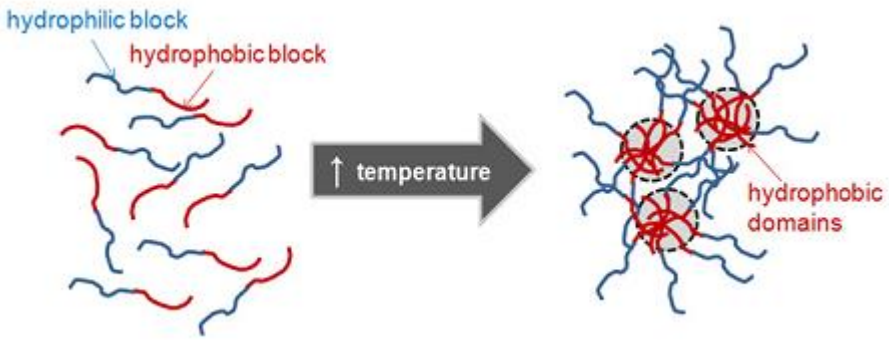

Figure 1.5 Mechanism of *in situ* physical gelation driven by hydrophobic interactions.

Chemical cross-linking

Chemical cross-linked hydrogels are strong and stable networks due to the presence of ionic and covalent bond.

- Cross-linking agents

Normally, most of hydrophilic polymers consist of functional groups such as hydroxyl(-OH), carboxyl(-COOH) and amine(-NH_2) that can cross-link trough chemical reaction in the presence of additional cross-linkers. For examples, chitosan hydrogels are obtained by cross-linking with glutaraldehyde (Figure 1.6) [23].

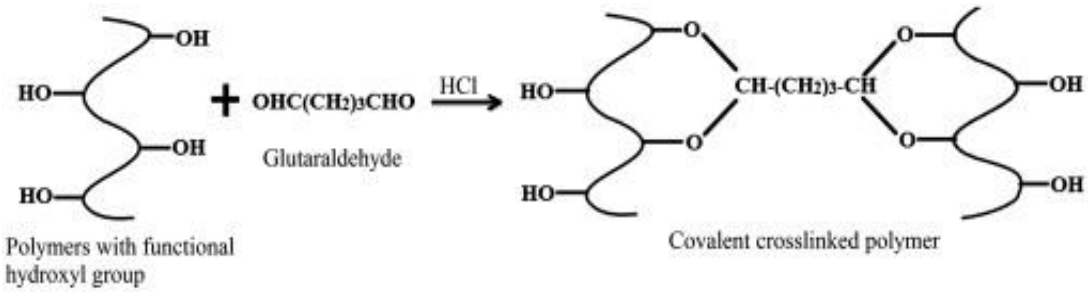

Figure 1.6 Covalently cross-linked chitosan hydrogel prepared using glutaraldehyde [23].

Cross-linking can also be achieved by addition reactions. The addition reactions are usually carried out in organic solvents because water can also react with the cross-linking agent. However, the cross-linking agents used in these reactions are usually toxic and need to be extracted from the hydrogels before use in biological applications.

- High energy radiation

In the water soluble polymers consist of vinyl groups can be formed into hydrogels using high energy radiation. High energy radiation, such as gamma and electron beam radiation can be used to polymerize unsaturated compounds. The high energy radiation directly creates free radicals which form intramolecular linkages as shown in Figure 1.7. For example, The Carboxymethyl cellulose hydrogels can be produced by electron beam irradiation. Carboxymethyl cellulose chains are grafted with acrlic acid follow by electron beam cross-linking [24].

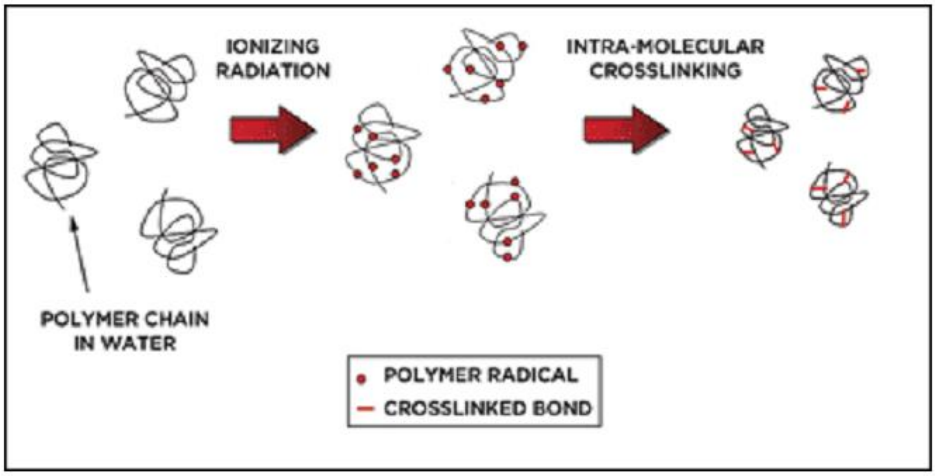

Figure 1.7 Intra-molecular cross-linking in hydrogels by irradiation.

1.1.3 Properties of Hydrogels

To development of materials, the properties such as physical, chemical and mechanical properties are necessary. In case of soft materials like hydrogels, there shown various properties including their absorption capacity, swelling behavior, permeability, surface properties, optical properties and mechanical properties which make them promising materials for a wide variety

of applications. The characteristics of the polymer chains and the cross-linking structures in these aqueous solutions play an important role in the outcome of the properties of the hydrogel.

Swelling behavior

Swelling degree is the most important property of a hydrogel which directly influences the rate of water sorption, the permeability of drugs, and the mechanical strength of the gel [25]. It represents the amount of solvent a gel will absorb at a given temperature and is defined as the ratio of swollen gel volume to the volume of dry polymer. Swelling leads to a three-dimensional expansion in which the network absorbs solvent and reaches an equilibrium degree of swelling at which the decrease in free energy due to mixing of the solvent with the network chains is perfectly balanced by the increase in free energy accompanying the stretching of the chains (elasticity). According to Flory, total free energy, and therefore swelling pressure, is represented as the sum of the individual contributions from polymer - solvent interactions, network elasticity, ionic osmotic pressure and electrostatic effects [5].Swelling pressure is therefore represented as follows:

$$P_{ext} = \Pi_{mix} + \Pi_{elas} + \Pi_{ion} + \Pi_{elec}$$

Where Π_{mix} represents the contribution from polymer-solvent interactions, which if favorable, increases swelling. Π_{elas} represents the contribution due to network elasticity which arises from restraints on swelling imposed by cross-links, opposing dissolution. For ionized gels, Π_{ion} represents the osmotic pressure of the counter-ions and Π_{elec} accounts for the interactions between the charged groups in the gel.

Permeability of Hydrogels

Permeability is the ability of a hydrogel to transmit another substance such as fluids, cells or proteins. Developing hydrogel membranes and coatings of appropriate permeability characteristics is key to the success of a number of bio artificial organ transplantations. The permeability of a hydrogel to water and solutes can be adjusted over a wide range by varying the cross-linker concentration at synthesis or copolymerizing with more hydrophilic or hydrophobic monomers [25]. Some of the real life situations where permeability of hydrogels is critical are oxygen permeation for contact lens applications, nutrient and immunological bio substance transport for immune isolation and release of drugs and proteins for drug delivery systems.

Surface Properties of Hydrogels

Biocompatibility is the ability of a hydrogel to reside in the body without inducing significant immune response or toxicity. The important question in biocompatibility is how the hydrogel transduces its structural makeup to direct or influence the response of proteins, cells and organisms. This transduction occurs through the surface properties of the hydrogel, i.e. the body reads the surface structure and responds to it. The surface of a hydrogel can be rough, smooth or stepped; it can be composed of different chemistries or could be highly crystalline, disordered and inhomogeneous. Studies have been performed on the importance of roughness, wettability, surface mobility, chemical composition, crystallinity and heterogeneity, however significant research has not yet been performed on determining which parameters are of utmost importance in understanding biological responses to surfaces. Some of the techniques used for determining the surface property include electron spectroscopy [26-28], secondary ion mass

spectrometry [29], scanning electron microscopy, Fourier transform infrared spectroscopy [30], scanning tunneling microscopy and atomic force microscopy. The information obtained using these methods can be used to monitor contamination, ensure surface reproducibility and explore the interaction of the hydrogels with living systems.

Mechanical Properties of Hydrogels

The mechanical properties of hydrogels depend on their composition and structure. Because of the high water content of fully swollen hydrogels, they normally have weak mechanical strengths. The mechanical properties of the hydrogel are affected by the co-monomer composition, cross-linking density, polymerization conditions and degree of swelling. The mechanical strength of the hydrogel is often derived entirely from the cross-links in the system, particularly in the swollen state where physical entanglements are almost nonexistent. The dependence of mechanical properties on cross-link density has been studied intensively by many researchers. However it should be noted that when the cross-linking density is altered, changes to properties other than strength also occur. For example, increasing the cross-linker concentration would make the polymer chains to come closer, thus reducing the diffusivity, release and swelling rates including the maximum degree of swelling. This would mean that these properties will need to be re-measured every time additional cross-links are added. The mechanical behavior of hydrogels is best understood by theories of elasticity and viscoelasticity. These theories are based on the time-independent and time-dependent recovery of the chain orientation and structure respectively. Elasticity theory assumes that when a stress is applied to the hydrogel the strain response is instantaneous. However for many biomaterials, including hydrogels and tissues, this is not a valid assumption. For example, if a weight is suspended from a specimen of ligament, the ligament continues to extend even though

load is constant. Similarly, if the ligament is elongated to a fixed length, the load drops continuously with time. This is due to creep and stress relaxation respectively and these are the result of viscous flow in the material. Despite this liquid-like behavior, hydrogels are functionally solids and are thus assumed to be perfectly elastic for the present study. In the next section a brief introduction to fundamentals of elastic theory is presented.

Theory of Elasticity

Elasticity is the physical property of a material by virtue of which it returns to its original shape after the force under which it deforms is removed. The applied force is usually referred to as stress, which is the force acting per unit cross-sectional area of the material, while the relative deformation is called as strain. The elastic regime is characterized by a linear relationship between stress and strain. The ratio of stress to strain is constant for a given material and is the defining mechanical property of the material. Based on whether the force applied is perpendicular or parallel to the area supporting it, the stresses and strains can be axial or shear. The proportionality constant obtained for the ratio of the axial stress to the axial strain is called as Young's modulus (represented by E) while the ratio of the shear stress to shear strain is referred to as shear modulus (represented by G). For a linearly, isotropic and homogenous material E and G are sufficient to completely characterize the mechanical properties of the material. However, most polymeric materials and tissue samples are anisotropic, meaning they have different properties in different directions. For example, bone, ligament and sutures are stiffer in the longitudinal direction as compared to the transverse direction. For such materials, on a macroscopic scale, more than two elastic constants are required to relate the stress and the strain properties. However, on a microscopic scale,

polymers are comparatively isotropic and the elastic and shear modulus are adequate to fully characterize their local mechanical properties.

1.2 Anisotropic Swelling of Hydrogels

It has been assumed that gels swell isotropically. In theories of gel swelling, the thermodynamics of the gel swelling is derived based on the assumption of isotropic swelling of gels and the structural parameters of gels are consequently predicted.

Li and Tanaka [31] explained the reason of isotropic swelling of gels by comparing the ink diffusion and gel swelling in water. Figure 1.8 shows schematically ink diffusion and gel swelling. The pure diffusion occurring in ink string placed in water produces the big change in the thickness of the string but the negligible change in its length. While in gel swelling, the changes in the length and thickness are similar. Li and Tanaka explain the reason of similar change in length and thickness is due to the nature of the modulus of gel to maintain its shape in order to minimize the shear energy, resulting in the isotropic swelling.

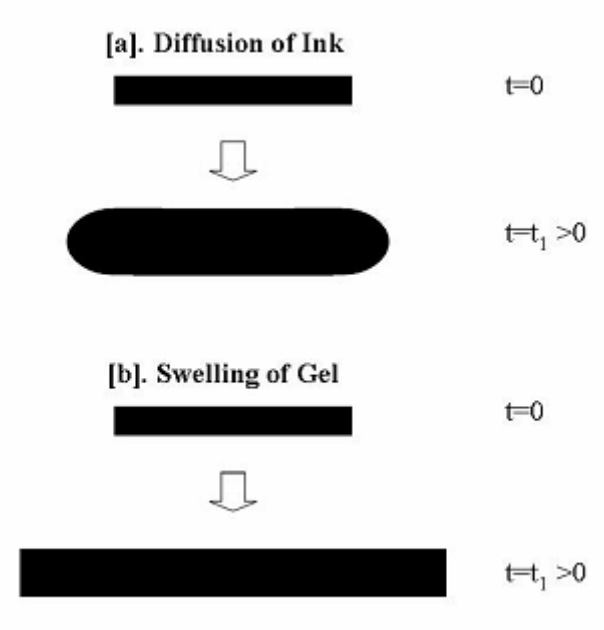

Figure 1.8 Schematic description of a diffusion process of ink molecules in (a) water and (b) the gel swelling process. For the former, the relative change of the length is negligible compared with that of the diameter. In the swelling of a long cylindrical gel, the relative change of the length and the diameter are the same [31].

There have been limited reports on the anisotropic swelling of some types of gels or hydrogels [32, 33, 34] unlike the assumption and reports of gel swelling. Brazel and Peppas [32] described the dimensional changes of HEMA/MMA and PVA hydrogels showing anisotropic swelling. As shown in Figure 1.9, there are three stages to change the hydrogel state during gel swelling. At the first stage, only the edge part of glassy and dry gel swells, glassy core remains, and only big change in the thickness occurs. At the second stage, the thickness of the gel with disappearing glassy core decreases and length increases. This was explained to be due to polymer relaxation, resulting in transparency of the hydrogel. At the third stage, the thickness increases while maintaining the length of the hydrogel and become fully swollen state.

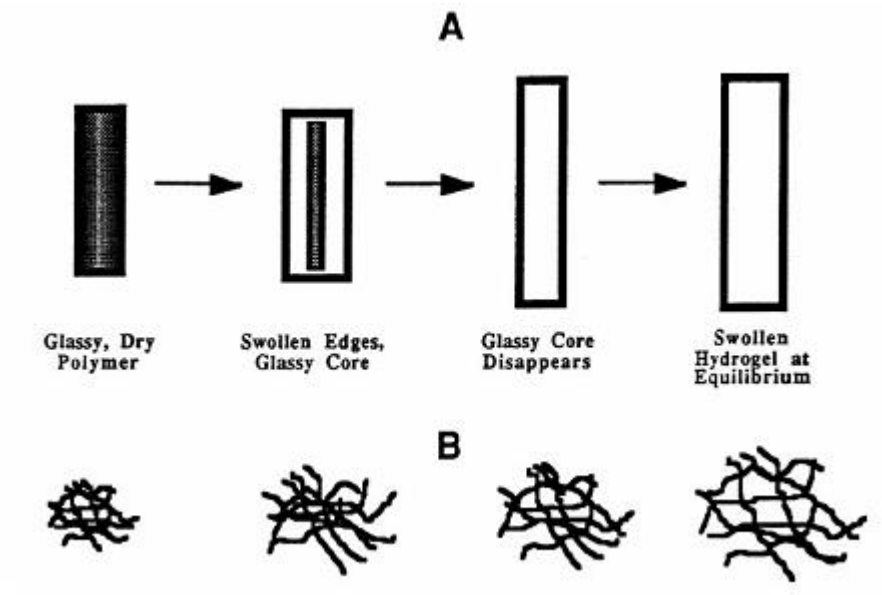

Figure 1.9 Depiction of polymer relaxation during water sorption into a slab geometry (A) and on the molecular level (B). Shaded area represents glassy polymer regions [32].

Edwards and coworkers [33] reported the anisotropic swelling of wet spun films of DNA showing 40 times expansion perpendicular to the molecular orientation and 1 or 2 times expansions parallel to chain orientation. The gel films showed the fast swelling initially, and continued to swell for 18 hours, until it eventually dissolved in the swelling medium. Boss and Stejskal [35] studied the hydrated vermiculite crystals (a clay possessing an ability to swell and shrink) with parallel silicate layers and observed about 100 times anisotropic expansion in thickness resulting from the water diffusion into the space between the parallel silicate layers from 100 to 1030 Å. In their study, pulsed magnetic-field gradient spin-echo NMR was used to investigate the diffusion of water. The anisotropy of sheared hydrogel composite of clay (LRD) and Polyethylene oxide (PEO) was studied by small angle neutron scattering (SANS) [36].

The swelling of stearic acrylate (SA) and acrylic acid AA co-polymeric gel films were investigated [34]. The SA/AA gels were characterized using wide angle x-ray scattering (WAXS) and determined to be crystalline with an oriented SA. The gels also showed temperature-dependent anisotropic swelling behavior in water/ethanol mixtures with greater than 50 wt. % ethanol. This behavior results from an anisotropic crystalline structure remaining in swollen state, with equilibrium swelling ratios in the range between 1 and 2.1. Harmon and coworkers [37, 38] reported the anisotropic swelling of UV cross-linked N-isopropylacrylamide (NIPAAm), 2-(dimethylmaleimido)-N-ethylacrylamide (DMIAAm) and N, N-dimethyl acrylamide (DMAAm). Anisotropic swelling behavior is sometimes seen in gel systems which either under the stress or confined. The anisotropic swelling of NIPAAm based terpolymeric hydrogels was also explained using models for anisotropic gel swelling. The models for anisotropic gel swelling were proposed by Tanaka and coworkers [39], Onuki [40], and Sekimoto and Kawasaki [41] as shown in Figure 1.10, which were based on either thin films coated on the substrate or volume instability of the gels at the phase transition resulting in buckling pattern.

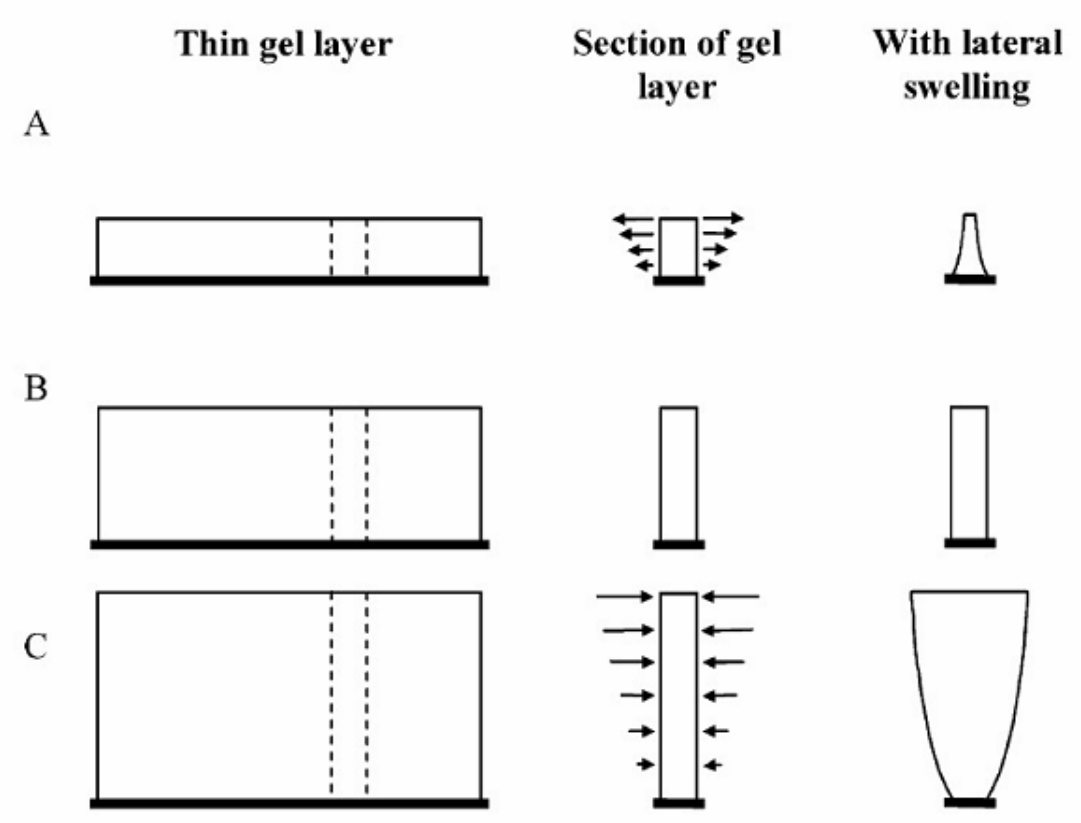

Figure 1.10 The hydrogel layer is cross-linked in some reference state (B), and the gel at the substrate remains in this reference state. The elastic energy of the network acts as compression when the gel layer is swollen (C) relative to the reference state and as elongation when the gel layer is collapsed (A) relative to the reference state. The compression or elongation increases monotonically and is greatest at the free surface of the gel. Our measurements are for infinitely wide films, but the exact shape of the gel with lateral swelling depends on both the film thickness and the aspect ratio of the gel layer [37].

1.3 Polysaccharides

Carbohydrates are biomolecules based on a ring unit containing 4 or 5 carbons and one oxygen (sugar units). These smallest sugar units of carbohydrate call as "monosaccharides". Polysaccharides are carbohydrates molecules composed of many monosaccharides units which are bonded together by glycosidic linkages. The use of polysaccharide is depend on types of sugar units in polysaccharides chain. Polysaccharides can be produced by animals, plants and bacteria which are extremely control their structural and functional. Cellulose are the most common polysaccharides from plants and glycogen are shown in animals. Bacteria and many other microbes including fungi and algae often produce various polysaccharides as an evolutionary adaptation to help them adhere to the surface as part of the cell wall component or storage units or virulence factors and also to prevent them from drying out. In bacterial polysaccharides can be divided into three groups by the morphological localization. The first is intracellular polysaccharides which are located inside or as part of the cytoplasmic membrane or cell wall. For examples, peptidoglycan, periplasmic glucans, lipo-polysaccharide, and lipo-oligosaccharide are intracellular bacterial polysaccharides. The second is capsular polysaccharides which are form a structural part of the cell wall [43]. The last is extracellular polysaccharides or called as "exopolysaccharides" consisting of branched, repeating units of sugars or sugar derivatives. There are two types of extracellular polysaccharides divided by sugar unit containing in molecules. The first is homo-polysaccharides such as cellulose, dextran and pullulan and the second is hetero-polysaccharides such as gellan and xanthan (Figure 1.11). Extracellular polysaccharides have shown wide industrial applications mainly in food and pharmaceutical products as gelling agents and medicines for wound dressings [44].

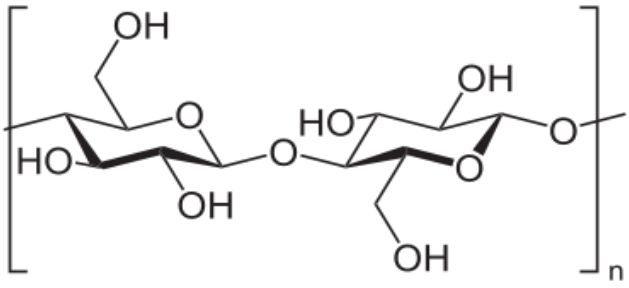

Cellulose

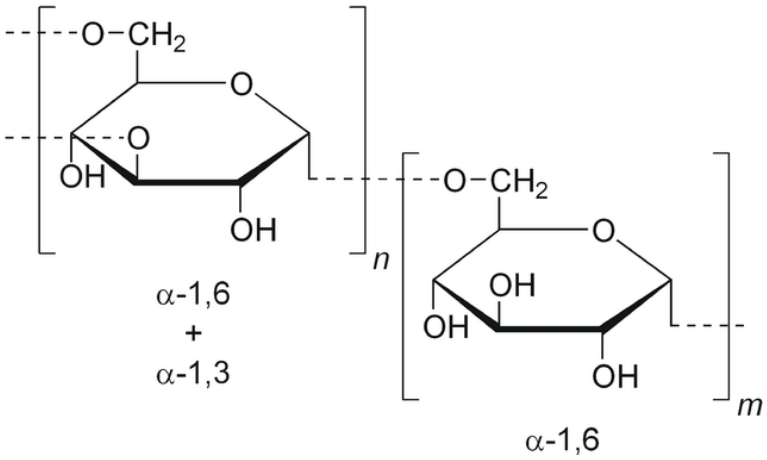

Dextran

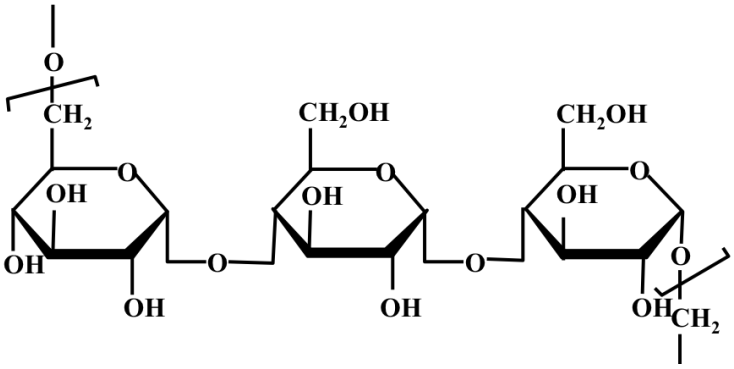

Pullulan

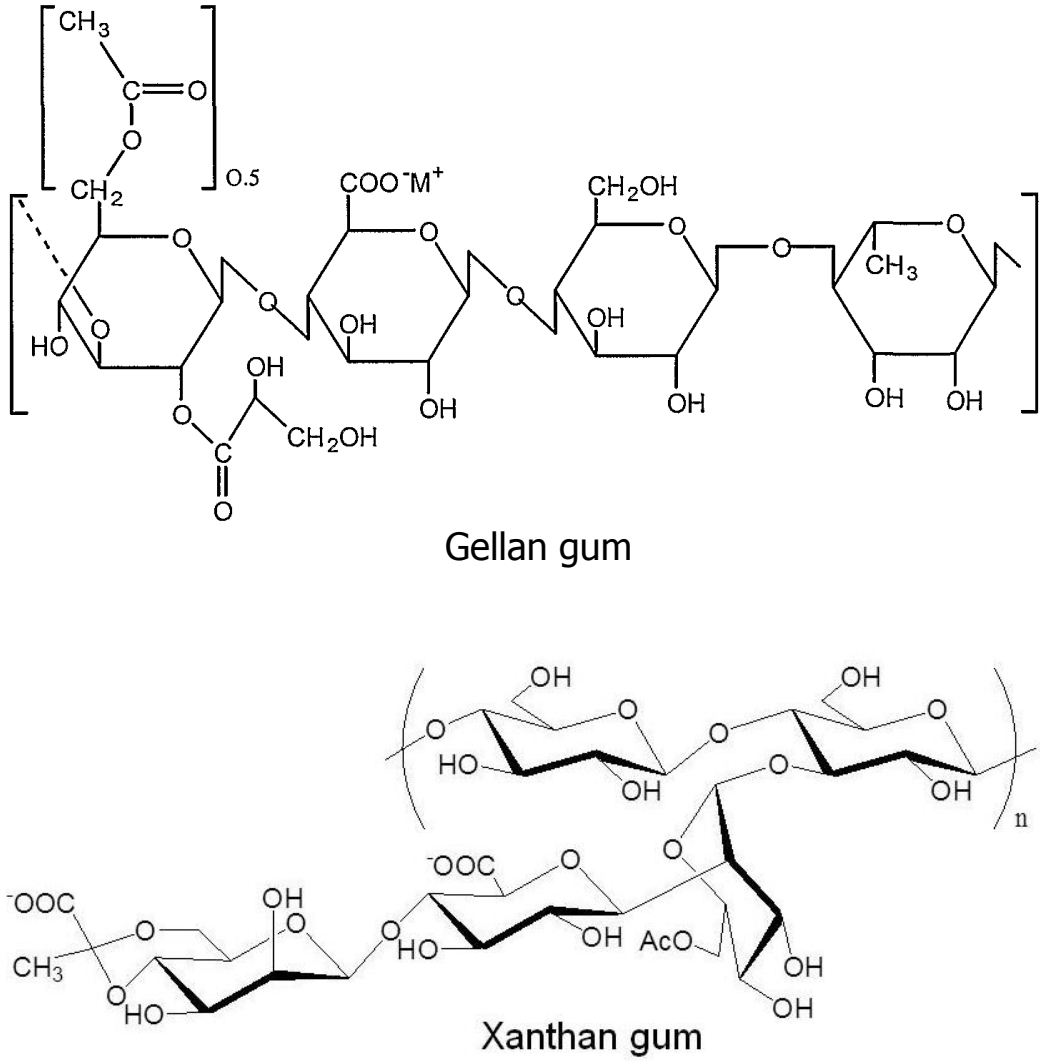

Figure 1.11 Structures of some extracellular polysaccharides.

1.4 Cyanobacterial polysaccharide "Sacran"

Sacran is cyanobacterial polysaccharide extracted from the jelly extracellular matrix of a river plant named *Aphanothece sacrum* (Figure 1.12). *Aphanothece sacrum* live in the river of spring water in Kumamoto and Fukuoka prefectures of Kyushu Island, Japan [45-46]. The structure of sacran chains are consist of 11% of sulfate groups, 22% of carboxyl groups and

about 250% of hydroxyl groups relative to the sugar residues (Figure 1.13) to having multifunctional anionic chains. Sacran can classified as hetero-polysaccharides composed of various sugar residues such as Glc, Gal, Man, Xyl, Rha, Fuc, GalA (anionic), and GlcA (anionic), with a composition of 25.9%, 11.0%, 10.0%, 16.2%, 10.2%, 6.9%, 4.0%, and 4.2%, and contain trace amounts (~1.0%) of Ara, GalN (cationic), and Mur (amphoteric).

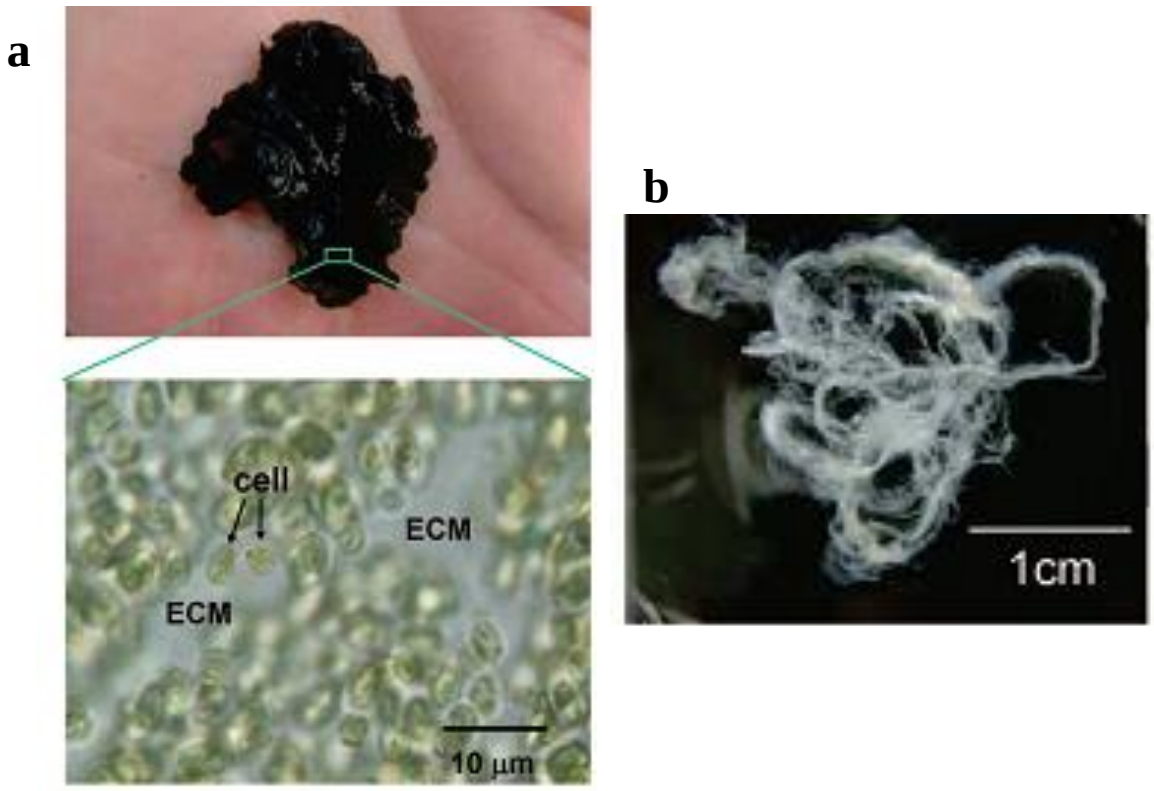

Figure 1.12 (a) Macroscopic view of *Aphanothece sacrum*. Inset: ECM is present between cells in microscopic image. (b) Macroscopic view of sacran in fibers formed [46].

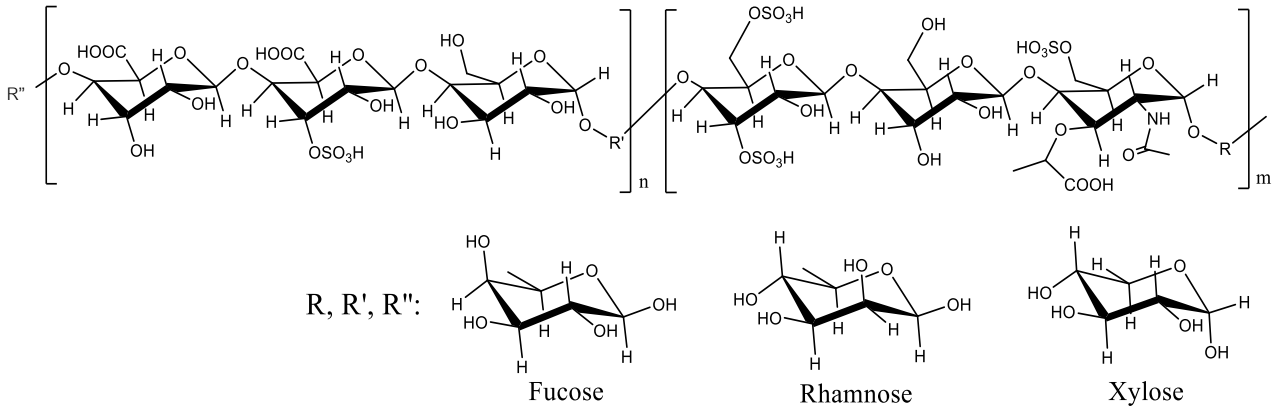

Figure 1.13 Partial structure of sacran.

The molecular weight of sacran is higher 16 Mg/mol. The previous research, sacran shows strong super-absorbent capacity not only for water (6100 ml/g) but also for 0.9 % saline (2700 ml/g) [46]. Sacran chains form double helixes at concentrations $c > 0.09$ wt% and form a weak gel at $c > 0.25$ wt%, and finally form huge domains of LC gels with centimeter scale at $c > 0.5$ wt%, which is quite a low concentration when compared to conventional LC polysaccharides [47]. The conformation of sacran chain in pure water are shown in Figure 1.14 [48].

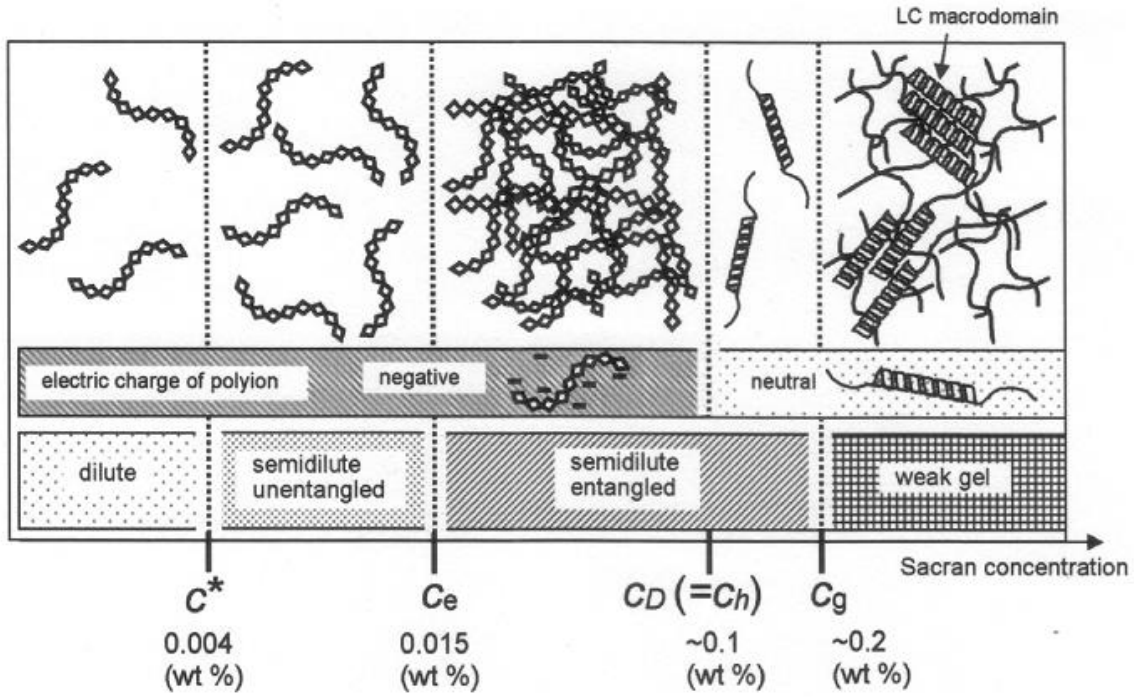

Figure 1.14 Schematic illustrations representing the chain conformation of sacran in salt-free solutions, [(c^*) overlap concentration, (c_e) entanglement concentration, (c_D) critical polyelectrolyte solution, (c_h) helix transition concentration, (c_g) gelation concentration] [48].

Sacran can easily form gels with trivalent metal ions by just mixing them together [49]. Additionally, it was recently discovered that sacran has an anti-inflammatory effect for atopic dermatitis model mice [50]. The sacran hydrogel is initially prepared water-casting method from sacran solution into the sacran film. This film shows molecularly-oriented and anisotropy swelling in water [51].

1.5 Objectives

In this research we tried to clarify the structure property relationship of orientated hydrogels with control materials structure. The special functions of hydrogels were important to develop the gel materials for biotechnological and chemical [51, 52]. Thus, we also tried to clarify the stimuli response of oriented sacran hydrogels.

References

[1] Peppas, N.A.; Mikos, A.G., Preparation methods and structure of hydrogels, in: Peppas, N.A. (Ed.), Hydrogels in Medicine and Pharmacy, Vol. 1, CRC Press, Boca Raton, FL, **1986**, pp. 1-27.

[2] Brannon-Peppas, L., Preparation and characterization of cross-linked hydrophilic networks, in: Brannon-Peppas, L.; Harland, R.S. (Eds.), *Absorbent Polymer Technology*, Elsevier, Amsterdam, **1990**, pp. 45-66

[3] Flory, P.J.; Rehner, J., *J. Chem. Phys.* **1943**, *11*, 521-526.

[4] Flory, P.J., *J. Chem. Phys.* **1950**, *18*, 108-111.

[5] Flory, P.J., Principles of Polymer Chemistry, Cornell University Press, Ithaca, NY, **1953**.

[6] Dumitriu, S. (Ed.). Polymeric Biomatrials, Marcel Dekker, Inc., New York, **2002**, ISBN: 0824705696.

[7] Hin, T., Engineering Materials for Biomedical Applications, World Scientific Publishing, Singapore, **2004**, ISBN: 981-256-061-0.

[8] Ratner, B.; Hoffman, A.; Schoen, F.; Lemons, J., Biomaterials Science: An Introduction to Materials in Medicine, Elsevier Academic Press, San Diego, CA, **2004**, ISBN 0-12-582463-7.

[9] Alpesh, P.; Kibret, M., Hydrogel Biomaterials, Biomedical Engineering - Frontiers and Challenges, Prof. Reza Fazel (Ed.), **2011**, ISBN: 978-953-307-309-5, InTech, DOI: 10.5772/24856.

[10] Omidian, H.; Park, K., Hydrogels. In: Fundamentals and Applications of Controlled Release Drug Delivery, Siepmann, J.; Siegel, R. A.; Rathbone, M. J., (Eds), Springer US: **2012**; pp 75-105.

[11] Hoare, T. R.; Kohane, D. S., *Polymer* **2008**, *49* (8), 1993-2007.

[12] Kuo, C. K.; Ma, P. X., *Biomaterials* **2001**, *22* (6), 511-521.

[13] Bajpai, A. K.; Shukla, S. K.; Bhanu, S.; Kankane, S., *Prog. Polym. Sci.* **2008**, *33* (11), 1088-1118.

[14] Zhao, Q. S.; Ji, Q. X.; Xing, K.; Li, X. Y.; Liu, C. S.; Chen, X. G., *Carbohydr. Polym.* **2009**, *76* (3), 410-416.

[15] Hennink, W. E.; van Nostrum, C. F., *Adv. Drug Deliv. Rev.* **2002**, *54* (1), 13-36.

[16] Martínez-Ruvalcaba, A.; Chornet, E.; Rodrigue, D., *Carbohydr. Polym.* **2007,** *67* (4), 586-595.

[17] Popa, N.; Novac, O.; Profire, L.; Lupusoru, C.; Popa, M., *J Mater Sci: Mater Med* **2010,** *21* (4), 1241-1248.

[18] Liu, J.; Lin, S.; Li, L.; Liu, E., *Int. J. Pharm.* **2005,** *298* (1), 117-125.

[19] Ricciardi, R.; Gaillet, C.; Ducouret, G.; Lafuma, F.; Lauprêtre, F., *Polymer* **2003,** *44* (11), 3375-3380.

[20] Xiong, X. Y.; Tam, K. C.; Gan, L. H., *J Nanosci Nanotechnol.* **2006,** *6* (9-1), 2638-2650.

[21] Chen, P.-C.; Kohane, D. S.; Park, Y. J.; Bartlett, R. H.; Langer, R.; Yang, V. C., *J Biomed Mater Res A* **2004,** *70A* (3), 459-466.

[22] Paavola, A.; Yliruusi, J.; Kajimoto, Y.; Kalso, E.; Wahlström, T.; Rosenberg, P., *Pharm Res* **1995,** *12* (12), 1997-2002.

[23] Giri, T. K.; Thakur, A.; Alexander, A.; Ajazuddin; Badwaik, H.; Tripathi, D. K., *Acta Pharm Sin B.* **2012,** *2* (5), 439-449.

[24] Said, H. M.; Abd Alla, S. G.; El-Naggar, A. W. M., *React. Funct. Polym.* **2004,** *61* (3), 397-404.

[25] Gehrke, S.H. Synthesis and properties of hydrogels used for drug delivery. In: Transport Processes in Pharmaceutical Systems, Amidon, G.L. (ed.), **2000**. pp. 473–546.

[26] Andrade J.D. Principles of protein adsorption. In: Andrade JD (ed.), Surface and Interfacial Aspects of Biomedical Polymers. New York: Plenum Press; **1985**. Pp. 1–80.

[27] Dilks A. X-ray photoelectron spectroscopy for the investigation of polymeric materials. In: A.D. Baker and C.R. Brundle (eds.), Electron Spectroscopy: Theory, Techniques, and Applications, Vol. 4, Academic Press, London, **1981** pp. 277–359.

[28] Ratner BD, McElroy BJ. Electron spectroscopy for chemical analysis: applications in the biomedical sciences. In: R.M. Gendreau (ed.), Spectroscopy in the Biomedical Sciences, CRC Press, Boca Raton, Fla., **1986**, pp. 107–140.

[29] Schuetzle, D.; Riley, T. L.; de Vries, J. E.; Prater, T. J., *Mass Spectrom. Rev.* **1984,** *3* (4), 527-585.

[30] Koenig, J., Fourier transform infrared spectroscopy of polymers. In: Spectroscopy: NMR, Fluorescence, FT-IR, Springer Berlin Heidelberg: **1984**; Vol. 54, pp. 87-154.

[31] Li, Y.; Tanaka, T., *J. Chem. Phys.* **1990,** *92* (2), 1365-1371.

[32] Brazel, C. S.; Peppas, N. A., *Biomaterials* **1999,** *20* (8), 721-732.

[33] Edwards, G. S.; Genzel, L.; Peticolas, W. L.; Rupprecht, A., *Biopolymers* **1986,** *25* (2), 223-227.

[34] He, X.; Takahara, A.; Kajiyama, T., *Polym. Gels Networks* **1997,** *5* (5), 429-438.

[35] Boss, B. D.; Stejskal, E. O., *J. Colloid Interface Sci.* **1968,** *26* (3), 271-278.

[36] Li, J.; Jiang, J.; Li, C.; Lin, M. Y.; Schwarz, S. A.; Rafailovich, M. H.; Sokolov, J., *Macromol. Rapid Commun.* **2006,** *27* (20), 1787-1791.

[37] Harmon, M. E.; Kuckling, D.; Pareek, P.; Frank, C. W., *Langmuir* **2003,** *19* (26), 10947-10956.

[38] Kuckling, D.; Harmon, M. E.; Frank, C. W., *Macromolecules* **2002,** *35* (16), 6377-6383.

[39] Tanaka, T.; Sun, S.-T.; Hirokawa, Y.; Katayama, S.; Kucera, J.; Hirose, Y.; Amiya, T., *Nature* **1987,** *325* (6107), 796-798.

[40] Onuki, A., *J. Phys. Soc. Jpn.* **1988,** *57* (6), 1868-1871.

[41] Sekimoto, K.; Kawasaki, K., *J. Phys. Soc. Jpn.***1987,** *56* (9), 2997-3000.

[42] Chawla, P.R.; Bajaj, I.B.; Survase, S.A,; Singhal, R.S., *Food Technol. Biotechnol.* **2009** *47*(2), 107–124.

[43] Sutherland IW, Microbial polysaccharides. Biotechnological products of current and future potential. In: Crescenzi V, Dea ICM, Paoletti S, Stivala SS, Sutherland IW (eds.), Biomedical and biotechnological advances in industrial polysaccharides. Gordon and Breach Science, New York, **1989**, pp 123–132.

[44] Okajima, M. K.; Ono, M.; Kabata, K.; Kaneko, T. *Pure Appl. Chem.* **2007**, *79*, 2039–2046.

[45] Okajima, M. K.; Bamba, T.; Kaneso, Y.; Hirata, K.; Fukusaki, E.; Kajiyama, S.; Kaneko, T. *Macromolecules* **2008**, *41*, 4061–4064.

[46] Okajima, M. K.; Kaneko, D.; Mitsumata, T.; Kaneko, T.; Watanabe, J., *Macromolecules* **2009,** *42* (8), 3057-3062.

[47] Mitsumata, T.; Miura, T.; Takahashi, N.; Kawai, M.; Okajima, M. K.; Kaneko, T., *Phys. Rev. E E* **2013,** *87* (4), 042607.

[48] Okajima, M. K.; Miyazato, S.; Kaneko, T., *Langmuir* **2009**, *25*, 8526−8531.

[49] Okajima, M. K.; Yokogawa, M.; Hirota, R.; Eitoku, M.; Muzembo, B. A.; Dumavibhat, N.; Takaishi, M.; Sano, S.; Kaneko, T.; Tanaka, T.; Nakamura, H.; Suganuma, N., *Ann Allergy Asthma Immunol* **2012,** *108* (2).

[50] Okajima, M. K.; Mishima, R.; Amornwachirabodee, K.; Mitsumata, T.; Okeyoshi, K.; Kaneko, T., *RSC Adv.* **2015,** *5* (105), 86723-86729.

[51] Jeong, B.; Gutowska, A., *Trends Biotechnol* **2002,** *20* (7), 305-311.

[52] Kikuchi, A.; Okano, T., *Prog. Polym. Sci.* **2002,** *27* (6), 1165-1193.

Chapter 2

Preparation of chemically cross-linked sacran hydrogels and their physical properties

2.1 Introduction

Hydrogels are network of polymer chains which absorb water but cannot be dissolved in water due to either physical or chemical cross-links. As the natural polymer of the polysaccharides possess a plurality of nucleophilic moieties (carboxyls, hydroxyls and sometimes amines) along their backbone, they are easily converted into hydrogels. Polysaccharide hydrogels can be prepared by covalent cross-linking. There are several methods and conditions which polysaccharides can be cross-linked directly to form into chemically conjugated hydrogels. The conjugation of polysaccharides can be accomplished *via* carbodiimide-mediated chemistry. Many carbodiimide compounds such as N,N'-dicyclohexylcarbodiimide (DCC) and 1-ethyl-3-(3-dimethylaminopropyl) carbodiimide (EDC) are used as cross-linking agents. The reaction initiates with the terminal carboxyl group of the material reacting with the carbodiimide to form an unstable *O*-acylisourea intermediate. The intermediate proceeds to react with nucleophiles forming an amide bond with a side product being an insoluble organo-urea which is typically removed by filtration. This chemistry has been applied for forming polysaccharide gels, for example the reacting of the hyaluronic acid with N-(3-aminopropyl) methacrylamide hydrochloride utilizing EDC as a carbodiimide reagent. The resulting hyaluronic acid derivative has chemical conjugates between the carboxylic acid units of the hyaluronic acid and the aminopropyl methacrylamide, allowing for

subsequent cross-linking with poloxamer diacrylate to form a thermally sensitive, chemically cross-linked hydrogel which served well as a scaffold for controlled release of human growth hormone [1]. However, Polysaccharides can be cross-linked as well by utilizing difunctional aldehyde such as glutaraldehyde or isocyanates like hexamethylene diisocyanate (HMDI). Some research shows that HMDI noticeably has lower cytotoxicity than glutaraldehyde [2]. HMDI is also used in the synthesis of biodegradable polyurethanes in combination with polycaprolactone diols [3]. The isocyanate moiety (R-N=C=O) is susceptible to reacting with nucleophiles. It has a higher reactivity towards alcohols, allowing for easier reactions along this route. Another method of cross-linking is by utilizing divinyl sulfone. Divinyl sulfone acts as a Michael's type reaction acceptor and is reactive preferentially towards nucleophiles such as amines, thiols and alcohols at high pH. This reaction has been done with hyaluronic acid to form hydrogels. This vinyl-sulfone-linked hyaluronic acid has been investigated for drug delivery as well as for use as biocompatible coatings and tissue scaffolds [4]. In addition to direct divinyl sulfone, a variety of sulfone-terminated PEGs have been used for this as well. The presence of the hydrophilic PEG spacer leads to an overall lower cross-linking density which allows for greater swelling and faster drug release [5].

To preparation of hydrogels, chemical cross-linking is a highly versatile method to create hydrogels with good mechanical stability. In this chapter, we focused on chemical cross-link between functional group of sacran to prepare sacran hydrogels. We used various types of cross-linkers to react with carboxyls and hydroxyls groups on sacran backbone.

2.2 Experimental

2.2.1 Materials

Sacran (MW 1.6 x 10^7 g/mol) was purchased from Green Science Material Inc. (Kumamoto, Japan). Dimethyl sulfoxide (DMSO; Sigma-Aldrich) used as solvent was used as received without further purification. Divinylsulfone (DVS; Sigma-Aldrich), hexamethylene diisocyanate (HMDI; TCI), 1-ethyl-3-(3-dimethylaminopropyl) carbodiimide HCl salt (WSC; TCI), and N-hydroxysuccinimide (NHS; Wako Pure Chemical), which were all used for cross-linking, were used as received without further purification. Sodium hydroxide (Kanto Chemical co. ltd) and hydrochloric acid (Kanto Chemical co. ltd) employed for pH adjustment were used as received.

2.2.2. Preparation of chemical cross-linked sacarn hydrogels

Preparation of sacran hydrogels with carbodiimides and L-lysine

Carboxylic acid of sacran in aqueous solution (1.0 % (w/v), 10 mL) was activated with WSC (85.2 mg, 0.4 mmol) and NHS (85.2 mg, 7.4 mmol). The solution was stirred for 20 min and then L-lysine (40.5 mg, 0.27 mmol) was added into the solution as a cross-linking agent. The solution was stirred vigorously, centrifuged to remove bubbles, and kept for 72 h at 4 ^{o} C in a refrigerator to form a hydrogel. The hydrogel was washed by immersion in a large volume of milli-Q water for 5 days and the external water was replaced every 12 h.

Preparation of sacran hydrogels with HMDI

Sacran was dissolved in DMSO to obtain 0.5 w/v % (20 mL) and then HMDI (0.15 g) was added into the solution. The solution was stirred for 20 min, centrifuged to remove bubbles, and kept for 24 h at 4 ^{o}C in a refrigerator to form an organogel. The DMSO of the organogel was replaced by milli-Q water by immersion in a large volume of milli-Q water for 7 days with replacement of the external water every 12 h [6].

Preparation of sacran hydrogels with DVS

Sacran was dissolved in 0.2 M NaOH solution (pH 13) at various concentration (Table 2.1). The mixture was stirred at around 60 ^{o} C for approximately 5 h or until a clear solution was obtained. After the solution was cooled to room temperature, DVS was added into the sacran solution (20 mL). Then, the mixture was stirred for 5 min and bubbles were removed by centrifugation for 1 min. The hydrogel was allowed to react completely for 4 h and the gel was neutralized by the addition of 0.2 M HCl, and then washed by immersion in a large volume of milli-Q water for 5 days with replacement of the external water every 12 h [7].

Table 2.1 Conditions of preparation sacran hydrogels cross-linked with divinylsulfone (DVS)

Sample No.	Conc. of sacran solution (w/v %)	DVS/OH (mol/mol)
S1	0.5	0.63
S2	0.6	0.63
S3-1	0.8	0.43
S3-2		0.63
S3-3		0.83
S3-4		1.10

2.2.3 Characterization

Fourier transform infrared spectrometry (FT-IR)

FTIR spectra were recorded with Perkin Elmer Spectrum One spectrometer between 4000-500 cm^{-1} using a diamond-attenuated total reflection (ATR) accessory.

Elemental analysis (EA)

Elemental analyses were made by Yanako CHN coder MT-6 and Mitsubishi chemical S coder AQF-100 (at the Center for Organic Elemental Microanalysis at Kyoto University). The degree of incorporation of DVS in each sugar unit in the sacran chain was calculated as following equation:

$$\begin{aligned} \frac{C_1}{S_1} &= \frac{C_0+\alpha}{S_0+\beta} \\ DVS\ incorporation(\%) &= \frac{6\times\beta}{C_1}\times 100 \end{aligned} \qquad (2.1)$$

where C_0 and S_0 are carbon and sulfur molar percentages of the uncross-linked sacran chains, and C_1 and S_1 are carbon and sulfur molar percentages of the sacran hydrogel, respectively. All these percentages were evaluated by elemental analyses. α and β are mol percentages of carbon and sulfur in DVS, respectively (α/β=4/1).

Swelling ratio measurements

The hydrogels were soaked in milli-Q water for 7 days to remove the unreacted cross-linker or condensation reagent, and the swelling ratio of the hydrogels was calculated by

$$Swelling\ ratio(Q) = \frac{W_s}{W_d} \tag{2.2}$$

where W_s is the weight of the sample in the equilibrated state at room temperature, and W_d is the weight of the dried sample. All experiments were performed at least in triplicate [4].

The water content of the hydrogels was calculated after equilibrium swelling by Equation 2.3.

$$Water\ \ content(\%) = \frac{W_s - W_d}{W_s} \times 100 \tag{2.3}$$

2.2.4 Mechanical properties of the hydrogels

The mechanical properties of sacran hydrogels were investigated using a compression test. A compression probe was set up on an Instron 3365 machine using a 5 kN load cell with a crosshead speed of 1.00 mm/min. Elastic modulus (E) of each sample was calculated using Equation 2.4 applied to unidirectional compression measurements carried out between two parallel plates [4].

$$\tau = \frac{F}{A} = E(\lambda - \lambda^{-2}) \tag{2.4}$$

where τ is the engineering stress, F is the applied force, A is the original cross sectional area of the hydrogels, and E is the elastic modulus. $\lambda = L/L_o$ where L is the hydrogel thickness under strain and L_o is the hydrogel thickness before compression. Plotting F/A versus (λ-λ^{-2}) resulted in a straight line with a slope of E, which is the modulus of elasticity of the swelling hydrogel.

The effective cross-link density (V_e) was calculated from swelling ratio and modulus using the following equation [8].

$$V_e = \frac{E}{RTQ^{-1/3}} \tag{2.5}$$

where E is the modulus and Q is the swelling ratio of the hydrogels.

The average molecular weight between cross-linking points (M_c) was calculated using the cross-link density as shown in Equation 2.6 [4].

$$M_c = \frac{\rho_p}{V_e} \tag{2.6}$$

where ρ_p is the density of the dry polymer (sacran ≈ 0.83 g/cm^3).

The degree of cross-linking (X) can be estimated theoretically by the average molecular weight between cross-linking points (M_c) as given equation [9].

$$X = \frac{M_0}{2M_c} \tag{2.7}$$

where M_0 is the molecular weight of the polymer repeating unit.

2.3 Results and Discussion

2.3.1 Preparation of sacran hydrogels with carbodiimides and L-lysine

To preparation of chemical cross-linked hydrogels, the active functional groups on sacran structure were selected for cross-linked. The structure of sacran contains 11 % of sulfate group, 22 % of carboxyl group and 250 % of hydroxyl group to sugar residues. In this work, we tried to cross-link sacran by L-lysine, HMDI and DVS. First, sacran was conjugated by carbodiimide-medaited chemistry. The reaction initiates with the carboxyl group of sacran reacting with the carbodiimide to form an unstable *O*-acylisourea intermediate, and N-hydroxysuccinimide (NHS) as the proton exchanger. The intermediate continue to react with amine group of L-lysine to form amide bond (Scheme2.1). Since the reaction did not occur immediately, we had enough time to remove the bubbles from solution by centrifugation.

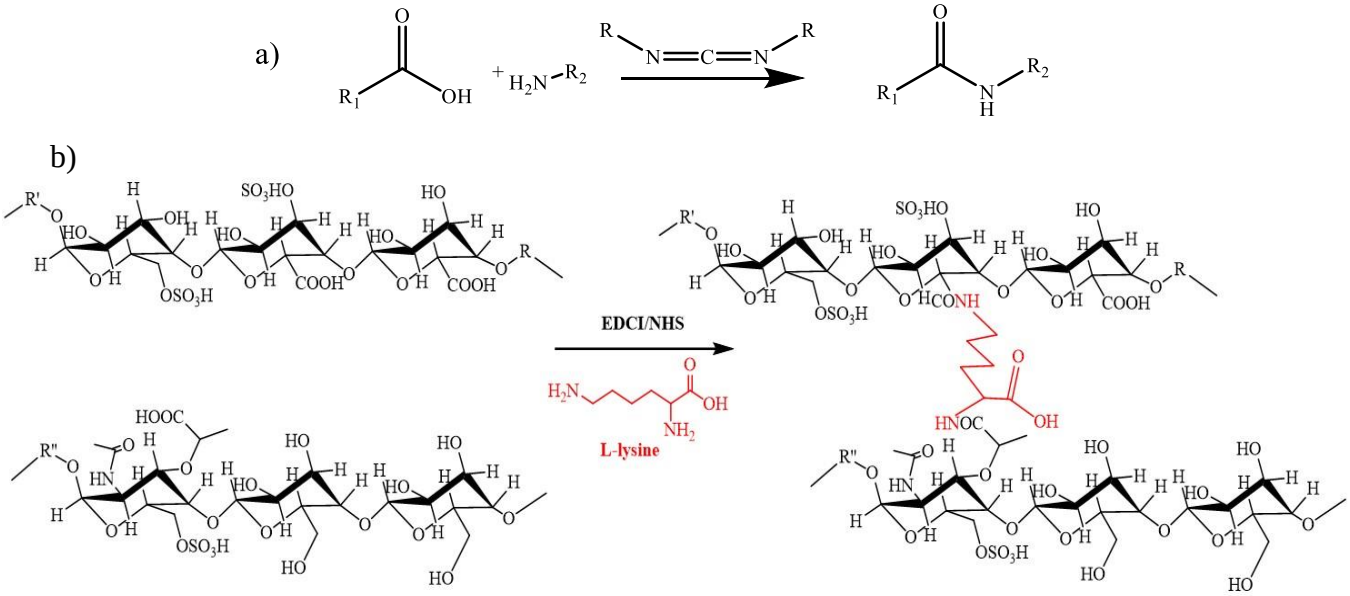

Scheme 2.1 Sacran hydrogels cross-linked by carbodiimide and L-lysine. a) generalized carbodiimide-mediated reaction between acid and amine. b) sacran cross-linked with EDCI and L-lysine forming an amide bond.

The hydrogels obtained from this method were very soft because the amount of carboxyl groups on sacran chain were not enough to cross-link by L-lysine (Figure 2.1).

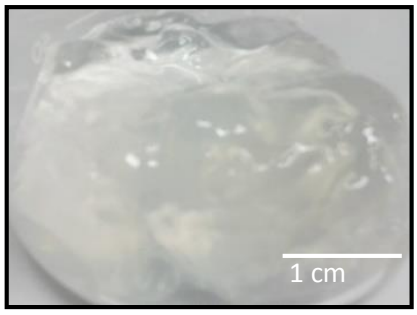

Figure 2.1 Representative picture of L-lysine cross-linked sacran hydrogel

2.3.2 Preparation of sacran hydrogels with HMDI

The stoichiometry of the reaction can be tuned in order to form hydrogels with different degrees of cross-linking, taking into consideration the number of active functional groups in sacran chain. To improving the cross-linking density upon chemical cross-linking, the high percentage of hydroxyl groups were selected for cross-link. Then, hydroxyl groups of sacran chain have been cross-linked with HMDI to form urethane bond. However, there were some drawbacks for reacting sacran with isocyanates, as the sacran was hydrophilic polysaccharides, the high amount of water in this reaction led to degradation of isocyanates into carbon dioxide gas (Scheme 2.2). Thus, the obtained hydrogels was spongy-like hydrogels (Figure 2.2).

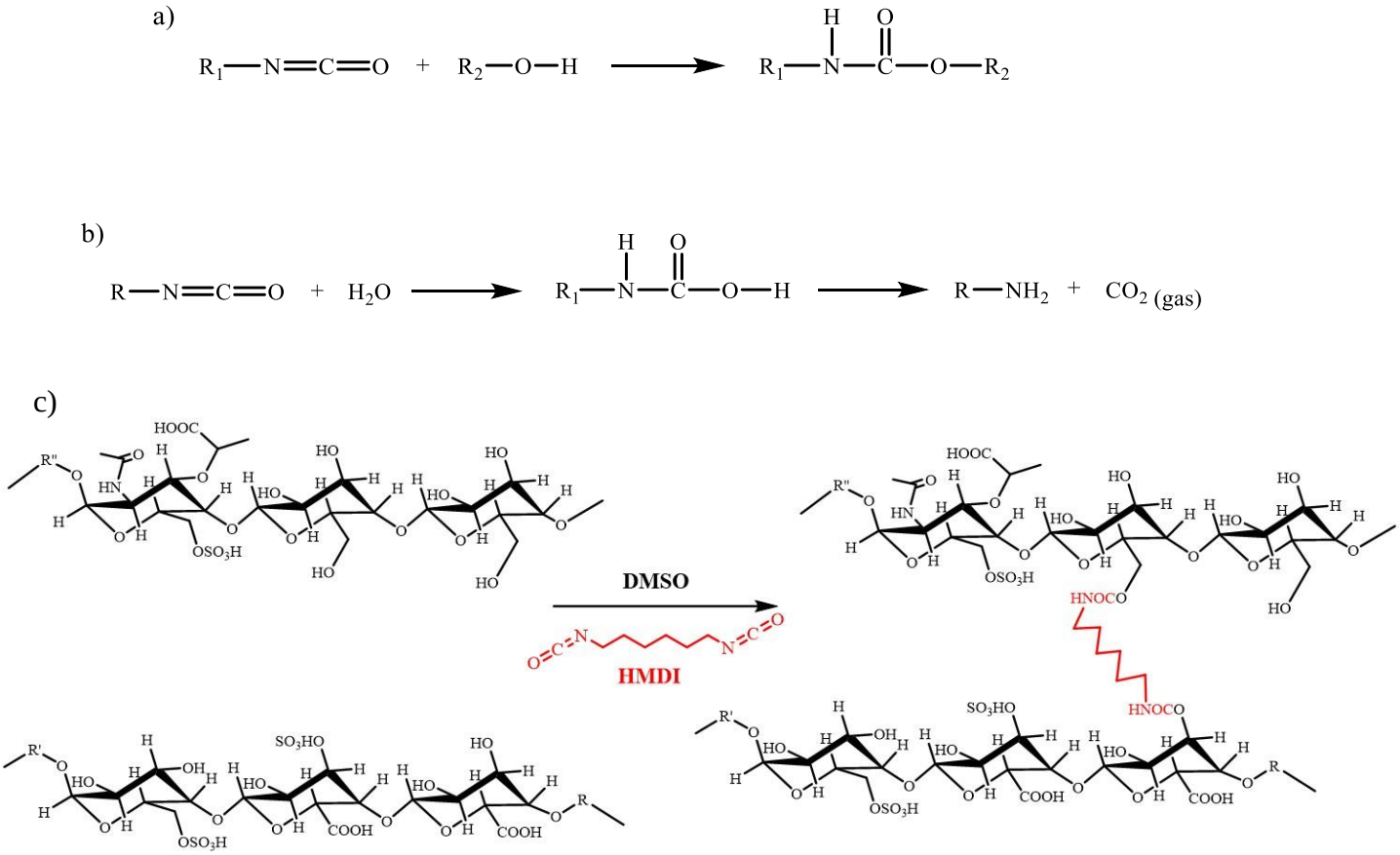

Scheme 2.2 Sacran hydrogels cross-linked by HMDI. a) generalized urethane reaction. b) carbon dioxide gas formed by reacting water and isocyanate. c) sacran cross-linked with HMDI forming an urethane bond.

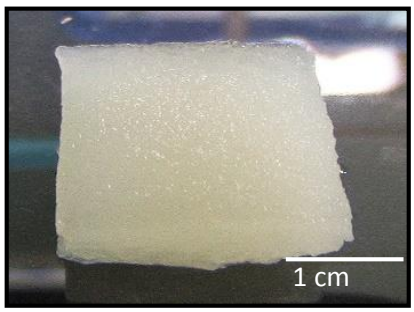

Figure 2.2 Representative picture of spongy-like sacran hydrogel from HMDI cross-linking.

2.3.3 Preparation of sacran hydrogels with DVS

Finally, divinyl sulfone was used as cross-linking agent. Divinyl sulfone operates as a Michael's type reaction acceptor and react with hydroxyl groups of sacran at high pH (Scheme 2.3). Then, clear hydrogels were obtained from DVS cross-linked (Figure 2.3). In this research the strong and clear hydrogels from DVS cross-linked were studied in the details.

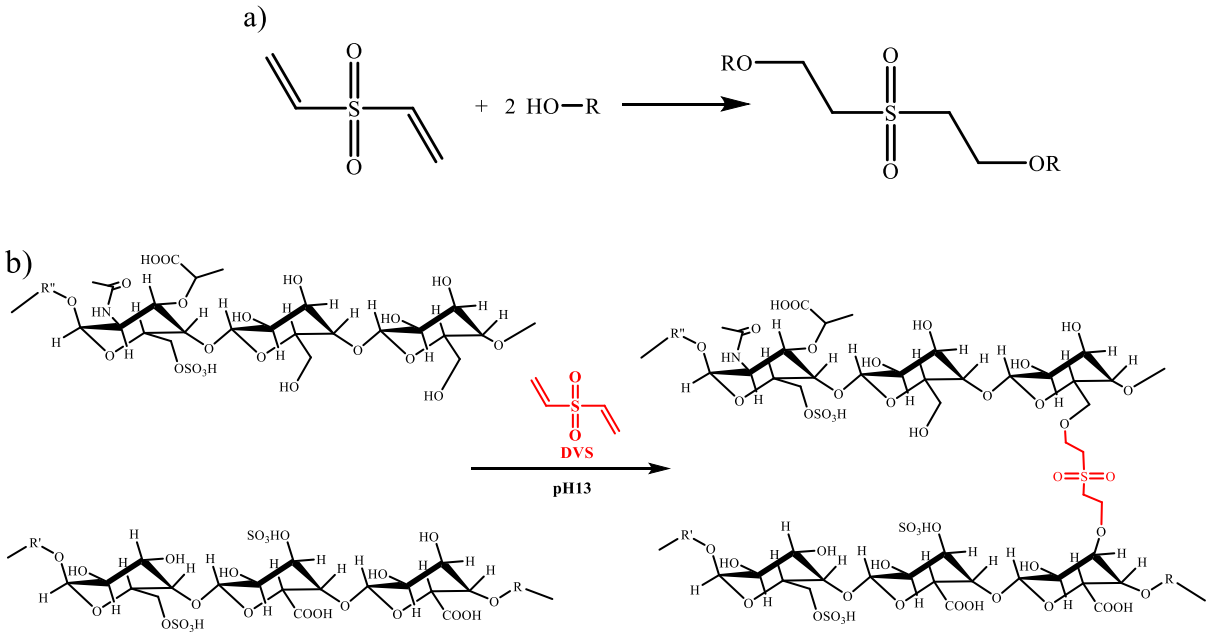

Scheme 2.3 Sacran hydrogels cross-linked by DVS. a) generalized vinyl sulfone-alcohol reaction. b) sacran cross-linked with DVS forming an ether bond.

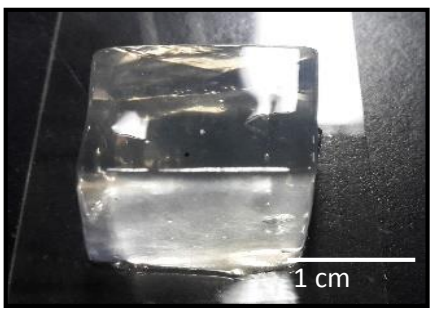

Figure 2.3 Representative picture of DVS cross-linked sacran hydrogel.

The nature of sacran solution at concentration more than 0.5% (w/v), sacran structure were self-orientation to form LC-gel. However, the gels were very soft and easily deformed without breaking, suggesting that sacran chains can form double helixes dynamically and interchain interactions may not so strong (Figure 2.4) [10].

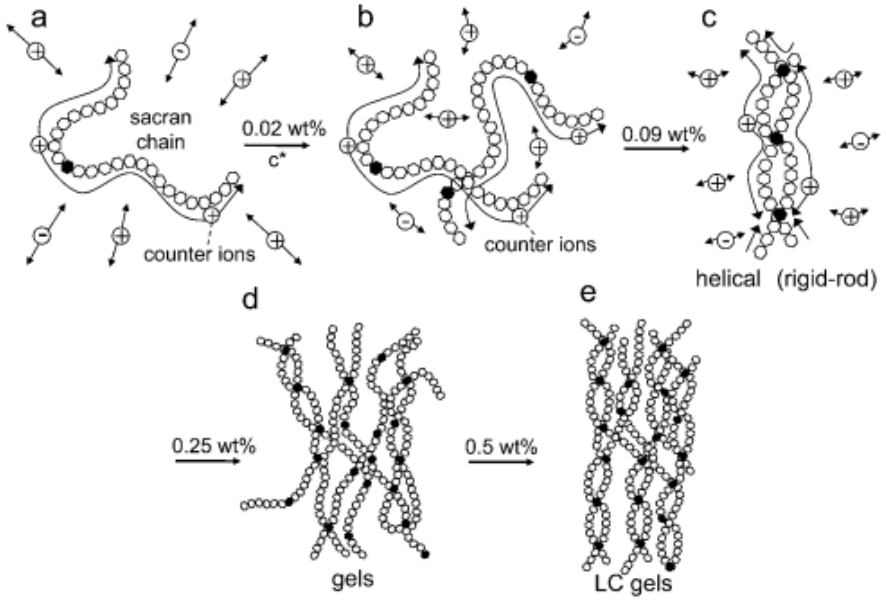

Figure 2.4 Schematic illustration of sacran self-organization upon a concentration increase. Circled + and - marks refer to counter cations and anions of sacran chains, respectively. Black points on sacran chains refer to moieties containing amino sugar residues. Arrow lengths correspond to fluctuation lengths [10].

In order to optimize the condition for preparing sacran hydrogels with DVS cross-linker, concentration of sacran solution and amount of DVS cross-linker were changed. First, sacran chain in solution at concentration of 0.5 %, 0.6 % and 0.8% (w/v) were cross-linked by DVS keeping molar ratio of DVS to sacran hydroxyl as 0.63. When the concentration of sacran solution were increased from 0.5 % to 0.8 %, the swelling ratio, q_0, of the prepared hydrogels decreased from 437 to 240 g/g (Figure 2.5).

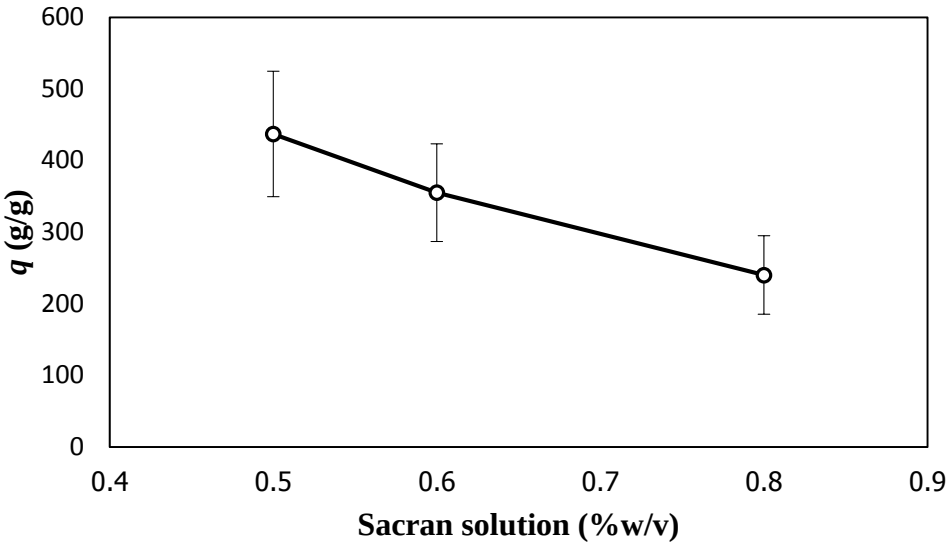

Figure 2.5 Swelling ratio (q_0) of DVS cross-linked sacran hydrogels at concentration of 0.5 %, 0.6 % and 0.8% (w/v) with molar ratio of DVS to sacran hydroxyl as 0.63.

The mechanical properties of these hydrogels were investigated. The results showed that elastic modulus (E_0) were increased by increasing concentration of sacran solutions as shown in Figure 2.6. After that, the effective cross-link density (V_e) were calculated from q and E (Equation 2.5). The V_e values were increased with increased the concentration of sacran solution (Figure 2.7). Moreover, the average molecular weight between cross-linking points (M_c) and degree of cross-linking (X) were also calculated (Equation 2.6 and 2.7, respectively) and the results were shown in Table 2.2.

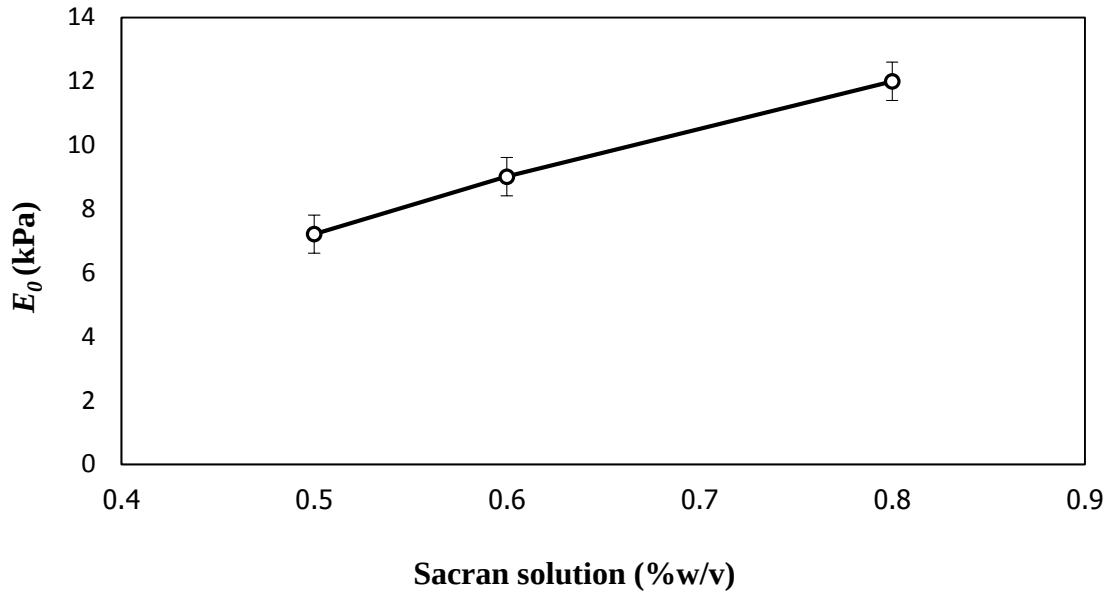

Figure 2.6 Elastic modulus by compression (E_0) of DVS cross-linked sacran hydrogels at concentration of 0.5 %, 0.6 % and 0.8 % (w/v) with molar ratio of DVS to sacran hydroxyl as 0.63

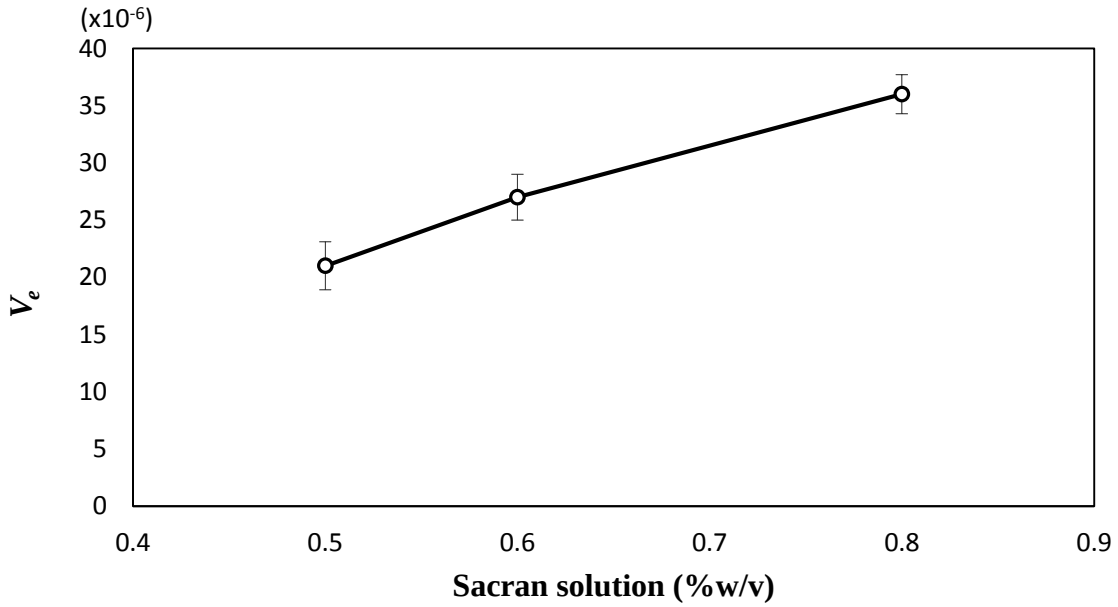

Figure 2.7 Cross-link density (V_e) of DVS cross-linked sacran hydrogels at concentration of 0.5 %, 0.6 % and 0.8 % (w/v) with molar ratio of DVS to sacran hydroxyl as 0.63

As a result, the high concentration of sacran solution was effective to prepare hydrogels. On the other hand, it was difficult to make homogeneous hydrogels in concentrations higher than 0.8 % due to bubble trapping in viscose precursor solutions, although harder hydrogels were prepared. The FT-IR spectroscopy was made in order to confirm the addition reaction of DVS vinyls with sacran hydroxyls to form ether linkage. FT-IR spectra show strong signals of hydroxyls in any samples to overlap with the ether signals, and then the samples of sacran fiber and xerogel were treated by D_2O to weaken hydroxyl signals before measurement. As a result, ether absorption appeared as a shoulder of glycoside peak around 1100 cm^{-1} in the IR spectra of DVS-cross-linked sacran hydrogel, to confirm the ether formation. Additionally, IR absorptions assigned to S=O were found around 1300 cm^{-1} (Figure 2.8), which indicate DVS incorporation by addition reaction with sacran hydroxyls.

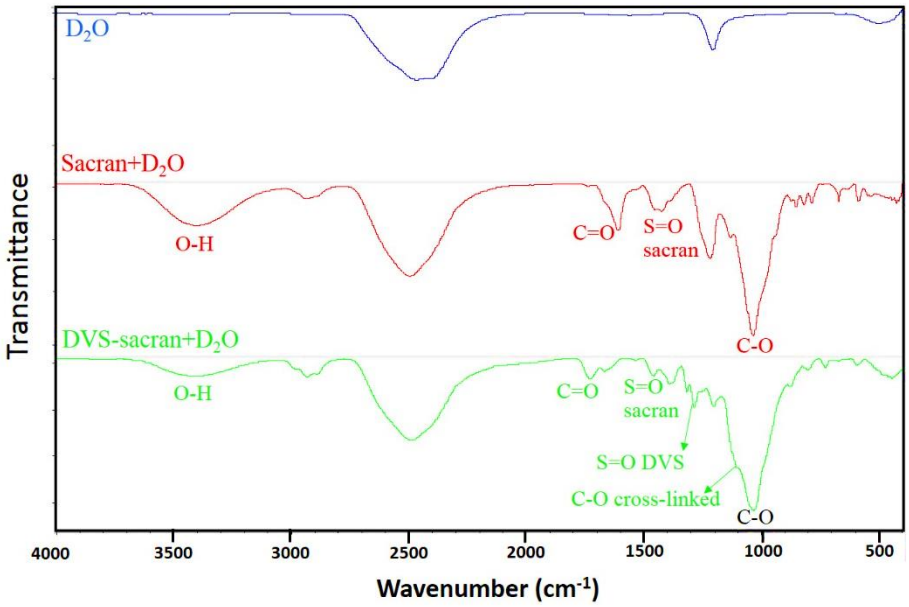

Figure 2.8 FT-IR-spectrum of pure sacran and DVS cross-linked sacran.

Table 2.2 Results of network structure analyses of sacran hydrogels cross-linked with divinylsulfone.

sample #	Conc. of sacran solution (w/v %)	DVS/OH (mol/mol)	DVS Incorporation degree[a)] (%)	Swelling ratio [b)], q_0 (g/g)	E_0 [c)] (kPa)	M_c (g/mol)[d)]	X [e)]	V_e (x10^{-6})[f)]
S1	0.5	0.63	7.5	437±87	7.0±0.6	98700±15	0.002 ± 0.0003	21±2.1
S2	0.6	0.63	7.8	355±68	9.0±0.6	30100±76	0.003 ± 0.0001	27±2.0
S3-1	0.8	0.43	8.0	312±54	10.0±1.5	27000±10	0.003 ± 0.0001	30±2.0
S3-2		0.63	16.0	240±12	12.0±0.6	22500±72	0.004 ± 0.0002	36±1.7
S3-3		0.83	21.5	220±12	18.0±0.6	15000±57	0.006 ± 0.0002	55±2.4
S3-4		1.10	28.0	145±4.8	19.0±1.0	14200±57	0.006 ± 0.0001	58±1.7

a) DVS incorporation degrees in hydrogels are simply calculated from increased C:S ratio by DVS reaction with sacran, determined by CHNS elemental analyses. b) q_0 refer to the swelling ratios of DVS cross-linked sacran hydrogels. c) E_0 refer to elastic moduli for DVS cross-linked sacran hydrogels, determined by compression mode. d) M_c refer to molecular weight between cross-linking points. e) X refer to the degree of cross-linking. f) V_e refer to the cross-linking density.

According to the results above, at 0.8 %wt of sacran solution was the limit of concentration to prepare DVS cross-linked sacran hydrogels. Then 0.8% sacran solution was selected to cross-link with various molar ratio of DVS to sacran hydroxyl as shown in Table 2.2.

After gelation, the properties of hydrogels were investigated. The results showed that an increased amount of DVS led to decreasing swelling ratio of hydrogels (Figure 2.9). However, the elastic modulus and cross-linking density were increased by increasing amount of DVS (Figure 2.10 and 2.11, respectively).

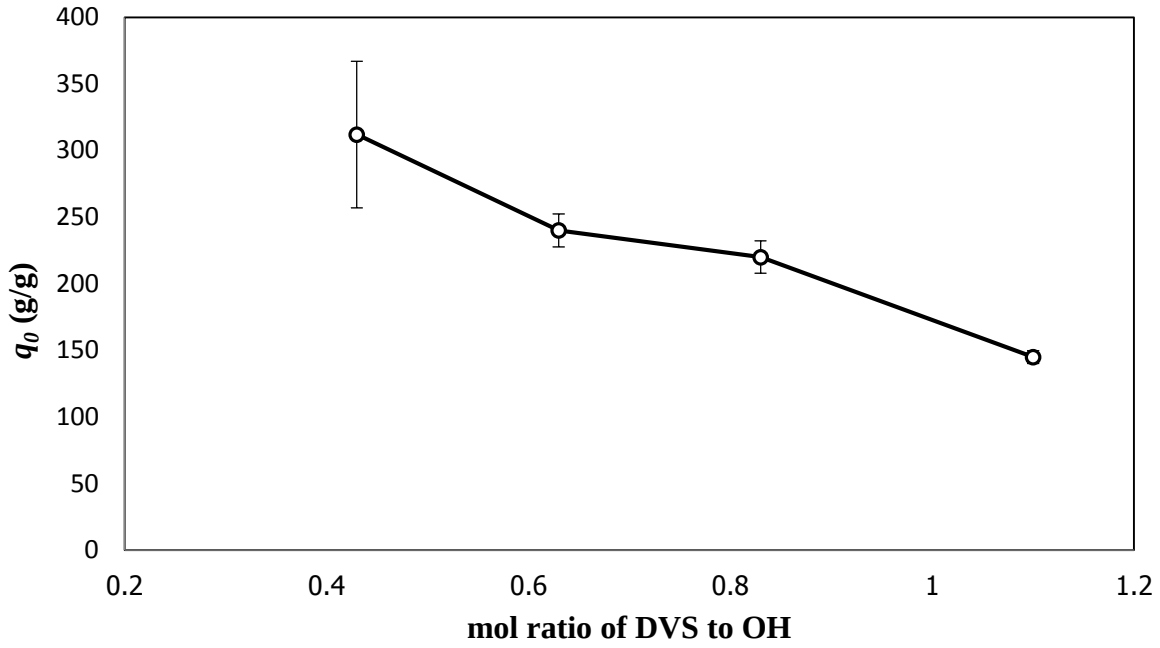

Figure 2.9 Swelling ratio (q_0) of 0.8 % sacran solution cross-linked with various mol ratio of DVS to OH.

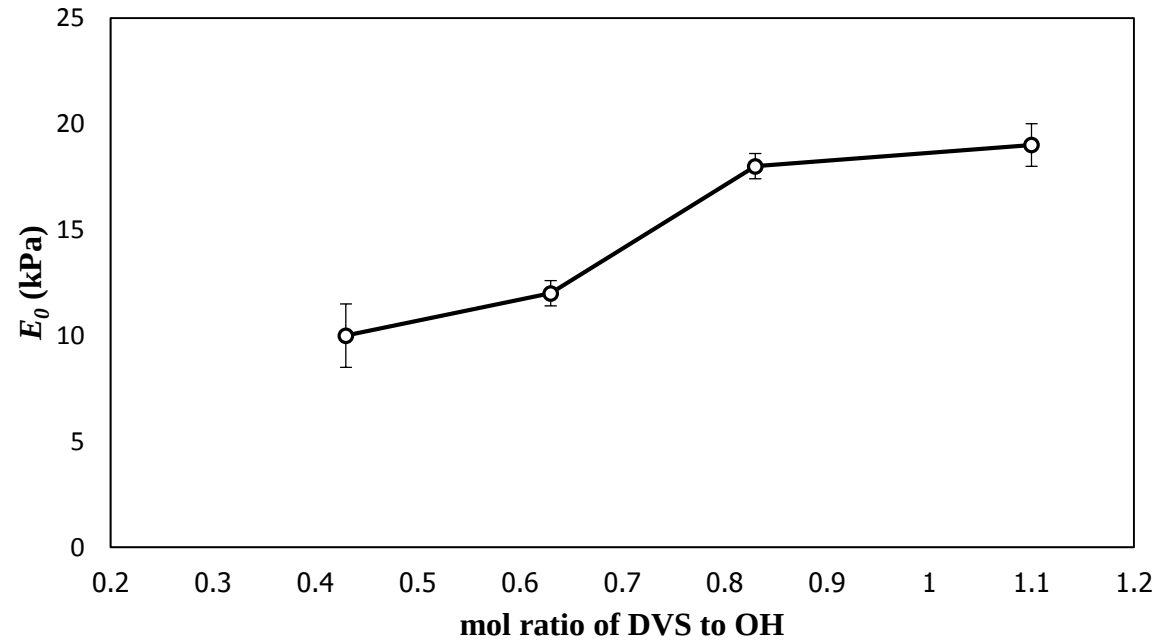

Figure 2.10 Elastic modulus by compression (E_0) of 0.8 % sacran solution cross-linked with various mol ratio of DVS to OH.

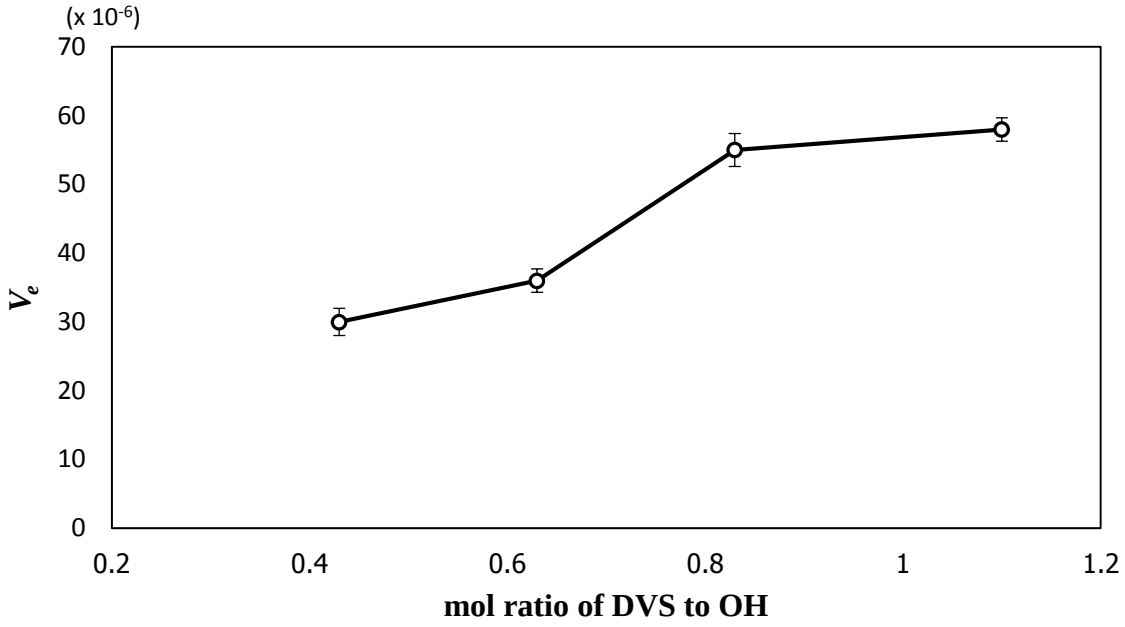

Figure 2.11 Cross-linking density (V_e) of 0.8 % sacran solution cross-linked with various mol ratio of DVS to OH.

The values of q0 ranged between 145 and 312 g/g and were too high for the amount of DVS used (Table 2.2), which might be attributed to the coexistence of DVS molecules not cross-linking but reacting with sacran hydroxyls at only one vinyl group. In order to clarify this hypothesis, the degree of DVS incorporation in the hydrogels was calculated from an increase in the S/C ratio between the original and DVS-reacted sacran (Table 2.2), which was measured by CHNS elemental analyses of the hydrogels. The degree of DVS incorporation ranged from 8.0 % to 28.0 %, which are also values too high for the soft hydrogels with a q0 of over 145 and an elastic moduli, E0, ranging from 10 to 19 kPa (Table 2.2) determined by a mechanical test in compression mode. Such a high degree of DVS incorporation supports the existence of non-cross-linking DVS side group in sacran networks (Scheme 2.4).

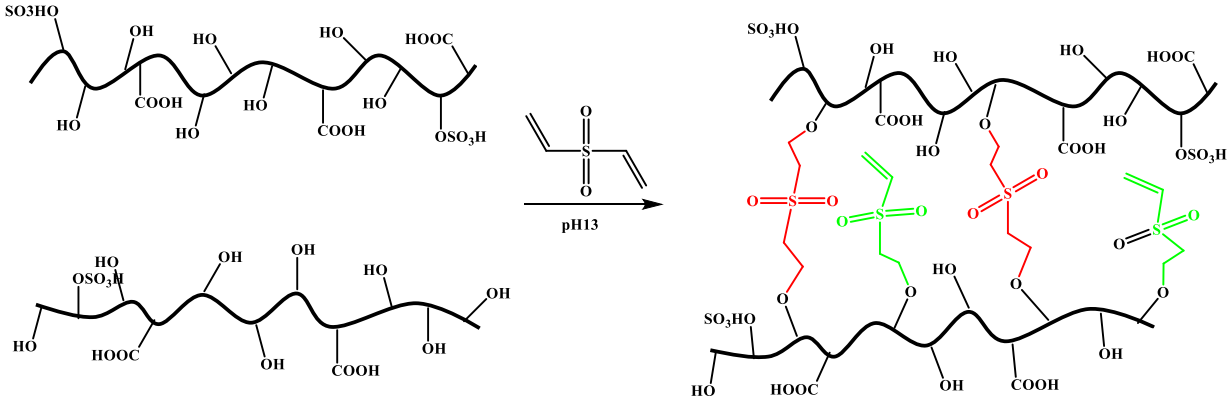

Scheme 2.4 Sacran networks after cross-linked by DVS molecules which some DVS not cross-linking but reacting with sacran hydroxyls at only one vinyl group. Bond in red color refer to reacting part and green color refer to un-reacting part.

2.4 Conclusion

Sacran hydrogel were prepared by chemical cross-link between functional group of sacran to prepare sacran hydrogels. The hydroxyl groups of sacran showed efficiently cross-linked presumably due to larger amount than other functional groups, by divinyl sulfone (DVS) forming an ether bond obtained strong and smooth hydrogels. The increasing of sacran concentration and amount of DVS showed the decreasing in swelling ratio, leading to higher elastic modulus. From data reported in this chapter, we deduced that the 0.8 %wt of sacran solution cross-linked with DVS at 1.1 mol ratio of DVS to OH was the best condition to prepare chemical sacran hydrogels. On the other hand, we considered that the DVS molecules was not completely cross-linked but reacted with sacran hydroxyls at only one vinyl group. Thus, the additional cross-linking would be studied in chapter 3.

References

[1] Jeong, B.; Kim, S. W.; Bae, Y. H., *Adv. Drug Deliv. Rev.* **2002,** *54* (1), 37-51.

[2] Luyn, M. J. A.; Wachem, P. B.; Olde Damink, L.; Dijkstra, P. J.; Feijen, J.; Nieuwenhuis, P., *J. Biomed. Mater. Res. A* **1992,** *26* (8), 1091-1110.

[3] Zhang, J.; Xu, J.; Wang, H.; Jin, W.; Li, J., *Mater Sci Eng C* **2009,** *29* (3), 889-893.

[4] Collins, M. N.; Birkinshaw, C., *J. Appl. Polym. Sci.* **2008,** *109* (2), 923-931.

[5] Hahn, S. K.; Jelacic, S.; Maier, R. V.; Stayton, P. S.; Hoffman, A. S., *J. Biomater. Sci. Polym. Ed.* **2004,** *15* (9), 1111-1119.

[6] Annabi, N.; Mithieux, S. M.; Boughton, E. A.; Ruys, A. J.; Weiss, A. S.; Dehghani, F., *Biomaterials* **2009,** *30* (27), 4550-4557.

[7] Ramamurthi, A.; Vesely, I., *Biomaterials* **2005,** *26* (9), 999-1010.

[8] Zhu, C.; Bettinger, C. J., *Macromolecules* **2015,** *48* (5), 1563-1572.

[9] Peppas, N. A.; Huang, Y.; Torres-Lugo, M.; Ward, J. H.; Zhang, J., *Annu Rev Biomed Eng.* **2000,** *2* (1), 9-29.

[10] Okajima, M. K.; Kaneko, D.; Mitsumata, T.; Kaneko, T.; Watanabe, J., *Macromolecules* **2009,** *42* (8), 3057-3062.

Chapter 3

Orientation control sacran hydrogel by one-dimensional drying process

3.1 Introduction

Most biological tissues are in a soft and wet gel-like state and contain a large amount of water; anisotropic structures are integrated from the molecular level to the macroscopic level [1]. The anisotropic structures of these biological tissues enable the elaborate functions of living organisms [2]. For example, actin and myosin show a liquid crystalline-like anisotropic structure in a muscle sarcomere, which contributes to the smooth motion of muscle contraction in one direction while limiting motion in the other direction [3-4]. In order to impart anisotropic properties to synthetic hydrogels, some techniques have been reported such as directional freezing [5], self-assembly [6-10], and mechanical reorientation [11]. Although one of the most attractive targets for anisotropic hydrogels is one-directional swelling, like a coiled spring, there have been no reports of this behavior as the water molecules move freely, rendering the network amorphous. Sacran chains are self-assembled by increasing the solution concentration enough so that a rigid-rod structure is formed [12], exhibiting liquid crystalline (LC) properties [13-14]. The long rigid polymer chains have the tendency to form in-plane orientation. When the rigid polymer chains are dissolved in a solvent with a low chain number density, the orientation of the chains are random in three dimensions, as shown in Figure 3.1(a). As the solvent evaporates, the thickness of the solution shrinks. Effectively the polymer chains

are compressed. When the solvent completely evaporates, the chains are randomly oriented in xy plane.

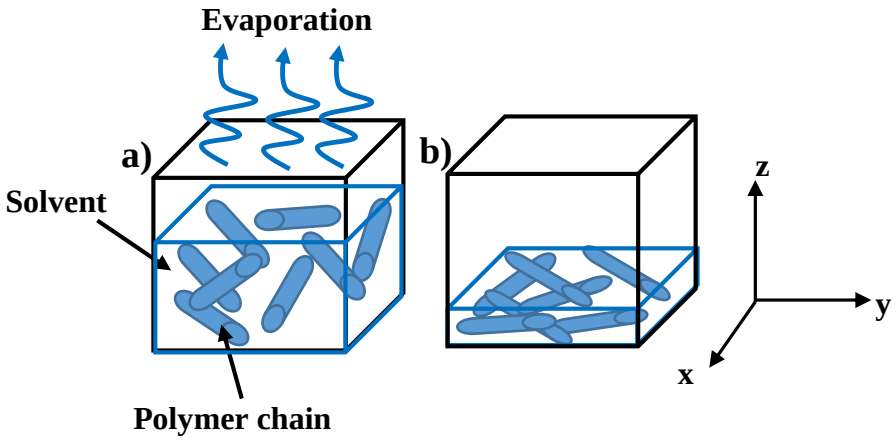

Figure 3.1 Schematic diagram showing how the in-plane orientation is formed from long rigid polymer chains. (a) random orientation in 3-D, (b) random orientation in 2-D (in-plane orientation)

Recently, we prepared self-supporting sheets of sacran hydrogels by a water-casting method from LC solutions, where precursor films cross-linked upon heating to a dry state displayed in-plane orientation by the cooperative alignment of sacran rigid rods. Moreover we found that molecularly-oriented hydrogels show anisotropy in water-swelling and mechanical properties [15]. These results encouraged us to prepare sacran gels with super-anisotropy of swelling.

According to chapter2, we were able to successfully prepared strong chemically cross-linked sacran hydrogels by DVS cross-linker. However, some molecule of DVS in this hydrogel not completely cross-linked but reacted with sacran hydroxyls at only one vinyl group. In this chapter, we tried to describe the new method to prepare one-dimensional swelling hydrogels by additional cross-linking. The molecular orientation and mechanical properties of obtained hydrogels were investigated.

3.2 Experimental

3.2.1 Materials

All of materials were used as same type as chapter 2.

3.2.2 Preparation of sacran xerogels by one-dimesional drying method

The oriented hydrogels were prepared by additional cross-linking during one-dimensional drying process. DVS cross-linked sacran hydrogels as prepared in chapter 2 were slowly dried on polypropylene substrate for 7 days at room temperature to form sacran xerogel. The obtained xerogel was re-swollen in water or other solvents [16].

3.2.3 Characterization of sacran xerogels

Swelling ratio and Mechanical properties

Swelling ratio of re-swollen sacran hydrogels in milli-Q water were measured by same method as described in previous chapter (see in 2.2.3). The mechanical properties of sacran xerogel was tested in compression and tensile mode. A probe for compression or tensile test was set up on an Instron 3365 machine using a 5 kN load cell with a crosshead speed of 1.00 mm/min. Elastic moduli, *E*, of the hydrogels were calculated using the initial inclinations of the stress-strain curves. The other mechanical properties such as cross-link density (V_e), average molecular weight between cross-linking points (M_c) and degree of cross-linking (X) were also calculated using same equations as mentioned in chapter 2.

Thermogravimetry (TGA)

Water content of the xerogel was measured by thermogravimetry (STA7000, Hitachi High Tech Science Coop.). A specimen of film was heated from 25 to 175 ^{o}C at a rate of 2 ^{o}C/min under a nitrogen atmosphere. Weight loss around 150 ^{o}C was regarded as water content due to the plateau appearance of the curve.

3.2.4 The orientation of the sacran hydrogel

Scanning electron microscopy (SEM)

Scanning electron microscope (SEM) measurements were performed using a Hitachi S-4500 scanning electron microscope at an accelerating voltage of 0.5 kV (500 V) for imaging.

Crossed-polarizing microscopy

Microscopic observations were investigaed by a microscope (BX51, Olympus) equipped with CCD camera (DP80, Olympus). A specimen of sacran hydrogels were cut to size for microscopic observation (ca. 5mm x 0.5mm x 1mm) and put on the glass slide at 25 ^{o}C. A first-order retardation plate ((λ = 530 nm) was inserted into the light path.

Wide-angle X-ray diffraction (WAXD)

Wide-angle X-ray diffraction (WAXD) patterns were measured using a graphite monochromatized CuKα radiation beam focused *via* a 0.3 mm pinhole collimator with a flat 20 x 20 cm^2 imaging plate (IP) detector of 1900 x 1900 pixels (Rigaku, R-AXIS IIc). A small

piece of the sample with an edge size less than 1 mm was mounted with the sample-IP distance of 10 cm. The exposure was performed for 3 min a shot in a geometrical condition by directing the X-ray beam in the front of samples. The degree of orientation was calculated by Hermann's orientation function (Equation 3.1) [17].

$$f = \frac{3\langle \cos^2 \varphi \rangle - 1}{2} \tag{3.1}$$

where;

$$\langle \cos^2 \varphi \rangle = \frac{\int_0^{\frac{\pi}{2}} I(\varphi) \cos^2 \varphi \sin \varphi \, d\varphi}{\int_0^{\frac{\pi}{2}} I(\varphi) \sin \varphi \, d\varphi}$$

Differential scanning calorimetry (DSC)

The orientation of water in the sacran hydrogel was measured by differential scanning calorimetry (DSC6000, Seiko Instruments Inc.) at a scan ratio of 2 ^{o}C/min from -150 ^{o}C to 20 ^{o}C under nitrogen gas. Samples were placed in aluminum pans and sealed. Samples were weighed before and after DSC measurements and no weight change was confirmed to determine that no water had vaporized.

3.3 Results and Discussion

3.3.1 Preparation of sacran xerogels by one-dimensional drying method

According to chapter 2, we investigated the degree of DVS incorporation in sacran hydrogels by elemental analyses (EA). The results from EA and E_0 values, indicated that molecule of DVS not completely cross-linked with both vinyl groups but there have some terminal vinyl group remaining in hydrogels. As the chemistry of DVS can easily react with nucleophile, we conjectured that these DVS side group should work as a chemical cross-linker by providing the proper reaction conditions such as an increased sacran concentration. If the network structures are deformed by an external stress and simultaneously cross-linked by DVS side group, the structures should be maintained deformed. Then, the first-step DVS cross-linked sacran hydrogels at 0.8 (w/v%) (Figure 3.1a) were slowly dried into xerogels (Figure 3.1b) after attaching them to a polypropylene substrate while the sacran concentration were gradually increased to make the pendant DVS cross-linkable with the pre-constructed networks and for the networks to be in a LC state (Scheme 3.1).

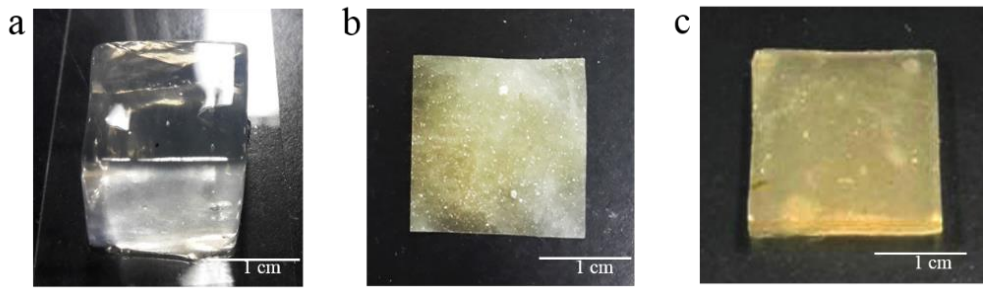

Figure 3.1 Representative images of sacran gels. (a) 1st step divinylsulfone cross-linked sacran hydrogels. (b) Xerogels formed by slow dry on attached substrate at room temperature. (c) Re-swollen gels from xerogels.

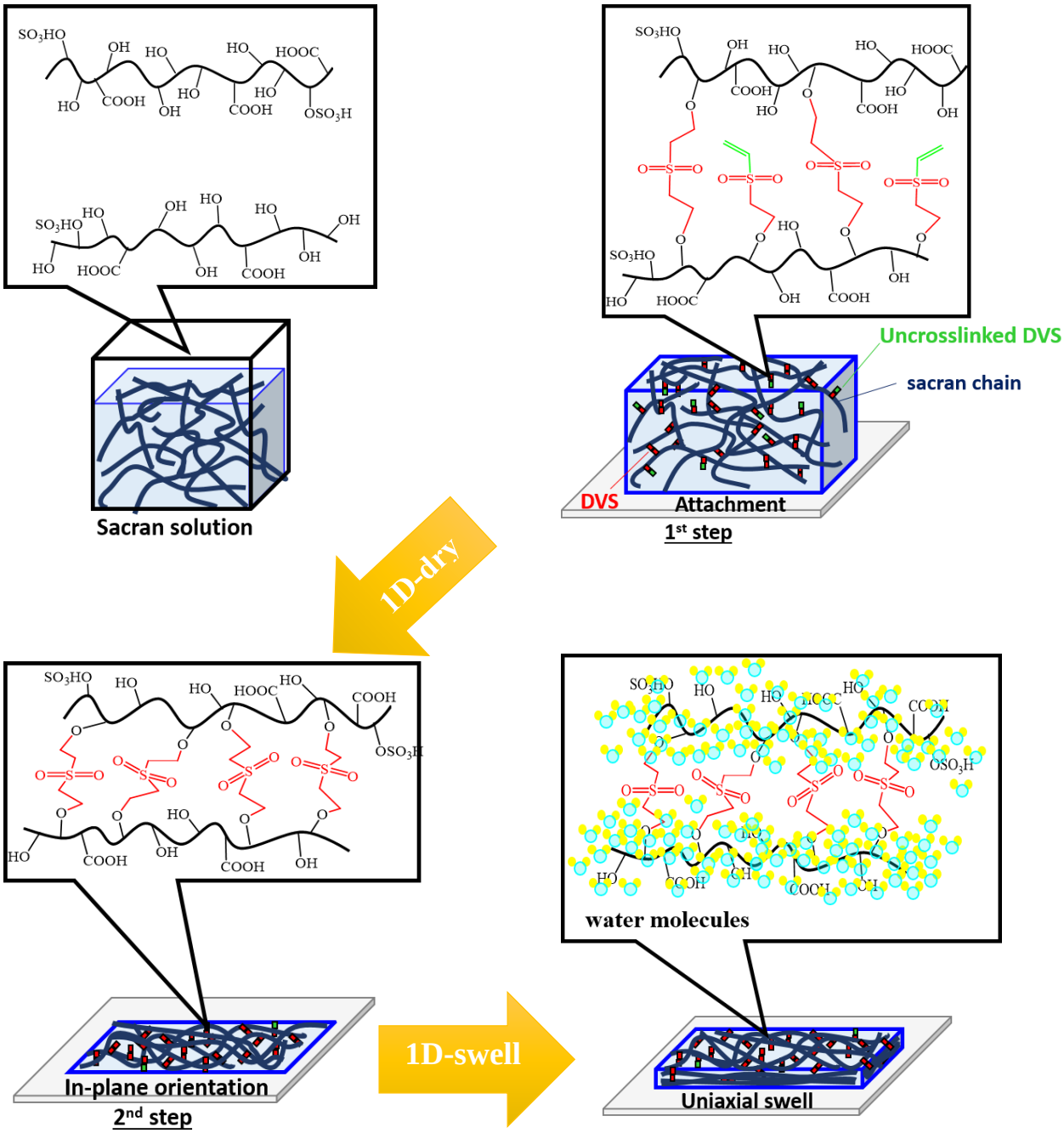

Scheme 3.1 Representative the formation process of hydrogels with one-dimensional swelling behavior by two-step cross-linking with divinylsulfone**.**

After drying process, the mechanical properties of sacran xerogels (film state) were measured by a tensile test. The obtained sacran xerogels at molar ratio of DVS to sacran hydroxyl as 0.43-1.10 had tensile strength values in the range of 0.08-0.16 MPa, tensile modulus in the 4.5-7.6 MPa and elongation in 1.9-3.2 % (Table 3.1). The water contents of the xerogels were determined by thermogravimetry (Table 3.1). The relationship between water content in xerogels and tensile modulus were investigated by sacran xerogel at molar ratio of DVS to sacran hydroxyl as 0.83. The results showed that tensile modulus were decreased with increasing of water content in xerogels (Figure 3.2).

Table 3.1 Mechanical properties and water contents of sacran xerogels (film state) cross-linked with divinylsulfone (DVS)

sample #	Conc. of sacran solution (w/v %)	DVS/OH (mol/mol)	Tensile strength (MPa)	Tensile modulus (MPa)	Elongation (%)	Water content by TGA (wt%)
S3-1	0.8	0.43	0.08	7.64	1.9	16.1
S3-2		0.63	0.12	4.93	2.9	14.0
S3-3		0.83	0.15	7.59	2.4	13.2
S3-4		1.10	0.16	4.53	3.2	13.1

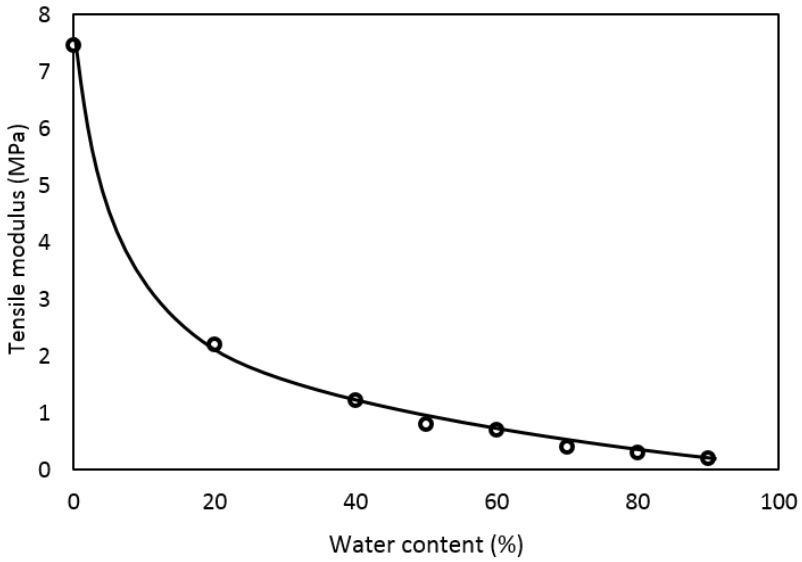

Figure 3.2 Tensile modulus of sacran xerogels with different of water content

Table 3.2 Swelling degrees and elastic moduli of sacran hydrogels cross-linked with divinylsulfone (DVS)[a)]

sample #	Conc. of sacran solution (w/v %)	DVS/OH (mol/mol)	DVS Incorporation degree[b)] (%)	Swelling ratio [c)], q_0 (g/g)	Re-swelling ratio [c)], q_r (g/g)	E_0 [d)] (kPa)	E_r [d)] (kPa)
S3-1	0.8	0.43	8.0	312±54	21±4.3	10.0±1.5	231.0±25
S3-2		0.63	16.0	240±12	18±6.2	12.0±0.6	384.0±25
S3-3		0.83	21.5	220±12	16±5.8	18.0±0.6	555.0±70
S3-4		1.10	28.0	145±4.8	10±4.3	19.0±1.0	836.0±32

a) Sacran was cross-linked by DVS in 0.2 M NaOH solution. b) DVS incorporation degrees in hydrogels are simply calculated from increased C:S ratio by DVS reaction with sacran, determined by CHNS elemental analyses. c) q_0 and q_r refer to the swelling ratios of original gels and re-swollen gels after drying, respectively. d) E_0 and E_r refer to elastic moduli for the original gels and for re-swollen gels after drying, respectively, determined by compression mode.

As a result, sacran xerogels in the LC orientation state were formed by additional cross-linking. If the xerogels were reswollen in water, the swelling ratio (re-swelling ratio, q_r) decreased to a range between 10 and 21 g/g and elastic moduli, E_r remarkably increased to 231-836 kPa, compared with the original DVS-cross-linked hydrogels, which strongly suggests that pendant DVS works as an additional cross-linker (Table 3.2).

In order to estimate the effects of the additional cross-linking on the network structure, the cross-link density (V_e) was calculated from q and E. The estimated results are summarized in Table 3.3. The V_e values of the re-swelled hydrogels after drying to xerogels were 20-45 times higher than those of the hydrogels before drying. The degree of cross-linking (X) and molecular weight between cross-linking points (M_c) were also calculated (Table 3.3). After drying and re-swelling, X became 20-45 fold higher than that of the primary hydrogels, while M_c dropped drastically. The results indicate that the treatment of primary hydrogels by drying/re-swelling was effective in inducing additional cross-linking by DVS in the highly-concentrated state. The hydrogel prepared with a sacran concentration of 0.8 wt% at a ratio of hydroxy group to DVS of 1.0:1.10 (S3-4 in Table 3.2) showed the highest E_r value (836 kPa, Table 3.2) of all the hydrogels prepared. This hydrogel had the consistency of soft rubber, and was used in the next experiment.

Table 3.3 Results of network structure analyses of sacran hydrogels cross-linked with divinylsulfone.

Sample #	Original gels			Re-swollen gels from xerogels		
	M_c (g/mol) [a)]	X [b)]	V_e (x10^{-5}) [c)]	M_c (g/mol) [a)]	X [b)]	V_e (x10^{-5}) [c)]
S3-1	27000±10	0.003 ±0.0001	3.0±2.0	1100±41	0.07±0.002	7.0±3.4
S3-2	22500±72	0.004 ±0.0002	3.6±1.7	700±10	0.12±0.008	11.7±4.7
S3-3	15000±57	0.006 ±0.0002	5.5±2.4	480±45	0.18±0.009	16.9±5.7
S3-4	14200±57	0.006 ±0.0001	5.8±1.7	320±26	0.27±0.003	25.6±5.3

a) M_c refers to molecular weight between cross-linking points; b) X refers to the degree of cross-linking; c) V_e refers to the cross-linking density

3.3.2 Anisotropic swelling

We found that the xerogels formed showed anisotropic re-swelling behavior in water, as expected. The swelling of the xerogels along their width was almost constant, whereas swelling along their thickness increased. The linear swelling ratio, α, of thickness to width was calculated by the following c:

$$\alpha = \frac{l_1 - l_0}{l_0} \qquad (3.2)$$

where l_1 is the length after swelling and l_0 is the length before swelling. In addition, the degree of anisotropy in swelling, α_t/α_w was calculated using the linear swelling ratio of thickness, α_t, to width, α_w.

The values of α_t/α_w ranged between 10,000 and 40,000 with small errors (Figure 3.3) and were much higher than those of physically cross-linked hydrogels created by thermal

treatment of dry sacran films, as previously reported [15]. Actually, these high values of α_t/α_w imply one-dimensional swelling in the thickness direction, like a coiled spring. Chemical cross-linking by DVS has the effect of reducing α_w (Figure 3.4), presumably due to stronger connections between sacran chains by covalent bonding than by physical cross-linking. Additionally, α_t/α_w values decreased with an increasing DVS ratio (Figure 3.3), which simply corresponds to a decrease in the degree of one-dimensional swelling described above due to an increase in the degree of chemical cross-linking.

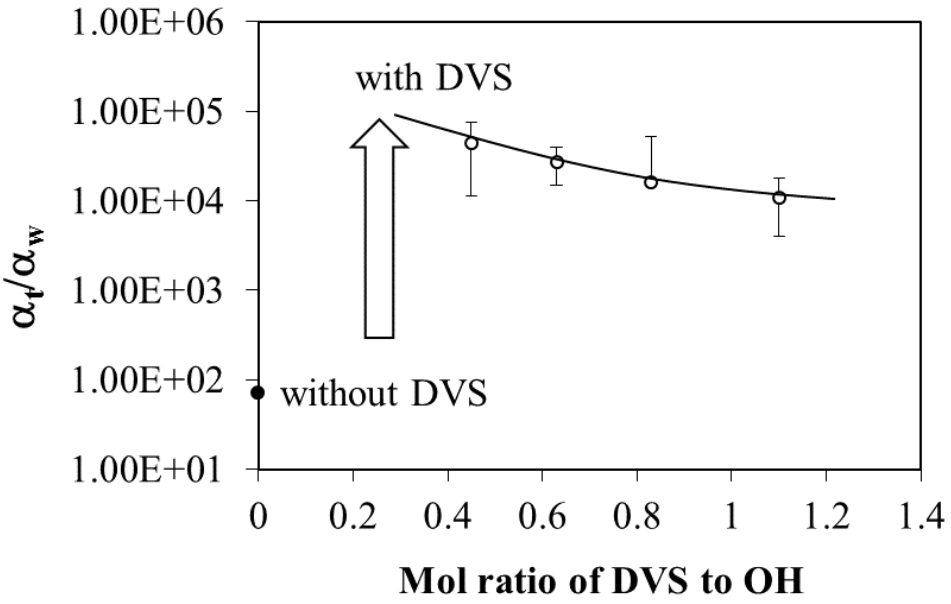

Figure 3.3 Anisotropy of swelling for sacran xerogels cross-linked by different amount of divinylsulfone.

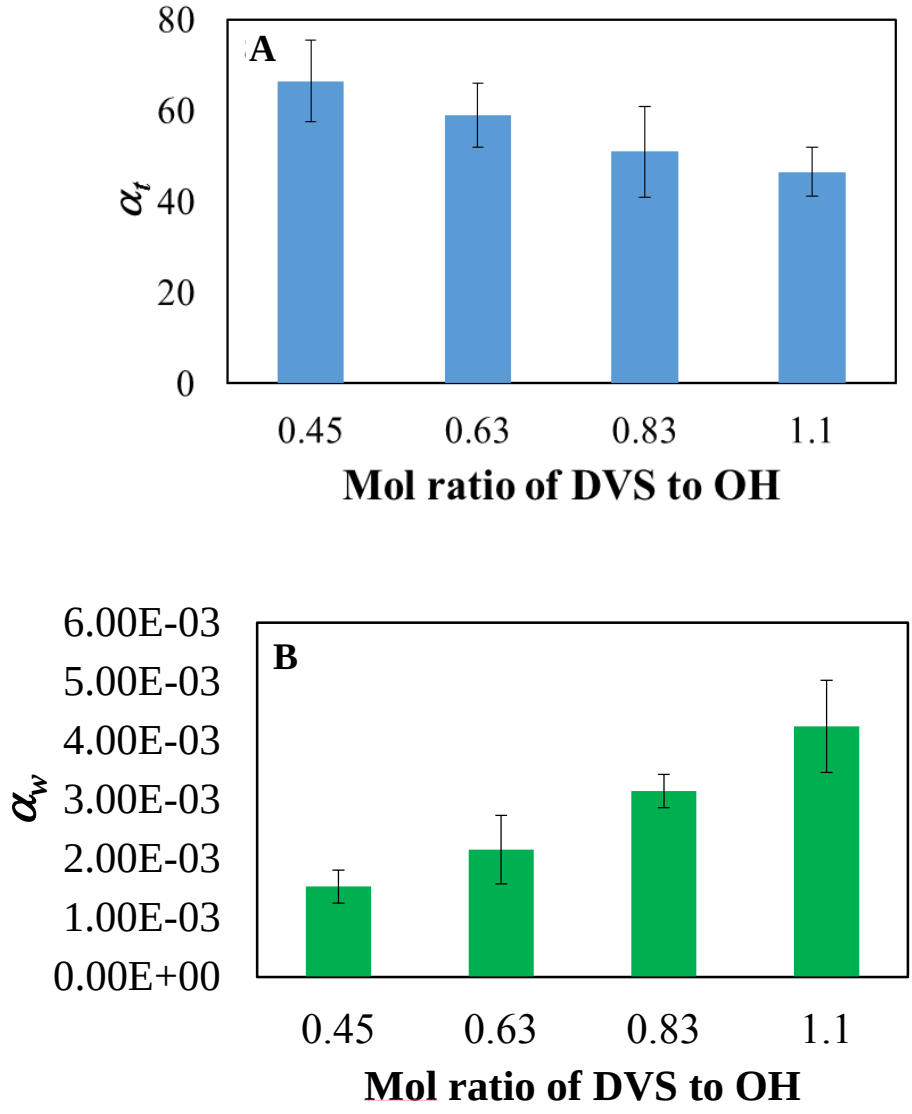

Figure 3.4 Representative linear swelling ratio of a) thickness (α_t) and b) width (α_w).

Figure 3.5 Xerogel formed by dehydration with ethanol and vacumm dried.

We prepared xerogels by other methods to observe the anisotropy in swelling, and found that the drying method strongly affected the anisotropy. If the hydrogels were dried by dehydration using ethanol (Figure 3.5) or under vacuum, no anisotropic swelling behavior was observed. On the other hand, slow drying on a polypropylene substrate which became spontaneously attached with sacran hydrogels at room temperature efficiently induced additional cross-linking of pendant DVS to fix the xerogel structure in an in-plane orientation (Figure 3.1b), which made possible unidirectional drying as illustrated in Figure 3.1d.

3.3.3 Structural orientation

Scanning electron microscopy images (SEM) of the xerogels swelled in one dimension are shown in Figure 3.6(a-b). While some aligned lines appeared in the image of the side surface (Figure 3.6a), the lines in the image of the top surface seem disordered (Figure 3.6b). Fourier-transformations (FTs) of the gray-scaled SEM images were made, and the output images are shown as an inset in each figure. FT converts information from data images in a real space into a mathematically-defined frequency space to better characterize surface structures [18]. As a result of FT, side view images showed a broad diagonal line from the upper right to the lower left, meaning that while the line direction on the real SEM images was very consistent, the distance between the lines was not constant, just like in nematic liquid crystalline structures. On the other hand, FT pictures of the top surface showed no specific patterns, implying randomness.

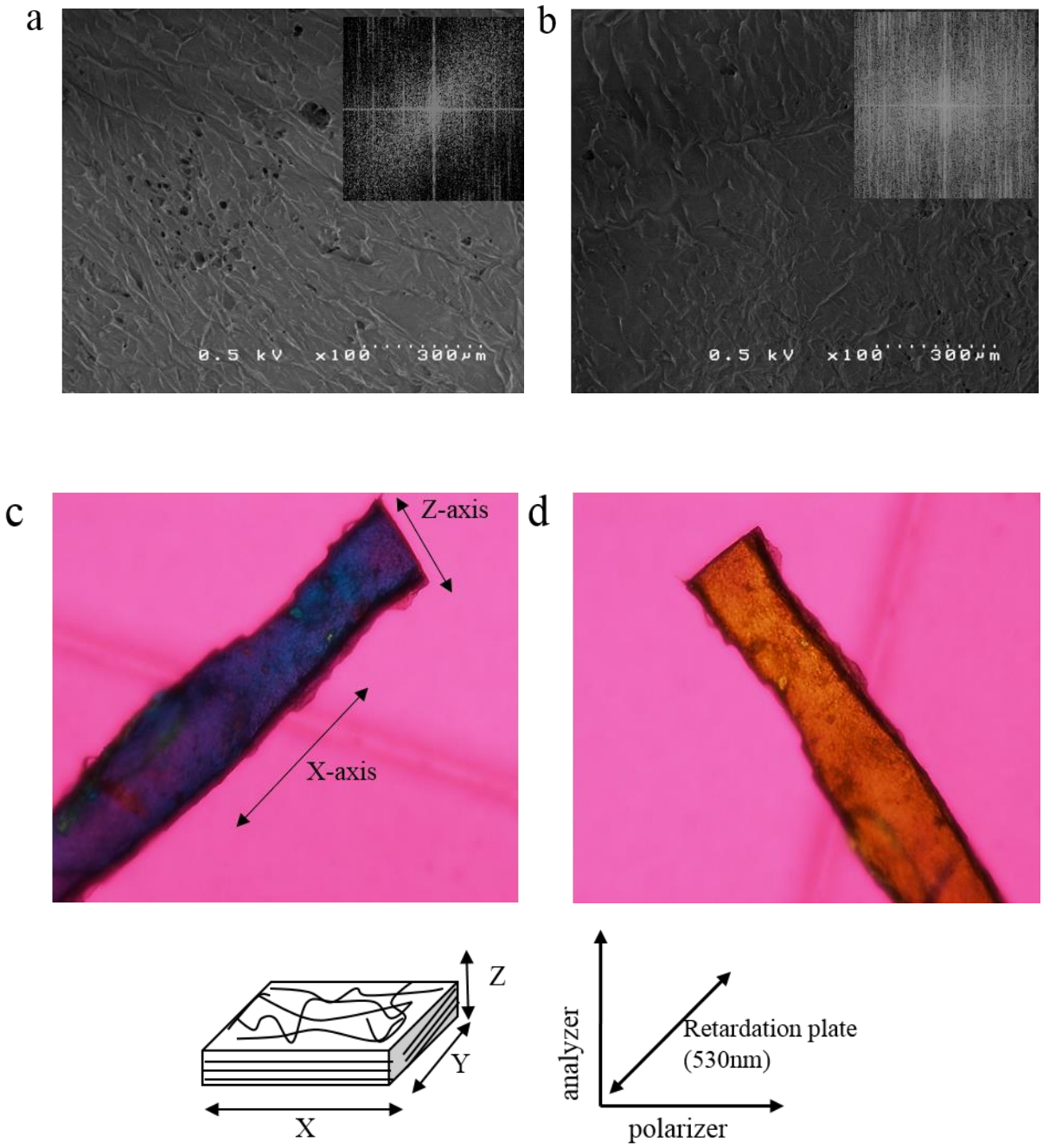

Figure 3.6 (a-b) Representative SEM images of re-swollen gels from xerogels (S3-4 in Table 1). Inset: Fourier-transformed images (a) ZX-surface. (b) XY-surface. (c-d) Representative crossed-polarizing microscopic photos of re-swollen gels from xerogels (S3-4 in Table 1) taken under a first-order retardation plate (530 nm). X-axis is long axis of sacran hydrogel. (c) X-axis is parallel to the direction of the first order retardation plate. (d) Z-axis is parallel to the direction of the first order retardation plate.

The nematic-like orientation of the sacran hydrogels was more clearly verified using a first-order retardation plate (λ=530 nm) inserted into the light path. The polarization microscopic observation showed that the sacran hydrogel birefringence was positive, as evidenced by both the additive birefringence (blue color) (Figure 3.6c) of the hydrogel lay from the upper right to the lower left, and by the subtractive birefringence (orange color) (Figure 3.6d) of the hydrogel lay from the upper left to the lower right. The positive birefringence strongly suggested that the orientation of the sacran polymer backbones was parallel to the XY-axis of the hydrogels. We studied the elastic behavior using compressive tests of re-swelled hydrogels targeting the oriented YZ- or XZ-sides or the non-oriented XY-side (Figure 3.7). The *E* value of the hydrogel when compressing the YZ- or XZ-side was 990 kPa and higher than the value when the non-oriented XY-side was compressed (836 kPa). The results strongly support the in-plane orientation of the hydrogels.

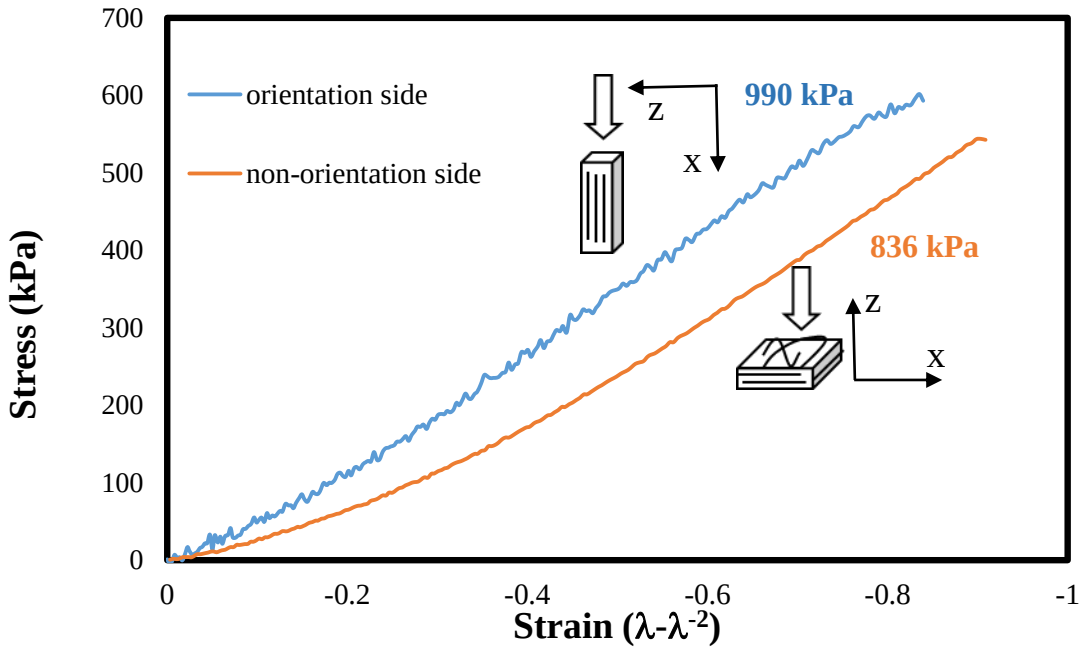

Figure 3.7 Stress-strain curves of re-swollen gels from xerogels (S3-4 in Table 3.1).

To investigate the molecular orientation, we performed wide-angle X-ray diffraction (WAXD) studies on the sacran xerogels and re-swelled hydrogels (Figure 3.8). The WAXD images of both sacran xerogel and re-swelled hydrogel in XY-side (Figure 3.8a and Figure 3.8g) exhibited symmetry Debye-circle, indicating that there was no in-plane orientation. In contrast, the WAXD images of sacran xerogel in XZ-side (Figure 3.8b) showing two broad halo arcs at a diffraction angle, 2θ, of around 20^{o} on the meridian line, revealing that sacran chains were oriented parallel to the XY-axis. The *d*-spacing of the diffraction arcs was calculated as 0.45 nm from Bragg's law: $2d\sin\theta = \lambda$, where λ = 0.154 nm (well-known spacing of molecules in the nematic state). Azimuthal scanning diagrams are shown in Figure 3.8e and the degree of orientation was estimated to be 0.24 using Hermann's orientation function. The degree of orientation was a little lower than the values typically reported for nematic molecules, presumably due to the disturbance in structure orientation by DVS cross-linkage. The WAXD images of the re-swelled hydrogel XZ-side (Figure 3.8j) also showed the diffraction arcs. However the diffraction angle (2θ) of the re-swelled hydrogel was 27 ^{o}, d-spacing was 3.40, and orientation degree was 0.047 (Figure 3.8k). Actually, diffraction was not attributed to the sacran chains but to water because the water content in the hydrogel state was around 95%, which eliminated the diffraction caused by the sacran networks. The fact that water molecules are responsible for these WAXD arcs that indicate orientation is unexpected because free water has too much mobility to show molecular orientation at room temperature.

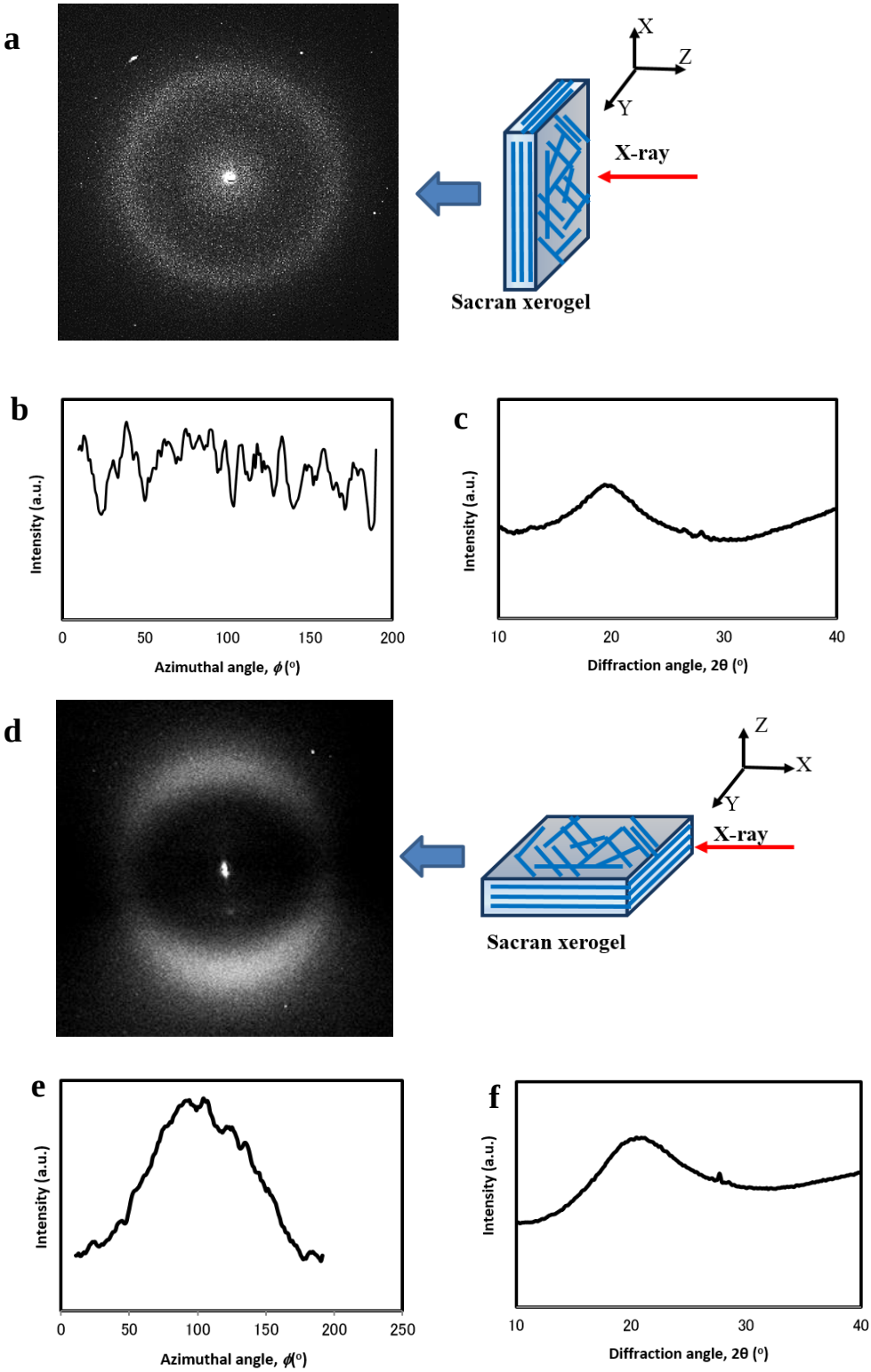
a
X
Z
Y
X-ray
Sacran xerogel
b
Intensity (a.u.)
0
50
100
150
200
Azimuthal angle, ϕ (°)
c
Intensity (a.u.)
10
20
30
40
Diffraction angle, 2θ (°)
d
Z
X
Y
X-ray
Sacran xerogel
e
Intensity (a.u.)
0
50
100
150
200
250
Azimuthal angle, ϕ(°)
f
Intensity (a.u.)
10
20
30
40
Diffraction angle, 2θ (°)

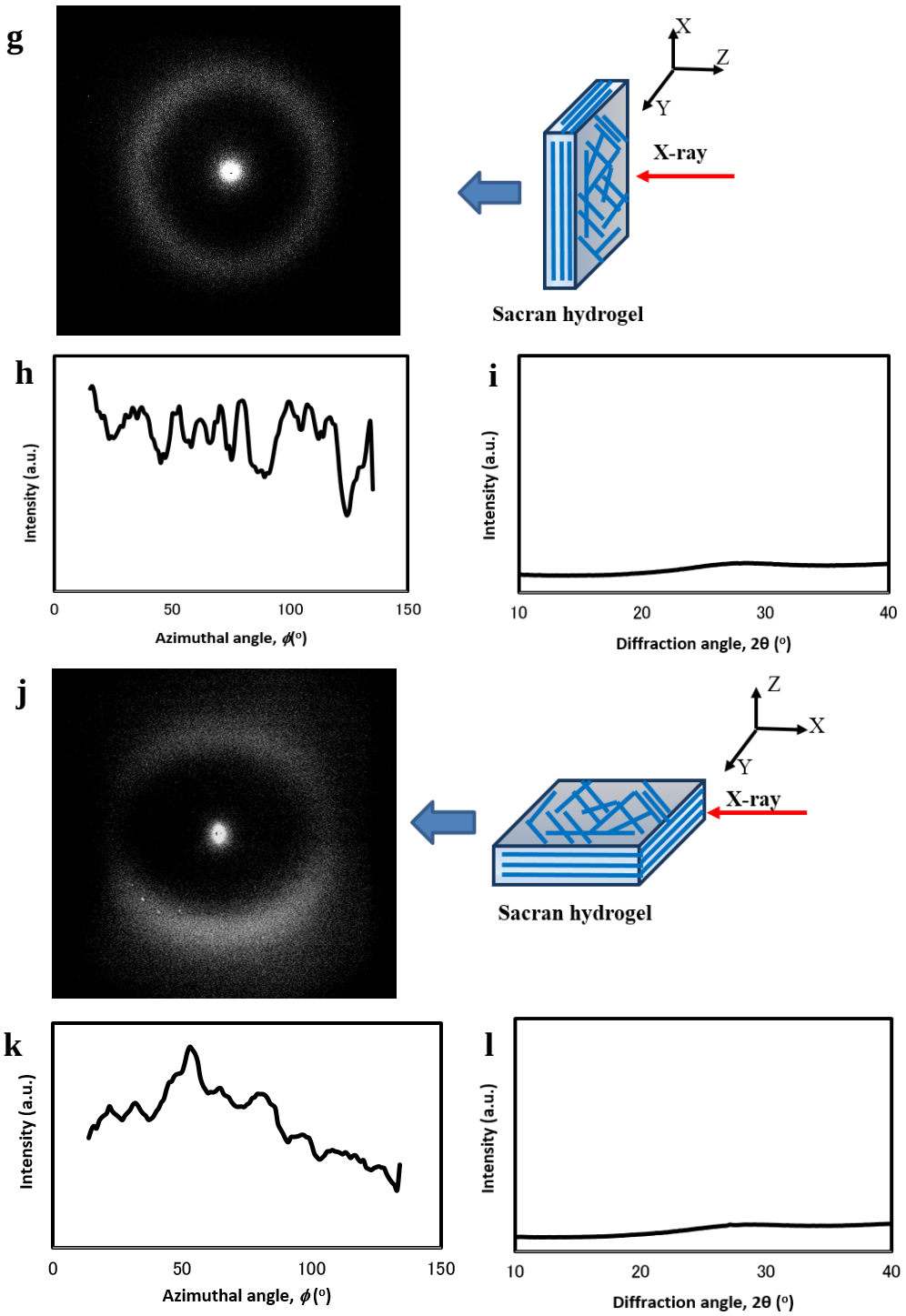

Figure 3.8 Wide angle X-ray diffraction (WAXD) images of sacran xerogels in (a) XY-side, (d) XZ-side, re-swelled hydrogels in (g) XY-side and (j) XZ-side. WAXD diagram of azimuthal scanning around diffraction arcs: (b and e) xerogels scanned around 2θ = 20° in WAXD image a and d, repectively. (h and k) re-swelled hydrogels scanned around 2θ = 27° in WAXD image g and j, respectively. WAXD diagram of 2θ diffraction angle : (c and f) xerogels and (i and l) re-swelled hydrogels.

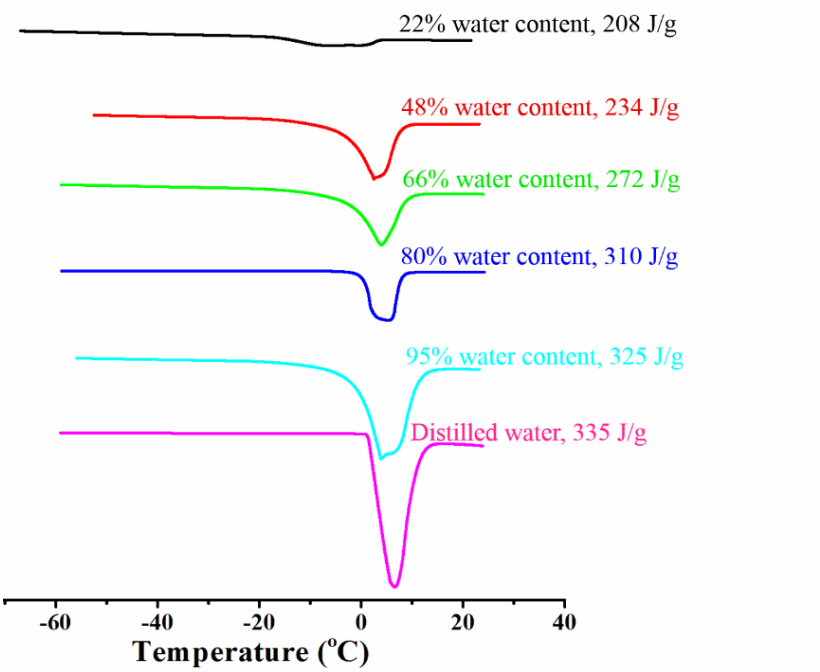

Figure 3.9 DSC thermograms of sacran hydrogels with various water contents scanned by heating from -100 °C to 25 °C. Inset values are fusion enthalpy of ice.

Table 3.4 Water composition in sacran hydrogel in various water content.

Sample#	Water content (%)	Fusion enthalpy of ice (J/g)	Free water (%)	Bound water (%)
Distilled water	-	335	100	-
S3-4	22	208	40	60
S3-4	48	234	57	43
S3-4	66	272	77	23
S3-4	80	310	92	8
S3-4	95	325	97	3

Next, we tried to confirm the state of water in the hydrogels by DSC study where the amount of the water binding to the sacran chains could be quantified. DSC measurements of sacran hydrogels with various water contents in distilled water were made at temperatures from -100 ºC to 25 ºC. The thermograms are shown in Figure 3.9, showing an endotherm with an onset temperature of around 0 ºC, corresponding to the melting point of ice. In all the hydrogels, ice melt started at temperatures slightly lower than 0 ºC. For the hydrogel with a water content of 22 wt%, the endotherm showed a multipeak, which can be attributed to the presence of at least two types of freezable water: (i) freezing free water which undergoes a thermal transition similar to normal water and (ii) freezing bound water, which undergoes a thermal phase transition at temperatures lower than that of normal water. The fusion enthalpy of ice made of distilled water was 335 J/g while the fusion enthalpy of ice in the sacran hydrogels was lower. For example, the fusion enthalpy of ice in the sacran hydrogel with 95 % water content was only 325 J/g. By comparing these values, the amount of bound water in the hydrogel was calculated and shown in Table 3.4. The sacran hydrogel with 95 % water content contained 0.8 wt% sacran fiber in the hydrogel, and 3 wt% water in the hydrogel bound to sacran chains. Taking these results, 0.8:3 (w/w) corresponds to a molar ratio of 37.5 mol of non-frozen bound water/mol of sacran sugar residues. Sacran hydrogels with water content ranging from 22 to 95 % showed 3 to 61 % bound water. On the other hand, xanthan gum, which is a rigid polysaccharide molecule ~10 mol of water/mol of the sugar unit of xanthan gum [19]. The amount of water bound in sacran is higher than that in xanthan gum. The bound water might directly attach to the polysaccharide chains through interactions with the hydroxyl, carboxyl, and sulfonate groups in sacran. According to the literature [20], bound water content in different polymer-water systems depends on both chemical composition as well as the higher-order structure of the polymer such as the helices of sacran chains reported previously [12,14]. The

above-mentioned unusual WAXD arcs associated with water in hydrogels are likely the result of the large amount of bound water arranged around sacran chains as shown in right picture of Figure 1d. However, the remaining free water might obscure the diffraction arcs of bound water and decrease the apparent degree of orientation.

Such anisotropic swelling behaviors of sacran hydrogels were reproducible, and this process was also applicable to prepare the oriented hydrogels of another LC polysaccharide. For example, anisotropic swelling of LC polysaccharide, xanthan gum, was investigated using the corresponding gels formed by the DVS cross-linking and successive drying. Actually xanthan gum solution at the concentration of 0.8 w/v% same with sacran gels was not high enough to cross-link by DVS, presumably because lower molecular weight ($M_w \approx 4.7\text{x}10^6$) or lower reactivity of xanthan gum than sacran. When increasing the concentration of xanthan gum solution to 2.0 w/v%, xanthan gum in the aqueous solution could be cross-linked by DVS at 2.75 mol ratio of DVS to xanthan hydroxyl. Then the 1st -step cross-linked hydrogel was dried on polypropylene substrate to generate additional cross-linkage. As a result of observation of the swelling behavior of the obtained xanthan gum xerogel (Figure 3.10), the xanthan gum hydrogel showed a one-dimensional swelling behavior at α_t/α_w value as 10,000, similarly to sacran anisotropic gels. The finding suggests that the present stepwise cross-linking for LC polysaccharides can be effective on the preparation of one-dimensionally swollen hydrogels.

3.3.4 Fused hydrogels

Moreover during drying process, two pieces of DVS cross-linked LC-polysaccharides could be fused into same piece of xerogel. For simplification, the color of sacran fiber was changed to pink by reacted with tetramethylrhodamine (TRITC).We prepared two types of fused hydrogels, the first was sacran-sacran (Figure 3.11a) and the second was sacran-xanthan gum hydrogels (Figure 3.11b). The two pieces of DVS cross-linked hydrogels were put on substrate and the surface of two hydrogels were stick together. After completely dried the homogenous xerogels were obtained. However, the swelling ratio of first-step DVS cross-linked hydrogels were required to make the fused hydrogel. If the swelling ratio of hydrogels were too much different, after re-swelling the hydrogels were cracked. This phenomenon indicated that the additional cross-linking of DVS not take place only inside hydrogel but also happen on the surface of hydrogel. Thus, the two-step cross-linking process was useful to prepare an anisotropic hybrid hydrogels. We hope that this hydrogels might be use as multi-functions hydrogel for physical or biological materials in the future.

Figure 3.10 Xanthan gum hydrogels prepared by two-step DVS cross-linking.

a

1st-stepDVS cross-linked sacran hydrogels

Arranged the surface of hydrogels adhere to each other

Re-swelling of fused sacran-sacran hydrogels

Fused sacran-sacran xerogels

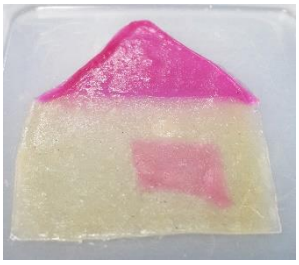

Fused sacran-sacran hydrogels like a home shape

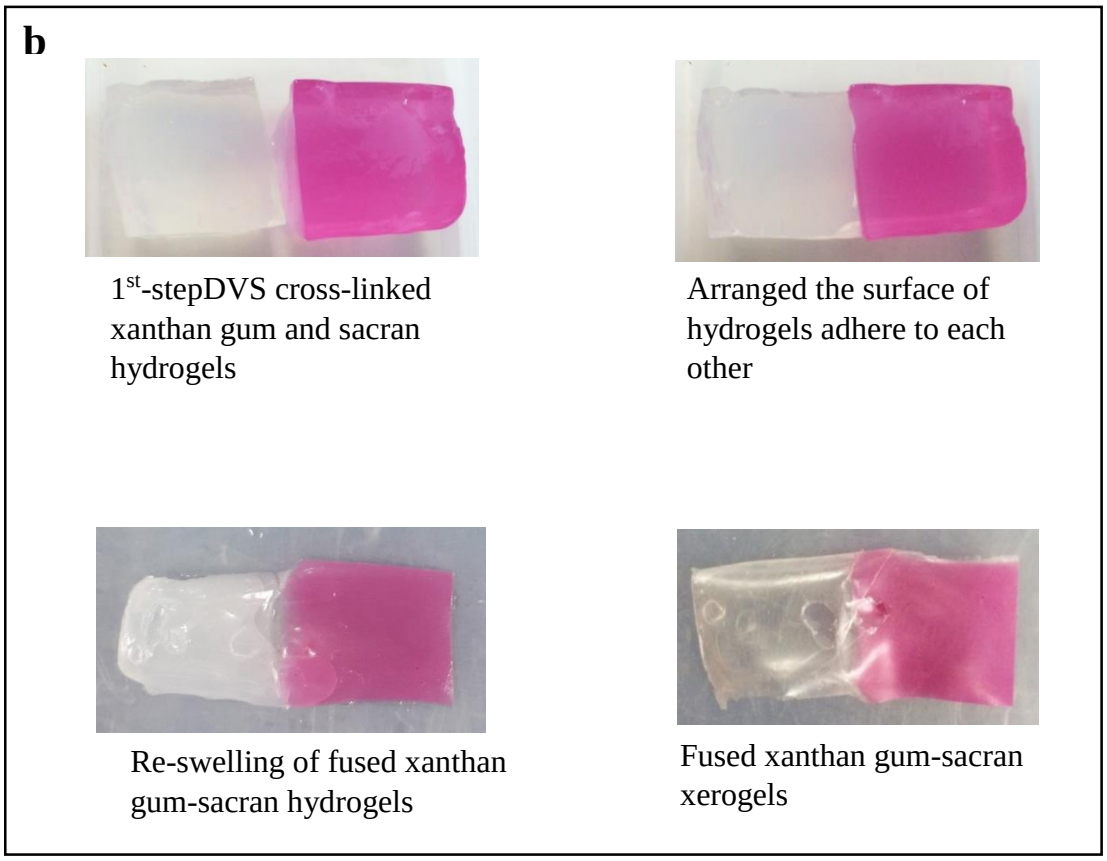

Figure 3.11 Representative fused DVS cross-linked LC hydrogels. (a) sacran-sacran hydrogels with no-color and pink color sacran. (b) sacran-xanthan gum hydrogels, no color xanthan gum and pink color sacran.

3.4 Conclusion

Sacran hydrogels with one-directional swelling were prepared by two-step chemical cross-linking of rigid-rod sacran chains in the LC state. Sacran chains at low concentration were partially cross-linked by DVS; some DVS also reacted with sacran hydroxyls through only one vinyl group without cross-linking. The hydrogels were slowly dried and attached to a substrate to create a film during which time the remaining DVS pendants cross-linked the pre-constructed networks in an oriented LC state. The resulting xerogels showed nematic orientation confirmed by X-ray diffraction imaging, SEM, and polarized microscopy. The xerogels also exhibited one-dimensional swelling just by immersion into water; the linear swelling ratio in the thickness direction of the hydrogel was 10,000-40,000 times higher than that in the width direction. This method for oriented hydrogel formation is simple enough to be applicable to many other LC polymers; drying the hydrogels on the substrate to which they are attached and re-swelling. Moreover this method can use to prepare multi-function hydrogels by additional cross-linking around surface. The liquid crystallinity and secondary cross-linkage are important factors in controlling the anisotropy. Because of the strong anisotropy, it was found that the water molecules bound to the oriented polymer chains were themselves oriented.

References

[1] Ahn, A. C.; Kaptchuk, T. J. *J. Anat.* **2011**, *219*, 515-524.

[2] Tamm, E. R.; Lütjen-Drecoll, E. *Microsc. Res. Tech.* **1996,** *33*, 390-439.

[3] Nishikawa, E.; Yamamoto, J.; Yokoyama, H.; Finkelmann, H. *Macromol. Rapid Commun.* **2004,** *25*, 611-617.

[4] Aßfalg, N.; Finkelmann, H. *Macromol. Chem. Phys.* **2001,** *202*, 794-800.

[5] Yokoyama, F.; Achife, E. C.; Momoda, J.; Shimamura, K.; Monobe, K. *Colloid. Polym. Sci.* **1990,** *268*, 552-558.

[6] Haque, M. A.; Kamita, G.; Kurokawa, T.; Tsujii, K.; Gong, J. P. *Adv. Mater.* **2010,** *22*, 5110-5114.

[7] Yang, W.; Furukawa, H.; Gong, J. P. *Adv. Mater.* **2008**, *20*, 4499-4503.

[8] Kaneko, T.; Yamaoka, K.; Gong, J.P.; Osada, Y. *Macromolecules* **2001**, *34*, 1470-1476.

[9] Shigekura, Y.; Chen, Y.M.; Furukawa, H.; Kaneko, T.; Kaneko, D.; Osada, Y.; Gong, J.P. *Adv. Mater.* **2005,** *17*, 2695-2699.

[10] Kaneko, T.; Shimokuri, T.; Tanaka, S.; Akashi, M. *Polym. J.* **2007,** *39*, 737-744.

[11] Osorio-Madrazo, A.; Eder, M.; Rueggeberg, M.; Pandey, J. K.; Harrington, M. J.; Nishiyama, Y.; Putaux, J.-L.; Rochas, C.; Burgert, I. *Biomacromolecules* **2012,** *13*, 850-856.

[12] Mitsumata, T.; Miura, T.; Takahashi, N.; Kawai, M.; Okajima, M.; Kaneko, T. *Phys. Rev. E* **2013**, *87*, 042607-9.

[13] Okajima, M.K.; Miyazato, S.; Kaneko, T. *Langmuir* **2009,** *25*, 8526-8531.

[14] Okajima, M. K.; Kaneko, D.; Mitsumata, T.; Kaneko, T.; Watanabe, J. *Macromolecules* **2009,** *42*, 3057-3062.

[15] Okajima, M. K.; Mishima, R.; Amornwachirabodee, K.; Mitsumata, T.; Okeyoshi, K.; Kaneko T. *RSC adv*. **2015**, *5*, 86723-86729.

[16] Ramamurthi, A.; Vesely, I. *Biomaterials* **2005,** *26*, 999-1010.

[17] Loizou, E.; Porcar, L.; Schexnailder, P.; Schmidt, G.; Butler, P. *Macromolecules* **2009,** *43*, 1041-1049.

[18] J. K. Alexander, B. Fuss, R. J. Colello, *Neuron Glia Neuron Glia Biol.* **2006,** *2*, 93.

[19] Yoshida, H.; Hatakeyama, T.; Hatakeyama, H. *Polymer* **1990,** *31*, 693-698.

[20] Qu, X.; Wirsén, A.; Albertsson, A. C. *Polymer* **2000,** *41*, 4589-4598.

Chapter 4

Evaluation of anisotropy of sacran hydrogels properties

4.1 Introduction

4.1.1 Stimuli-responsive hydrogels

There are numerous applications of these hydrogels, in particular in the medical and pharmaceutical sectors. Hydrogels resemble natural living tissue more than any other class of synthetic biomaterials. This is due to their high water contents and soft consistency which is similar to natural tissue. Furthermore, the high water content of the materials contributes to their biocompatibility. The discovery of hydrogels as a class of materials designed for medical use started from contact lens. Poly(2-hydroxyethyl methacrylate) commonly known as P-HEMA was the first synthetic hydrogel to be synthesized in 1936 by DuPont scientists, but it was not until 1960, that Wichterle and Lim [1] established the importance of P-HEMA hydrogels as excellent candidates for contact lens applications. This innovation led to the contact lens industry and to the modern field of biomedical hydrogels. The commercial success of soft contact lenses generated enormous interest in hydrogels, and eventually led to the development of "smart hydrogels", that can change their properties upon application of an external stimuli. Many physical and chemical stimuli have been applied to induce various responses of the smart hydrogel systems. The physical stimuli include temperature, electric fields, solvent composition, light, pressure, sound and magnetic fields, whereas the chemical

or biochemical stimuli include pH, ions and specific molecular recognition events (Figure 4.1) [2]. Smart hydrogels have been used in diverse applications, such as in making actuators [3-5] and valves [6], in the immobilization of enzymes and cells [7-8], in concentrating dilute solutions in bio separation [9-10].

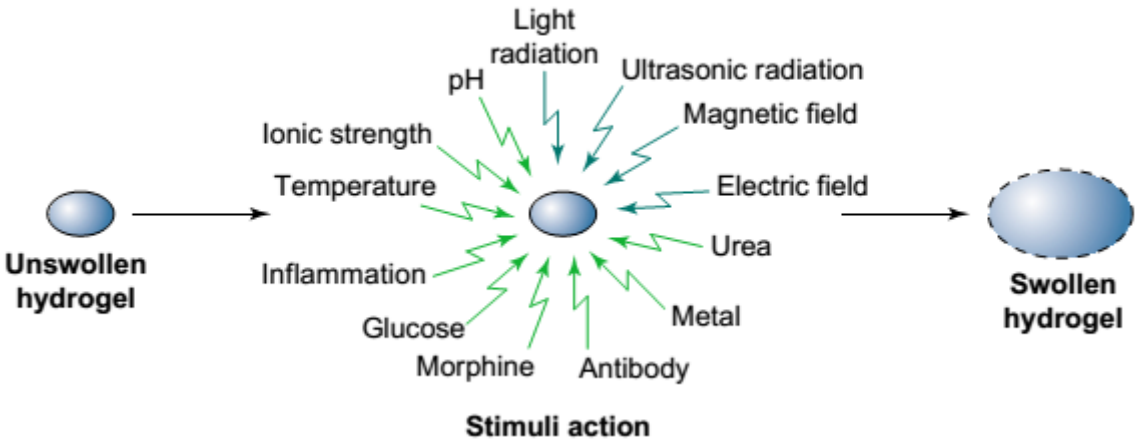

Figure 4.1 Stimuli responsive swelling of hydrogels [2].

4.1.2 Hydrogels for tissue engineering

Tissue engineering is aimed at the realization of in vitro engineered tissues/organs or thein vivo restoration of tissues/organs by a suitable three-dimensional matrix, called scaffold, which can properly interact with cell components. In any organ and tissue, the extracellular matrix (ECM) regulates the communication between the adjacent cells and the external environment; therefore, the organization and composition of ECM impact organ development and function [11]. Thus, a promising approach in tissue engineering strategies is the design of scaffolds with biomimetic properties inspired by natural ECM, which can suitably drive cell response. The ECM is generally composed of structural proteins (such as collagen and elastin),

cell-adhesive proteins (such as collagen, fibronectin, laminin and tenascin), glycosaminoglycans (such as hyaluronic acid, dermatan sulfate, keratan sulfate, chondroitin sulfate and heparin sulfate), proteoglycans and interstitial fluid. The development of tissue engineering has progressed significantly from the original concepts. The current paradigm involves constructing scaffolds from biodegradable polymers with seeded cells that proliferate and deposit extracellular matrix (ECM) molecules, such as collagen and fibronectin, eventually regaining their native structure and tissue morphology as the scaffold degrades. Some success was achieved for cell-sparse tissues (using large amounts of ECM and relatively few cells) such as heart valves [12], bone [13], and cartilage [14].

In this chapter, we tried to clarify stimuli responsive of anisotropic swelling sacran hydrogels with pH, ionic strength, solvent and metal ion. According to the stimuli responsive hydrogels can use as biomaterials, the cytocompatibility of sacran hydrogels were also investigated.

4.2 Experimental

4.2.1 Materials

Neodymium(III) chloride hexahydrate ($NdCl_3.6H_2O$), tetrasodium ethylene diamine tetra acetic (EDTA), phosphoric acid, 2-hydroxethylamine, sodium dihydrogenphosphate and disodium hydrogen phosphate were purchased from KANTO chemical. Sodium hydroxide hydrochloric acid (Kanto Chemical co. ltd) employed for pH adjustment were used as received.

4.2.2 Stimuli-responsive of sacran hydrogels

Swelling behavior in different ionic strength solutions

A series of NaCl solutions with different concentrations were prepared to investigate the ionic strength sensitivity of fully swollen hydrogels. Sacran xerogels were immerged in mill-Q water to equilibrium swelling. Then the hydrogel samples were put in NaCl solutions for equilibrium swelling at 25 °C for the time required to attain equilibrium (24 h). Then, the swelling ratio (q) and anisotropic swelling (α_t/α_w) were investigated.

Swelling behavior in different pH solutions

To study the gel swelling at different pH-values, sacran xerogels were immerged in mill-Q water to equilibrium swelling. Then the hydrogel samples were put in buffer solutions of the desired pH which maintained ionic strength using sodium chloride (1.54). The hydrogel samples remain in the solutions at 25 °C for the time required to attain equilibrium (24 h). After that, the swelling ratio (q) and anisotropic swelling (α_t/α_w) were measured.

Swelling behavior in water/ethanol systems

Sacran xerogels were immerged in mill-Q water to equilibrium swelling. Then hydrogels were put in the different percentages of ethanol in water at 25 °C for 24 h and swelling ratio (q) and anisotropic swelling (α_t/α_w) were measured.

Swelling behavior in Nd^{3+}- EDTA system

The equilibrium swelling sacran hydrogels were immersed in 0.01 M of Neodymium(III) Chloride Hexahydrate ($NdCl_3.6H_2O$) solution at 25 ^oC for 3 h. Then, the hydrogels were changed 0.5 M of ethylene diamine tetra acetic (EDTA) solution at 25 ^oC for 3 h. The swelling ratio (q) and anisotropic swelling (α_t/α_w) were investigated in both solvents.

4.2.3 In vitro cytocompatibility of sacran hydrogels

A mouse fibroblast-like cell line (L929) was selected for all the biological assays in order to evaluate the cell adhesion on sacran hydrogels. The L929 fibroblast cell line was obtained from the American Type culture collection (Manassa, VA, USA). The cells were cultured in Dulbecco's Modified Eagle's Medium (DMEM, Sigma-Aldrich, USA), supplemented with 10% of heating inactivated fetal bovine serum (FBS, Biochrom AG, Germany) incubated at 37 °C in humidified atmosphere with 5% of CO_2. Prior to culturing, all sacran xerogels were sterilized with 70 % ethanol and dried. Then xerogels were swelled in PBS and seeded with 100 µL of a cell suspension (2.5×10^4 cells.mL^{-1}) and cultured for 1, 2 and 3 days at 37 °C in 24-well multiplates. Well plate was used as controls. The number of

cells adhering to the surface of hydrogels were investigated by Cell Counting Kit-8 (CCK-8) colorimetric assay, (Dojindo Molecular Technologies, Inc., Rockville, US).

4.3 Results and discussion

4.3.1 Stimuli-responsive of sacran hydrogels

Swelling behavior in different ionic strength solutions

In the study on ionic strength sensitivity, the equilibrium swelling of sacran hydrogels in Milli-Q water were exposed to NaCl solutions. The water swelling ratio of the sacran hydrogels decreased dramatically as the concentration of NaCl solutions increased to 0.2 M. Then gradually changes with further increasing of concentration to 2.0 M (Figure 4.2a). The reduction of the water swelling ratio with ionic strength is very common for carboxy-containing hydrogels. In milli-Q water, sacran molecular chains extend because of electrostatic charge repulsion of $–COO^-$ groups, which results in an increase of osmotic pressure in the hydrogel networks [15] which in turn causes the swelling of the sacran hydrogels. The chain expansion is limited as negative electrostatic repulsion is depressed by the shielding of Na^+ counter ions. However, the sacran hydrogels shrank in one-dimension by their anisotropic swelling character. The anisotropic swelling ratio were decreased due to decreasing of swelling ratio as shown in Figure 4.2b.

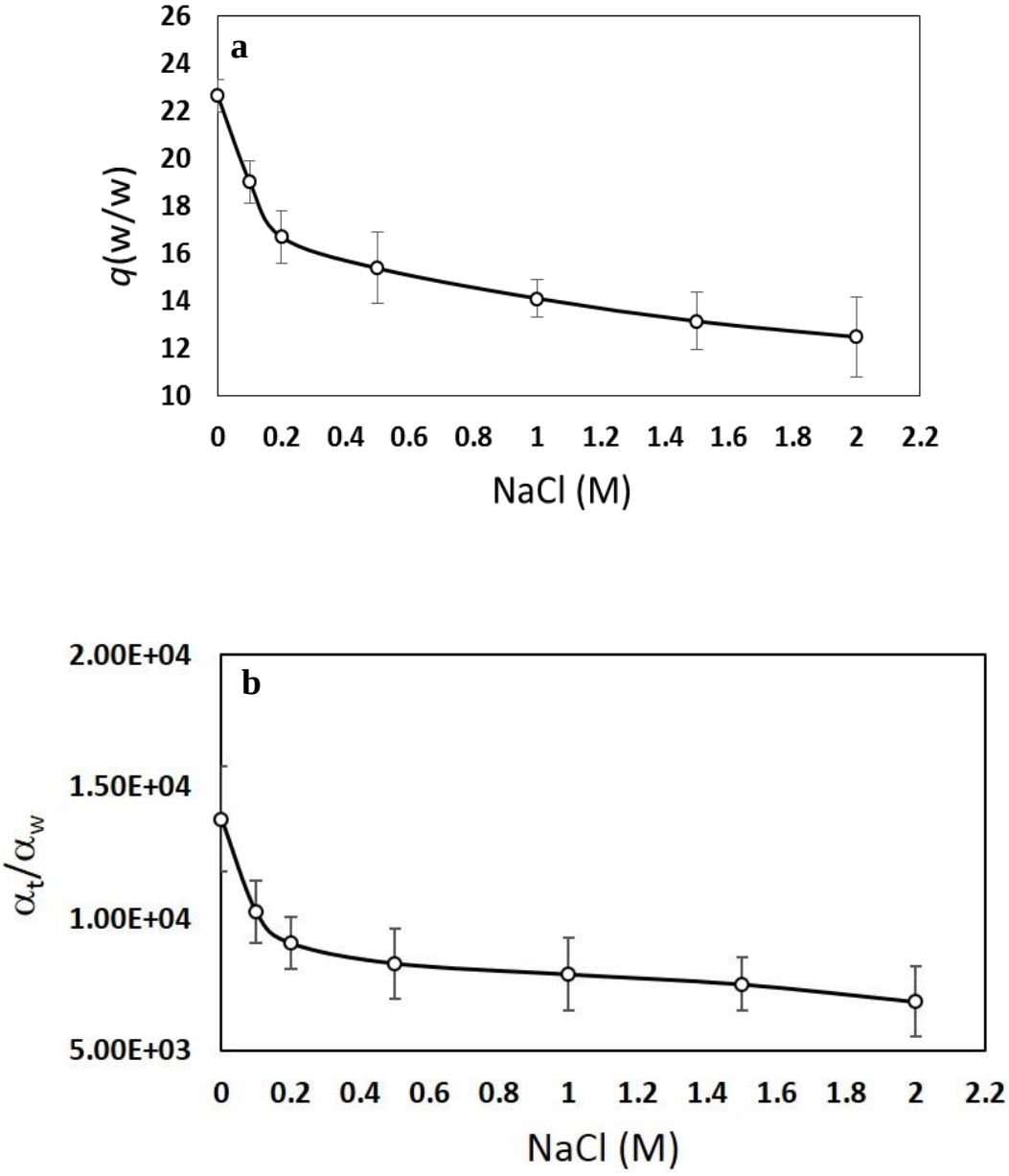

Figure 4.2 Swelling ratio of sacran hydrogels in NaCl solution with varied concentration.

(a) swelling ratio and (b) anisotropic swelling ratio.

Swelling behavior in different pH solutions

The pH sensitive characteristic of hydrogels were studied by swelling sacran hydrogels under buffer in different pH (I = 1.54). When the pH was lowered to 1.9, the hydrogels shrunk because of the deprotonation of carboxyl groups, which resulted in weaker charge repulsion and weaker osmosis. However, swelling ratio significantly increased when pH was higher than 10.0 (Figure 4.3a). From results shown that sacran hydrogels expanded in one-dimensional, the anisotropic swelling ratio were also calculated (Figure 4.3b). This results indicated that not only carboxyl groups can induced the swelling behavior, hydroxyls groups also showed high effect on swelling ratio of sacran hydrogels. When pH was higher than pKa of hydroxyl groups of sugar unit (≈12), the hydrogels exhibited high swelling with enlarged volume due to the osmosis and charge repulsion from deprotonation of hydroxyl groups. The swelling ratio at pH > 10 were too high due to large amount of hydroxyl groups in sacran chains. However, the pH responsive in this anisotropic swelling sacran hydrogels were irreversible. To explain this phenomenon, we presumed that the sacran hydrogels had layer structures. According to the slowly drying process, a layer by layer staking of sacran films were generated as xerogels. At high pH, the distance between each layers were strongly expanded and some of layer were broken. The broken of layer structure were observed with dehydration hydrogels (pH13) by ethanol (Figure 4.4). Thus, the protonation of hydroxyl groups when decreasing pH were not induced hydrogels shrank.

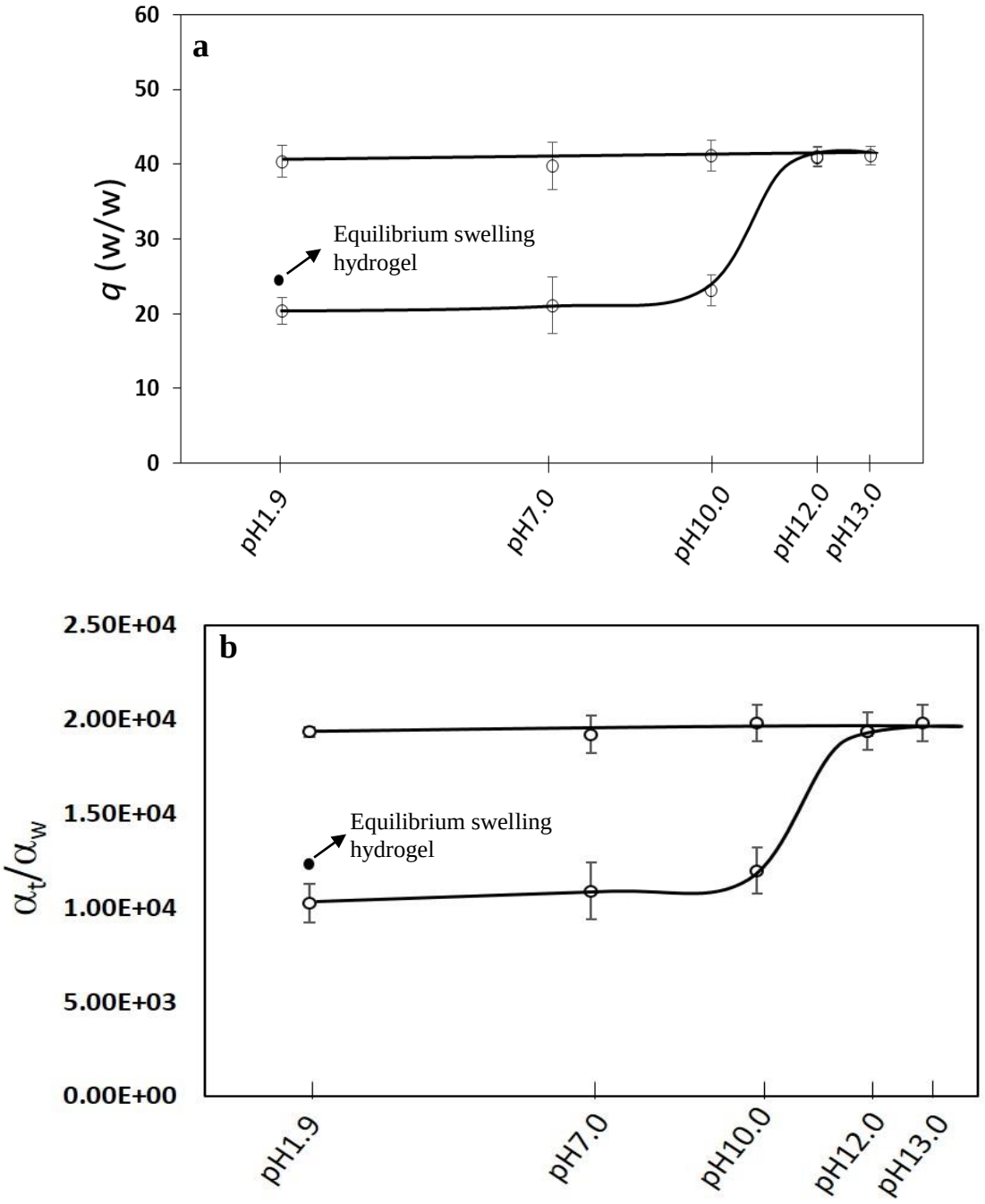

Figure 4.3 Swelling ratio of sacran hydrogels in pH buffer solution at pH in range of 1.9 to 13 (I=1.54). (a) swelling ratio and (b) anisotropic swelling ratio.

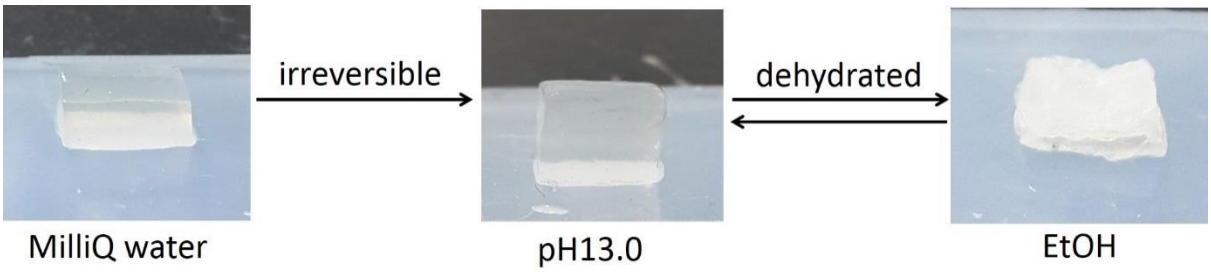

Figure 4.4 Sacran hydrogel showed high swelling ratio at pH 13 and the broken structure was clearly observed by dehydration in EtOH.

Swelling behavior in water/ethanol systems

The phenomenon of Volume Phase Transition (VPT) in both of xerogels and equilibrium swelling hydrogels were observed with ethanol/water mixed solvent at 25 ^{o}C. Both of sacran xerogels and hydrogels shown decreasing of swelling ratio at ethanol concentration of 70% (Figure 4.5). This behavior is due to attractive interactions between the polymer chain and the solvent molecules (hydrogen bonding) that dominate over the attraction between the polymer chains (hydrophobic interaction). In the case of a mixed solvent, the solvent–solvent interaction dominates over the solvent–polymer interaction, thereby increasing the affinity among polymer segments. This would induced the collapse of the polymer network. Therefore, the hydrogels were in collapsed state in the intermediate range of mixtures [16].

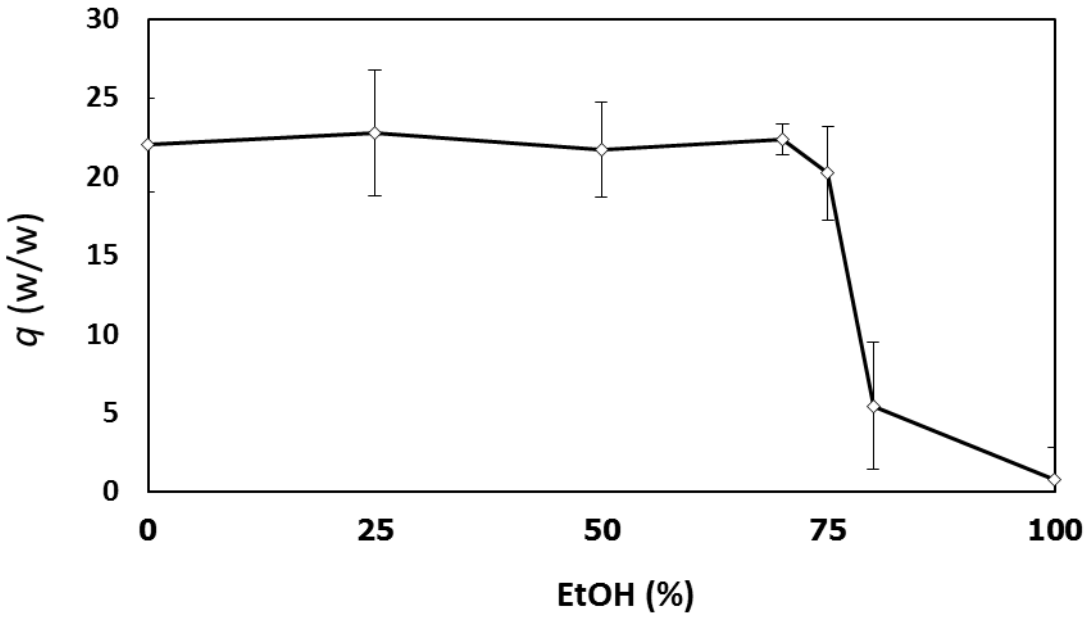

Figure 4.5 Swelling ratio of sacran xerogels and equilibrium swelling hydrogels in ethanol/water mixture.

Swelling behavior in Nd^{3+}- EDTA system

As previous research, sacran can easily cross-linked by trivalent metal ion. The swelling behavior in trivalent metal ion were observed by immersed equilibrium swelling sacran hydrogels in 0.01M Nd^{3+} solution. The results shown the volume change of the hydrogels in one-direction (Figure 4.6). This phenomenon indicated that hydrogels were additional cross-linked by Nd^{3+}. However, when Nd^{3+} sacran hydrogels were soak into EDTA solution for extracted metal ion, the hydrogels expanded to same condition as spring-like hydrogels. From the results, more strong hydrogels can produced by this reversible methods with remain anisotropic behavior.

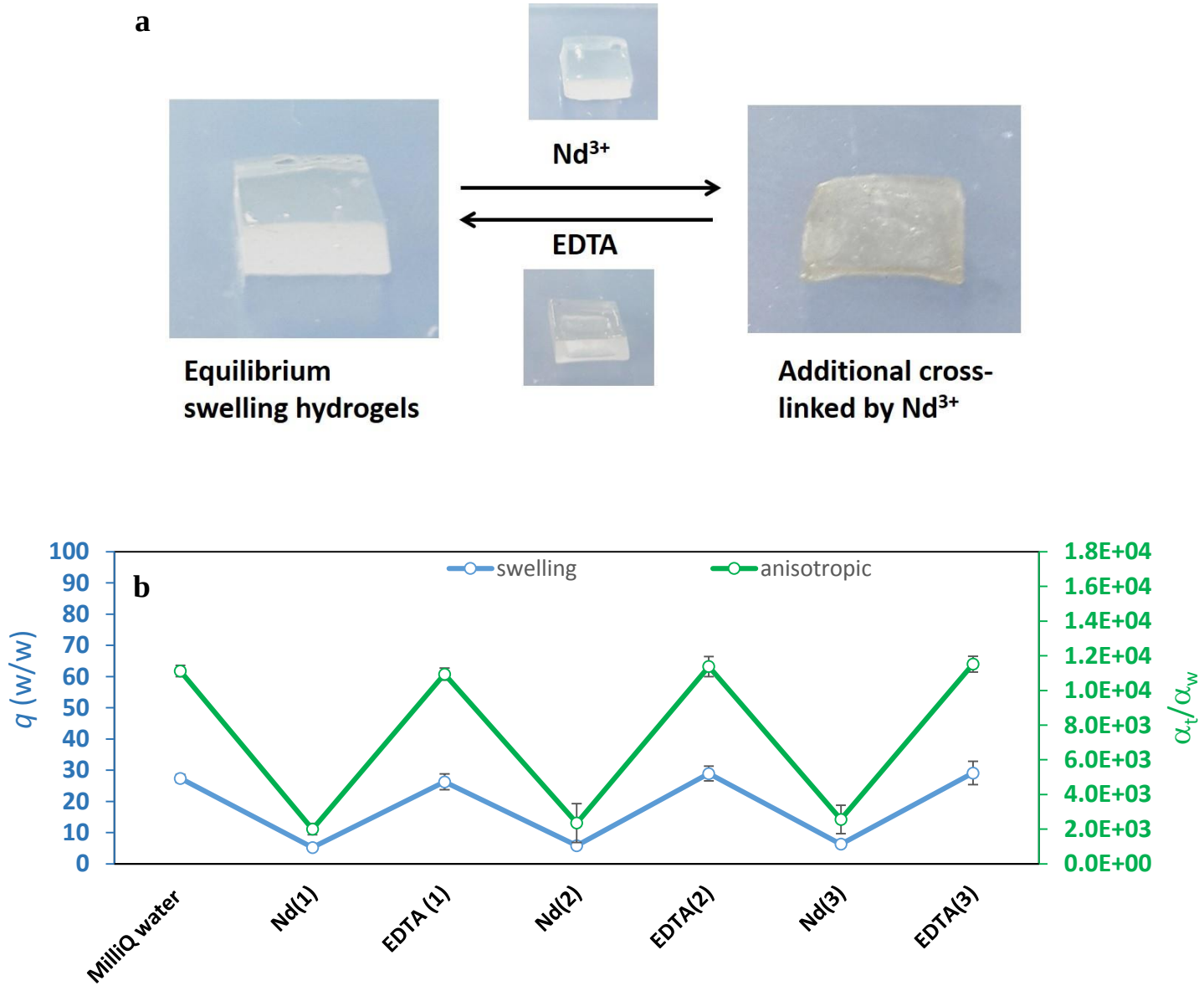

Figure 4.6 Swelling behavior of sacran hydrogels in Nd^{3+} and EDTA solutions. (a) reversible swelling and de-swelling behavior, (b) swelling ratio and anisotropic swelling ratio.

4.3.2 In vitro cytocompatibility of sacran hydrogels

The anisotropic sacran hydrogels with molecular orientation of sacran fiber were used in cytocompatibity test with L929 fibroblast cells. The adhesion of L929 cells were investigated in both of orientation (XZ) side and non-orientation (XY) side. As expected, the results shown L929 cells adhered and proliferation on sacran hydrogels without modified surface by cells adhesive protein. To describe this phenomenon, back to the origin of sacran, this polysaccharide was extracted from extracellular matrix of cyanobacteria and their structure was consisted of uronic acid like glycosaminoglycans (GAGs). Then, we tried to compare the number of cell between unmodified surface and collagen modified surface of sacran hydrogels. The sterilized sacran xerogels was immersed in 0.6 mg.ml^{-1} collagen solution at 4 ^{o}C for 24 h and 3 times washed with PBS solution. After that, collagen modified surface sacran hydrogels were incubated with L929 cells. The number of L929 cells slightly increased with the presented of collagen. The cells density were calculate and shown in Figure 4.7.

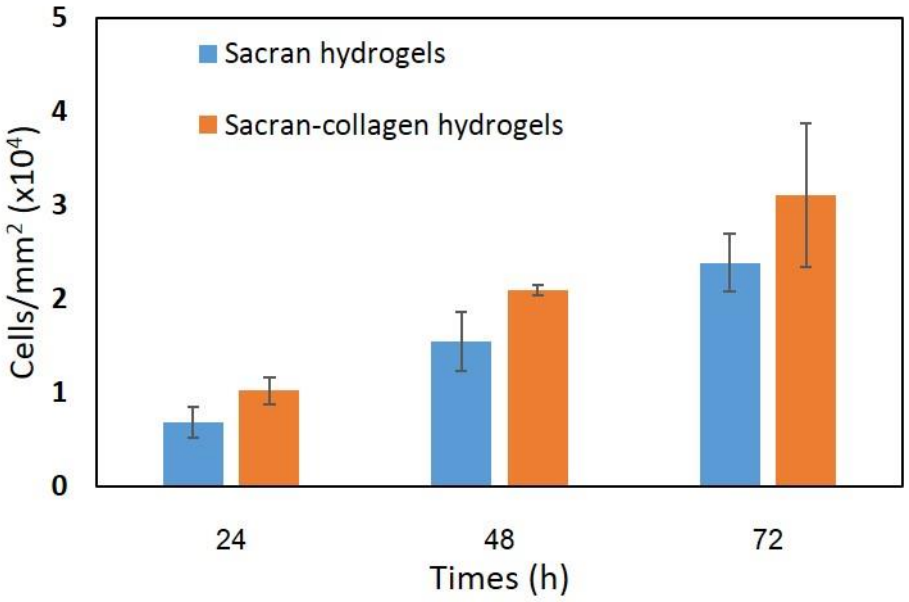

Figure 4.7 L929 Cells density on sacran and sacran-collagen hydrogels at 24, 48 and 72 h.

Figure. 4.8 shows the adhesion of L929 cells on the sacran hydrogels after 48 h incubation. Adherent cells were stained with Calcein-AM for visualization. In XY-side the cells were random alignment but some alignment was found in XZ-side. We suspected that L929 cells recognized and aligned at obviously oriented area such as the border of layer structures. Then, sacran hydrogels at equilibrium swelling state were freeze-dried to induce clearly layer structure. After that, freeze-dried hydrogels were used to culture with L929 cells. The cells alignment were observed and shown in Figure 4.9. The alignment of L929 cells were clearly observed after freeze dried because the signal of orientation were enhanced by layer structure.

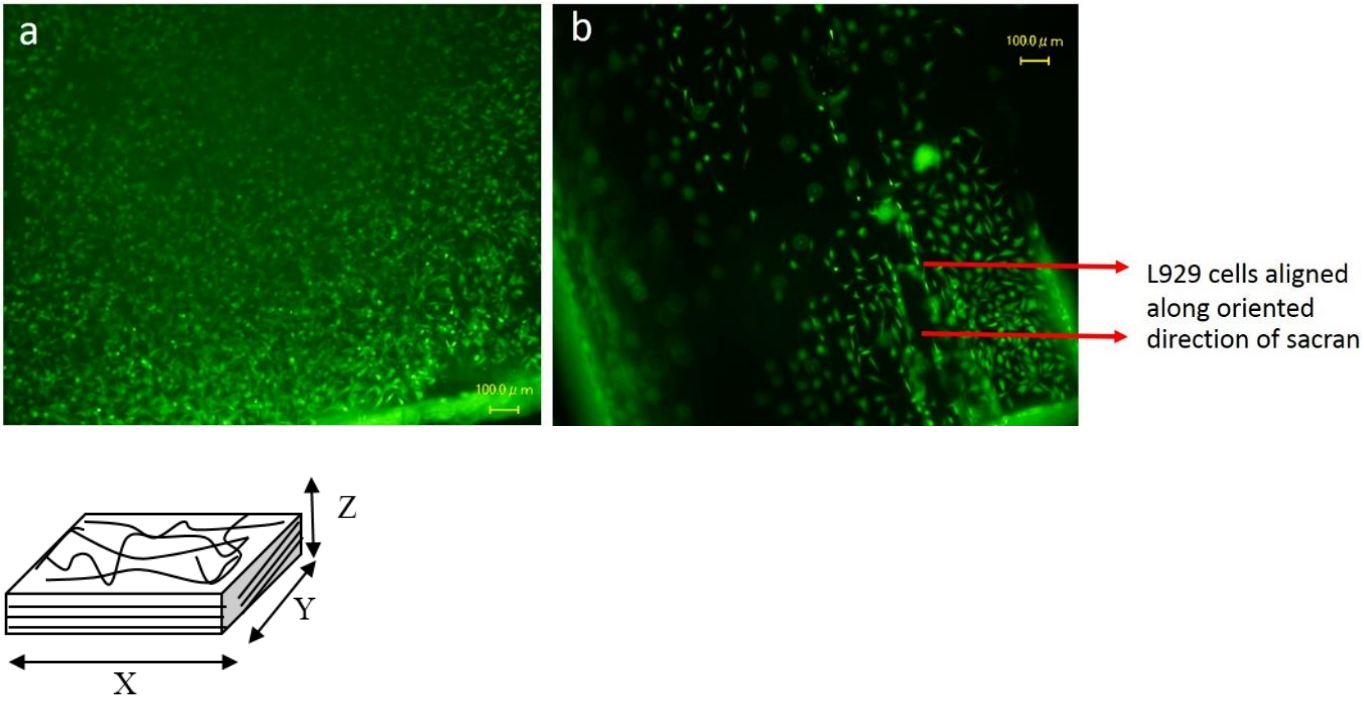

Figure 4.8 L929 cells adhered to sacran hydrogels, random alignment on non-oriented (XY) side (a) and some alignment on oriented (XZ) side (b).

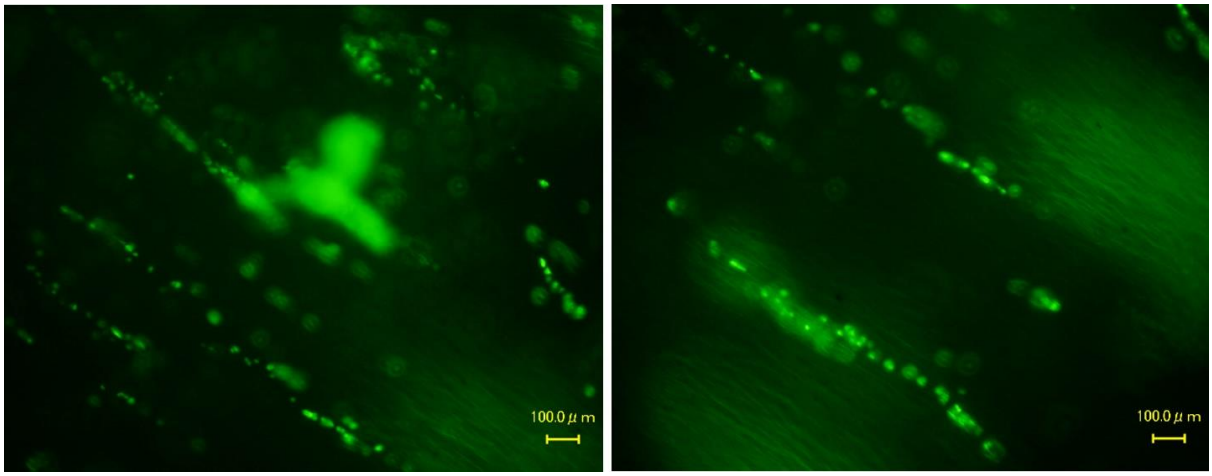

Figure 4.9 L929 alignment on oriented sacran hydrogels after freeze dried.

4.4 Conclusion

Sacran hydrogels with molecular oriented structure showed swelling behavior response to ionic strength, pH, solvent and metal ion. These characteristic of sacran hydrogels lead to development of biomaterials, we will be able to use high safely in biomedical applications owing to good cells adhesion and inducing cells alignment.

References

[1] Wichterle, O.; Lim, D., *Nature* **1960,** *185* (4706), 117-118.

[2] Gupta, P.; Vermani, K.; Garg, S., *Drug Discov Today* **2002,** *7* (10), 569-579.

[3] Asoh, T.-a.; Matsusaki, M.; Kaneko, T.; Akashi, M., *Adv. Mater.* **2008,** *20* (11), 2080-2083.

[4] Maeda, S.; Hara, Y.; Sakai, T.; Yoshida, R.; Hashimoto, S., *Adv. Mater.* **2007,** *19* (21), 3480-3484.

[5] Techawanitchai, P.; Ebara, M.; Idota, N.; Asoh, T.-A.; Kikuchi, A.; Aoyagi, T., *Soft Matter* **2012,** *8* (10), 2844-2851.

[6] Beebe, D. J.; Moore, J. S.; Bauer, J. M.; Yu, Q.; Liu, R. H.; Devadoss, C.; Jo, B.-H., *Nature* **2000,** *404* (6778), 588-590.

[7] Ebara, M.; Yamato, M.; Aoyagi, T.; Kikuchi, A.; Sakai, K.; Okano, T., A., *Adv. Mater.* **2008,** *20* (16), 3034-3038.

[8] Kim, Y.-J.; Ebara, M.; Aoyagi, T., *Angew. Chem. Int. Ed.* **2012,** *51* (42), 10537-10541.

[9] Feil, H.; Bae, Y. H.; Feijen, J.; Kim, S. W., *J. Membr. Sci.* **1991,** *64* (3), 283-294.

[10] Freitas, R. F. S.; Cussler, E. L., *Chem. Eng. Sci.* **1987,** *42* (1), 97-103.

[11] Hynes, R. O., *Science* **2009,** *326* (5957), 1216-1219.

[12] Shinoka, T.; Breuer, C. K.; Tanel, R. E.; Zund, G.; Miura, T.; Ma, P. X.; Langer, R.; Vacanti, J. P.; Mayer, J. E., Jr., *Ann Thorac Surg*. **1995,** *60* (6 Suppl), S513-6.

[13] Puelacher, W. C.; Wisser, J.; Vacanti, C. A.; Ferraro, N. F.; Jaramillo, D.; Vacanti, J. P., *J Oral Maxillofac Surg* **1994,** *52* (11), 1172-1177.

[14] Vacanti, C. A.; Langer, R.; Schloo, B.; Vacanti, J. P., *Plast Reconstr Surg* **1991,** *88* (5), 753-9.

[15] Lei, L.; You-Lo, H., *Nanotechnology* **2005,** *16* (12), 2852.

[16] Katayama, S.; Hirokawa, Y.; Tanaka, T., *Macromolecules* **1984**, *17*, 2641–2643

Chapter 5

General conclusion

The research in this thesis focused on preparation of chemical cross-linked sacran hydrogels. The cross-linking conditions and method to prepare anisotropic swelling sacran hydrogels were studied. The important and interesting results throughout this study were summarized as follows.

In Chapter 2, the cross-linking condition of sacran to prepare hydrogel were investigated. There were many factors to control cross-linking reaction such as percentages of active functional groups, concentration of polymer and amount of crosslinker. For sacran, hydroxyl groups showed efficiently cross-linked presumably due to larger amount than other functional groups, by divinyl sulfone (DVS) forming an ether bond obtained strong and smooth hydrogels. The increasing of sacran concentration and amount of DVS showed higher mechanical properties. From the number of DVS incorporate with sacran chain and the calculated M_c values make we considered that the DVS molecules was not completely cross-linked but reacted with sacran hydroxyls at only one vinyl group. Thus, the next step of cross-linking was studied in next chapter.

In Chapter 3, According to chapter2, sacran chains were partially cross-linked by DVS and remained some unreacted vinyl groups. The remained DVS cross-link the pre-constructed networks during drying process to obtain molecular oriented xerogels. This xerogels show super-anisotropic swelling behavior, where the values of α_t/α_w ranged between 10,000 and 40,000 are prepared by two-step chemical cross-linking. From this results, we present a new

method for oriented hydrogel formation which is simple enough to be applicable to many other LC polymers; drying the hydrogels on the substrate to which they are attached and re-swelling (Figure 5.1). The liquid crystallinity and secondary cross-linkage are important factors in controlling the anisotropy.

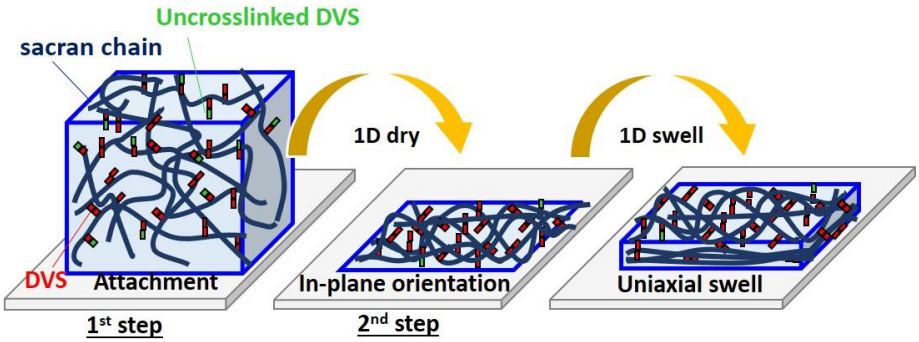

Figure 5.1 Two-step chemical cross-linking to prepare oriented hydrogel from LC-polymers.

In Chapter 4, oriented sacran hydrogel showed swelling behavior response to many different environments such as ionic strength, pH, solvent, metal ion. Moreover, sacran hydrogels showed cytocompatibility with L929 cells. The alignment of cells also observed on surface of oriented sacran hydrogels.

Moreover, although the oriented sacran hydrogels showed good properties such as high anisotropic swelling ratio, high mechanical properties, response to stimuli environments and cytocompatibility, this hydrogel requires further studies and develops for using in daily life.

ACHIEVEMENTS

Publications:

1. Kittima Amornwachirabodee, Maiko K. Okajima, Tatsuo Kaneko.
   Uniaxial Swelling in LC Hydrogels Formed by Two-Step Cross-Linking.
   Macromolecules **2015**, *48* (23), 8615-8621.

Other Publications:

1. Kittima Amornwachirabodee, Khajeelak Chiablaem, Sumrit Wacharasindhu, Kriengsak Lirdprapamongkol, Jisnuson Svasti, Viwat Vchirawongkwin, Supason Wanichwecharungruang.
   Paclitaxel delivery using carrier made from curcumin derivative: Synergism between carrier and the loaded drug for effective cancer treatment.
   J. Pharm. Sci. **2012,** *101* (10), 3779-3786.

2. Maiko K. Okajima, Ryosuke Mishima, Kittima Amornwachirabodee, Tetsu Mitsumata, Tatsuo Kaneko.
   Anisotropic swelling in hydrogels formed by cooperatively aligned megamolecules.
   RSC Advances **2015**, *5* (105), 86723-86729.

3. Sunatda Arayachukiat, Jiraporn Seemork, Porntip Pan-In, Kittima Amornwachirabodee, Naunpun Sangphech, Titiporn Sansureerungsikul, Kamonluck Sathornsantikul, Chotima Vilaivan, Kazuki Shigyou, Prompong Pienoinijtham, Tirayut Vilaivan, Tanpat Palaga, Wijit Banlunara, Tsutomu Hamada, Supason Wanichwecharungruang.

   Bringing Macromolecules into Cells and Evading Endosomes by Oxidized Carbon Nanoparticles.

   Nano Letters **2015,** *15* (5), 3370-3376.

Presentations:

1. Kittima Amornwachirabodee, Maiko K. Okajima, Tatsuo Kaneko.

   Syntheses of chemically cross-linked hydrogels of cyanobacterial polysaccharides.

   The CSJ academic conference (Kinki-branch of Japanese chemical society), Oct. 12, 2013 Japan Advance Institute of Science and Technology (JAIST), Ishikawa, Japan.

2. Kittima Amornwachirabodee, Maiko K. Okajima, Tatsuo Kaneko.

   Syntheses of anisotropy hydrogels of cyanobacterial polysaccharides.

   International Symposium for Green-Innovation Polymers (GRIP2014) & The 13th Symposium of the Research Center for Highly Environmental and Recyclable Polymers, Mar. 6-7, 2014, Kanazawa, Japan.

3. Kittima Amornwachirabodee, Maiko K. Okajima, Tatsuo Kaneko.

   Preparation of anisotropic chemical hydrogels of cyanobacterial polysaccharides and its stimuli-responsibility.

   The IUPAC World Polymer Congress, 'Macro (2014)' Chiang Mai, Thailand.

4. Kittima Amornwachirabodee, Maiko K. Okajima, Tatsuo Kaneko.

   One-dimensional swelling hydrogels from supergiant LC polysaccharides.

   64th Symposium on Macromolecules, Sep. 15-17, 2015, Kawauchi Campus, Tohoku University, Japan.

5. Kittima Amornwachirabodee, Maiko K. Okajima, Tatsuo Kaneko.

   Anisotropic swelling of in-plane oriented hydrogels from supergiant LC polysaccharides.

   7th Annual and 1st International Symposium on Sacran, Nov. 21, 2015, Kyushu Institute of Technology, Kitakyushu, Japan.

6. Kittima Amornwachirabodee, Maiko K. Okajima, Tatsuo Kaneko.

   One-dimensional swelling of in-plane oriented hydrogels of supergiant LC polysaccharides.

   The 2015 International Chemical Congress of Pacific Basin Societies (PAC CHEM™), Dec. 15-20, 2015, Honolulu, Hawaii, USA.

7. Kittima Amornwachirabodee, Maiko K. Okajima, Tatsuo Kaneko.

   Super-anisotropic swelling hydrogels from LC cyanobacterial-polysaccharide.

   27th Polymer Gel Research Symposium, Jan. 18-19, 2016, Tokyo, Japan.

Awards:

1. Syntheses of anisotropy hydrogels of cyanobacterial polysaccharides.

   Poster award on International Symposium for Green-Innovation Polymers (GRIP2014) & The 13th Symposium of the Research Center for Highly Environmental and Recyclable Polymers, Mar. 6-7, 2014, Kanazawa, Japan.
2. JASSO Scholarship for Doctoral Students, April 2013-March 2014.
3. Grant for PhD student, the Royal Golden Jubilee Ph.D. Program, Thailand.

Minor research

Introduction

The use of carriers to improve the water solubility of hydrophobic drugs, slow down their clearance from and degradation in the body, increase their shelf-life and target the drugs to the required sites, have all been well recognized. Various diverse forms of carriers have been proposed and these include conventional liposomes, polymeric micelles or vesicles, self-assembled polymer aggregates and porous inorganic particulates. However, most carriers offer a drug loading of less than 10% (w/w), thus enforcing the administration of a relatively large amount of carrier material that has no therapeutic function into the body. With this rationalization, it would be advantageous if the carrier could possess a therapeutic function on its own (bioactive carrier). The concept of a bioactive carrier has been demonstrated in a few works, including the use of nano-vesicles constructed from pro-anticancer drug molecules to deliver another anti-cancer agent to cancer cells,[1] and the use of an UV absorptive carrier in the form of organic polymeric nanoparticles (NPs) or hybrid organic-inorganic NPs for topical delivery of the bioactive agent while at the same time the carriers act as sunscreening agents to protect both the skin and the loaded drugs from UV radiation.[2,3] Here, we propose a novel bioactive carrier, polyethylene oxide – palmitate modified curcumin (mPEO-CUR-PA), that not only possesses a therapeutic function alone but can also work synergistically with the loaded drug (paclitaxel), thus enabling (i) an effective administration of the drugs into the cells with no extra burden of non-therapeutic carrier materials for the cells, and (ii) an improvement in the treatment derived from the additive or synergistic (as in the case shown here) therapeutic action of the carrier material and enhancement of the loaded drug action. With this arrangement, the synergism of the two drugs can be maximized since the ratio of the two drugs delivered into the same cells at the same time can be more precisely controlled.

It is well accepted that curcumin (CUR), [1,7-bis(4-hydroxy-3-methoxyphenyl)-1, 6-heptadiene-3,5-dione], a pharmaceutically safe yellow pigment isolated from the rhizomes of

the turmeric plant (*Curcuma longa* L.), is an effective anticancer agent that can block NF-κB activation.[4,5] Curcumin can reverse drug resistance in cancer cells by down-regulating the expression levels of P-gp, MRP-1 and ABCG2, which are three of the major ABC drug transporters responsible for the increased drug efflux rate in multidrug resistant cancer cells.[6,7] Moreover, curcumin has been shown to be able to improve the therapeutic outcome of paclitaxel treatment by suppressing the activation of the NF-κB and Akt survival signals induced by paclitaxel.[8,9] Indeed, curcumin has been reported to suppress the paclitaxel-induced expression of NF-κB–regulated gene products and to prevent breast cancer metastasis to the lung in nude mice.[10-12] Thus, the use of a paclitaxel-curcumin combination is a promising way to potentially kill cancer cells more effectively.[13]

However, the use of curcumin is not easy because it not only degrades easily,[14,15] but it also typically has a low bioavailability due to its water insolubility and fast clearance from the circulation.[16,17] Both the chemical derivatization of curcumin and/or the use of delivery systems have been proposed to solve these problems.[18,19]

Since the administration of paclitaxel also requires a suitable drug carrier[20,21] and, as mentioned above, curcumin needs either a suitable chemical modification or delivery technology to obtain an effective therapeutic result, then we synthesized an amphiphillic curcumin derivative and used this obtained derivative to construct a carrier for paclitaxel delivery. Curcumin is nontoxic and is usually is administered at a much higher dose than paclitaxel, and so it is reasonable to make curcumin into carrier which may typically be used at a greater level relative to the amount of the loaded drug (in this case paclitaxel). By incorporating paclitaxel into the curcumin-carrier, the possibility that the two drugs will be delivered into the same cells at the same time is maximized and so the potential of taking full advantage of their synergistic action is attained. To this end we modified the curcumin structure by attaching to it polyethylene oxide (PEO) moieties, so as to give a hydrophilic and stealth

character for good water dispersion with minimal blood clearance, and to palmitate (PA) moieties, to give a hydrophobic character for the formation of a stable micellar core with the ability to hold hydrophobic paclitaxel, and so make the modified curcumin molecules (mPEO-CUR-PA) amphiphillic and capable of self-assembling into water dispersible micellar architectures. The ability to form mPEO-CUR-PA microspheres, to encapsulate paclitaxel at two different doses, and its *in vitro* cytotoxicity against cancer cell lines was evaluated and compared to those for the unmodified curcumin and free paclitaxel. In addition, the cellular uptake of mPEO-CUR-PA microspheres, with or without paclitaxel loading was evaluated and the results were compared to the observed cytotoxicity levels.

Experimental Section

Chemicals. Curcumin (>98%), succinic anhydride were purchased from Acros organics (Geel, Belgium) while poly(ethylene glycol) methyl ether (mPEO, Mn ≈ 750) plamitic anhydride (97%), dicyclohexylcarbodiimide (DCC), 4-(N,N-dimethylamino)pyridine (DMAP) and lipophillic Sephadex LH-20 were purchased from Aldrich (Steinheim, Germany). Silica gel 60 (0.063-0.200 nm) for column chromatography was purchased from Merck KGaA (Darmstadt, Germany). Triethylamine (Carlo Erba reagent, MI, Italy), pyridine (Carlo Erba) and dimethylformamide (RCI Labscan, BKK, Thailand) were dry and triply distilled before use. All other chemicals were reagent grade and were triply distilled before use.

Spectrometric analysis. ^{1}H-NMR spectra were acquired at 400 MHz (Varian Company, USA) while UV-Visible absorption spectra were taken at 200-600 nm using an UV2500 spectrophotometer (Shimadzu Corporation, Kyoto, Japan). Infrared spectra were obtained on germanium reflection element using a Nicolet 6700 ATR-FTIR spectrometer (Thermo Electron Corporation, Madison, WI, USA). Mass spectra were acquired on Microflex MALDI-TOF mass spectrometer (Bruker Daltonik GmbH, Germany) and fluorescent images

were acquired by confocal microscopes using a Nikon Ti-E Inverted Microscope Confocal Nikon C1si-system (Nikon Corporation, Tokyo, Japan).

Synthesis of palmitoylcurcumin (CUR-PA). The attachment of the palmitoyl group to the hydroxyl moiety of curcumin was carried out by reacting curcumin with palmitic anhydride. Palmitic anhydride (0.5 g, 1.0 mmol) was added to a solution of curcumin (1.84 g, 5.0 mmol) in 100 ml of dry ethyl acetate (EtOAc). The mixture was stirred at 0 °C under a nitrogen atmosphere for 15 min. Then, triethylamine (0.7 ml, 5.0 mmol) was slowly added to the mixture, and stirring was continued at room temperature overnight (Scheme 1a). The solvent was evaporated and the residual crude mixture was purified on a silica gel column, using a 20-40% (v/v) EtOAc gradient in hexane to elute the CUR-PA fraction from the unreacted curcumin, palmitic anhydride and $(PA)_2$-CUR.

CUR-PA: ^{1}H-NMR($CDCl_3$, 400 MHz) δ 7.60 (dd, J = 15.8, 1.9 Hz, 2H), 7.17 – 7.09 (m, 3H), 7.04 (d, *J* = 8.2 Hz, 2H), 6.93 (d, *J* = 8.2 Hz, 1H), 6.58 – 6.46 (m, 2H), 5.88 (s, 1H), 5.83 (s, 1H), 3.95 (s, 3H), 3.87 (s, 3H), 2.58 (t, *J* = 7.5 Hz, 2H), 1.81 – 1.71 (m, 2H), 1.46-1.21 (m, 24H) and 0.88 (t, *J* = 6.8 Hz, 3H). UV-visible spectroscopy (MeOH) λ_{max} at 412 nm; FT-IR (cm^{-1}) 2914.02, 2847.60, 1754.98, 1625.46, 1585.61, 1507.69, 1207.01 and 1123.08. MALDI-TOF observed M^+ = 607 (calculated M.W. = 607). The final yield was 52.8%.

Synthesis of methoxy poly(ethylene oxide) acetic acid (mPEG-COOH). Succinic anhydride (6.6 g, 66.6 mmol) was added to a solution of methoxy poly(ethylene glycol) (10 g, 13.3 mmol) in dry DMF. The mixture was stirred at 80 °C under a nitrogen atmosphere for 30 min. Then, pyridine was slowly added to the mixture, and stirring was continued at 80 °C for 3 days (Scheme 1b). Succinic acid was eliminated by Sephadex column chromatography, using 100% (v/v) MeOH for the eluting solvent. The mPEO-COOH spectrum showed signals of terminate methoxy proton in two peak at 3.22 and 3.18 ppm which at 3.18 ppm was the same

as pure mPEO, so the obtained product were the mixtures of mPEO and mPEO-COOH. The amount of mPEO-COOH in the mixtures was 40.32%.

Synthesis of mPEO-CUR-PA. The attachment of mPEO-COOH to the synthesized CUR-PA (see above) was carried out through esterification using dicyclohexylcarbodiimide (DCC) and 4-(N,N-dimethylamino)pyridine (DMAP) as coupling agents. DCC (48 mg, 0.2 mmol) was added to the solution of mPEO-COOH (0.1 g, 0.1 mmol) in dry CH_2Cl_2 (5 ml). The mixture was stirred at 0 °C under a nitrogen atmosphere for 15 min. Then, a catalytic amount of DMAP was added to the mixture and stirred at 0 °C for 60 min. The solution of CUR-PA (0.14 g, 0.2 mmol) in dry CH_2Cl_2 (15 ml) was added to the mixture and stirred continuously at room temperature overnight (Scheme 1c). Residual DCC in the crude product was eliminated by repeated (5 times) precipitation with cold CH_2Cl_2. The unreacted CUR-PA and CUR were then partially removed by precipitation in methanol. The crude product was then subjected to Sephadex column chromatography, using 100% (v/v) MeOH as the mobile phase. Finally, the liquid product was dispersed in water and further purified by centrifugation based filtration (Millipore, MWCO 100,000) to obtain mPEO-CUR-PA at a final yield of 43.78%.

mPEO-CUR-PA: ^{1}H-NMR ($CDCl_3$, 400 MHz) δ 7.67 – 7.46 (m, 2H), 7.14 - 6.98 (m, 6H), 6.53 (d, J = 15.9 Hz, 2H), 5.83 (s, 2H), 4.27 – 4.21 (m, 2H), 3.83 (s, 6H), 3.70 – 3.49 (m, 58H), 3.34 (s, 3H), 2.89 (dd, J = 14.3, 7.5 Hz, 2H), 2.75 (t, J = 6.8 Hz, 2H), 2.54 (dd, J = 15.1, 7.6 Hz, 2H), 1.80 – 1.65 (m, 2H), 1.49 – 1.05 (m, 24H) and 0.84 (t, J = 6.6 Hz, 3H). UV-visible spectroscopy (MeOH) λ_{max} at 400nm, FT-IR (cm^{-1}) 2917.34, 2857.56, 1764.94, 1735.06, 1116.23, 1021.99 and 937.17. MALDI-TOF (m/z) 1000-1500.

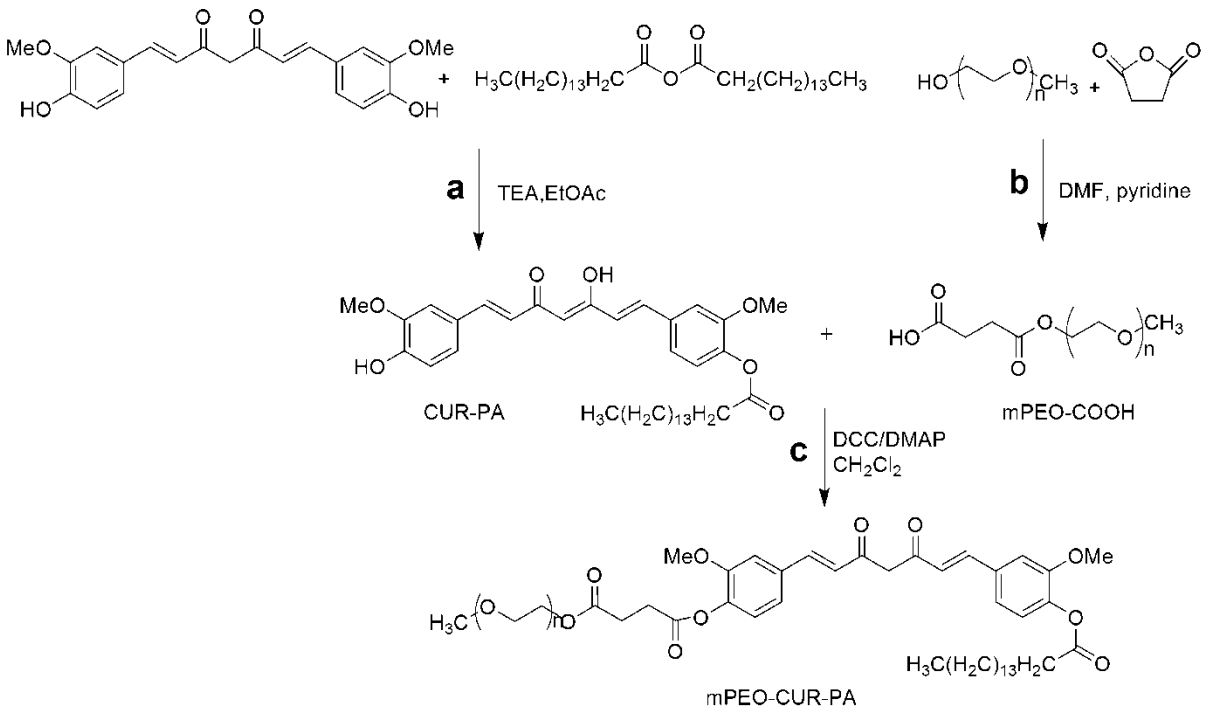

Scheme 1. Synthesis of (a) palmitoylcurcumin (CUR-PA), (b) methoxy poly(ethylene oxide) acetic acid (mPEO-COOH) and (c) mPEO-CUR-PA.

Critical micellar concentration (CMC). The pure liquid mPEO-CUR-PA was added to deionization water at various (v/v) ratios and then sonicated for 30 min to obtain the liquid mixtures at various (v/v) concentrations. The critical micellar concentration (CMC) of mPEO-CUR-PA was determined by measuring the ability of these mixtures to scatter light. Light scattering was acquired in a 1 cm path-length quartz cuvette with the use of monochromatic laser radiation (533 nm, at 100 mW) set perpendicularly to the detector as light source and using the ocean optics® USB2000 as the detector.

Encapsulation of paclitaxel. Paclitaxel was added to the water suspension of mPEO-CUR-PA and sonicated for 30 min to obtain paclitaxel loaded mPEO-CUR-PA micelles. The encapsulation was performed at 0.01:100 and 0.1:100 paclitaxel: curcumin molar ratios.

Particle morphology. The shape and size of the mPEO-CUR-PA micelles, before and after paclitaxel loading, were characterized by confocal laser microscopy using both differential interference contrast (DIC) and fluorescent modes. Suspensions of particles in water were also subjected to dynamic light scattering (DLS) on a Zetasizer nanoseries model S4700 (Malvern Instruments, Worcestershire, UK) for determination of the hydrodynamic size.

***In vitro* uptake of mPEO-CUR-PA by cells in tissue culture.** The *in vitro* cellular uptake of mPEO-CUR-PA was investigated on HEp-2 (Human laryngeal carcinoma) cells in tissue culture. The HEp-2 cells were grown on tissue culture plastic-ware in CM (RPMI 1640 medium with 2.05 mM L-Glutamine (Hyclone Laboratory, Inc., Logan, UT, USA), 10% (v/v) fetal bovine serum and 1% (v/v) antibiotic-antimycotic solution (Gibco BRL Laboratories, Grand Island, N.Y.)) at 37 °C in a 5% CO_2 (v/v) and 80% relative humidity atmosphere. *Uptake experiment.* The HEp-2 cells were cultured in 6 well plates in 1 ml of CM and allowed to adhere overnight. The following day cells were treated with the indicated final concentration of mPEO-CUR-PA in CM media and incubated at 37 °C under 5% (v/v) CO_2 and 80% relative humidity for 2 hours. Then, the media was removed and the cells were washed twice with RPMI 1640 medium and then incubated in CM supplemented with 100 ppm acridine orange for 1 hour. The media was then removed and the cells washed with RPMI 1640 before being subjected to confocal laser fluorescent microscopy (Nikon Digital Eclipse C1-Si/C1Plus (Tokyo, Japan) equipped with Plan Apochromat VC 100×, a 32-channel-PMT-spectral-detector and Nikon-EZ-C1 software). Excitation was carried out using a Diode Laser (405 nm, Melles Griot, Carlsbad, CA, USA), and fluorescent spectral signals at 420–750 nm were collected. The obtained spectrum of each pixel was then unmixed into the mPEO-CUR-PA and acridine orange components, using chemometric analysis (image algorithms) based on the spectral database for each compound constructed from the fluorescent spectrum of the standard

mPEO-CUR-PA and acridine orange when stained on the HEp-2 cells, using the EZ-C1 software (Nikon, Tokyo, Japan). Images indicating the locations of mPEO-CUR-PA were then constructed using the obtained resolved signals.

***In vitro* cytotoxic activity against tissue culture cells.** The HCC-S102 hepatocellular carcinoma cell line was established from a Thai patient.[22] The A549 human lung adenocarcinoma cell line was obtained from the American Type Culture Collection (ATCC), whilst A549RT-eto, a multidrug resistant cancer cell line, was developed from A549 cells.[23] All cell lines were grown in CM, supplemented with 100 U ml^{-1} penicillin, 100 μg ml^{-1} streptomycin and 125 ng ml^{-1} amphotericin B (all antibiotics were from Gibco, Grand Island, NY, USA), in a 80% relative humidified atmosphere of 5% (v/v) CO_2 at 37 ºC. The cell viability after 3 days treatment in 96-well plates was determined by the MTT method as previously described.[19]

Results and discussion

The amphiphillic mPEO-CUR-PA was successfully synthesized by esterifying mPEO-COOH with one of the two-curcumin hydroxyl groups and then esterifying palmitic acid onto the other hydroxyl group (Scheme 1). The obtained mPEO-CUR-PA was purified from the other products through Sephadex column chromatography, multiple DCU precipitations in cold CH_2Cl_2, and centrifugal based filtration through a 100 kDa M.W. cut-off membrane that retained the self-assembled mPEO-CUR-PA microspheres while letting the left-over mPEO-COOH pass through. ^{1}H-NMR, FTIR and mass spectroscopy derived data confirmed the successful synthesis and purification (see the spectral data in SI).

The mPEO-CUR-PA structure was designed to be an amphiphillic molecule in which the PA and PEO moieties are the hydrophobic and hydrophilic segments, respectively. PEO

was chosen not only because of its hydrophillicity, but also because PEO is non-toxic, biocompatible and possesses stealth characteristics with respect to the immune system. As expected, mPEO-CUR-PA self-assembled in water into a spherical architecture, and was observed by confocal microscopy using the DIC mode to have a diameter of ~ 1.7 μm (Figure 1). A clear fluorescent signal of the curcumin chromophore from the particles was observed through the fluorescent mode of the microscope (inset of Figure 1), thus confirming that the observed spheres were the mPEO-CUR-PA material. DLS analysis also revealed an average hydrodynamic diameter of 1.794 ± 0.197 μm. The CMC of this amphiphillic molecule in water was 20 μM. During self-assembly in water, the PA moieties are expected to arrange themselves to be at the core of the micelles in order to have minimum contact with water molecules, while the PEO moieties should be directed outwards to maximize their interactions with the water. The presence of PA should increase the hydrophobic interaction at the micellar core and so make the spheres more stable, while the presence of the mPEO at the outer surface should make the sphere water dispersible. When the mPEO-CUR-PA microspheres were tested on the HCC-S102 cell line, in tissue culture, the material could kill the cancer cells more effectively than the standard curcumin at concentrations above 100 to 200 μM depending upon the cell line. In fact, the activity of mPEO-CUR-PA started to significantly increase at between 25 - 80 μM, a concentration that is slightly higher than the CMC value (~ 20 μM) (Figure 2a), and was more effective than the free unmodified curcumin at concentrations above 100 μM. Although a higher cytotoxic activity, or lower LC_{50} value, for the mPEO-CUR-PA over curcumin cannot be excluded, the notion that the observed increase in the cytotoxicity of mPEO-CUR-PA is due to a more efficient cellular uptake of these microspheres is supported by the confocal fluorescent microscopy based data (Figure 3). Under this scenario, at high concentrations more mPEO-CUR-PA could be delivered into the cells, and so a higher cytotoxic activity was observed. In contrast, in the case of unmodified curcumin, high concentrations did not deliver

significantly higher levels of the curcumin carrier into the cells, and so no significant increased cytotoxicity was observed, since curcumin has only limited water solubility. Thus if used as a drug carrier, more drug would be expected to be delivered inside the cells by mPEO-CUR-PA at high concentrations (>100-200 μM) than by free curcumin.

To confirm that the observed increase in the observed cytotoxic activity on the HCC-S102 cell line of mPEO-CUR-PA near the CMC concentration was not just a co-incidence, the assay was also evaluated in the A549 cell line. A broadly similar dose response, with a significantly greater decrease in the cell viability with mPEO-CUR-PA levels starting from 25-80 μM and higher concentrations and exceeding that of the free curcumin from 200 μM, was seen (Figure 2b). This supports the notion of a better uptake of microspherical mPEO-CUR-PA than free curcumin but, as stated above the possibility of a higher cytotoxicity (LC_{50}) for the modified (mPEO-CUR-PA) curcumin over the native form cannot be excluded.

To help distinguish whether the increased cytotoxicity (as cellular mortality) observed for mPEO-CUR-PA was derived from an increased affectivity (LC_{50}) or cellular uptake level of the microspherical mPEO-CUR-PA pro-drug, its *in vitro* uptake in tissue culture cells was evaluated using the HEp-2 cell line. When HEp-2 cells were incubated with 100 μM mPEO-CUR-PA (a concentration well above the CMC value) for 120 min, the fluorescent signal of the curcumin chromophore could be clearly detected inside the HEp-2 cells, and was most likely to be located within the lysosomes in the cytoplasm (Figure 3), indicating a good uptake of the mPEO-CUR-PA into the cells. The uptake of mPEO-CUR-PA was likely to have occurred *via* endocytosis since the spherical morphology of the mPEO-CUR-PA was clearly observed inside the cells. If so, the endocytosis of mPEO-CUR-PA then potentially explains the situation in which the *in vitro* cytotoxic activity of mPEO-CUR-PA against the cell lines in tissue culture started to increase at concentrations slightly above the CMC value of the material.

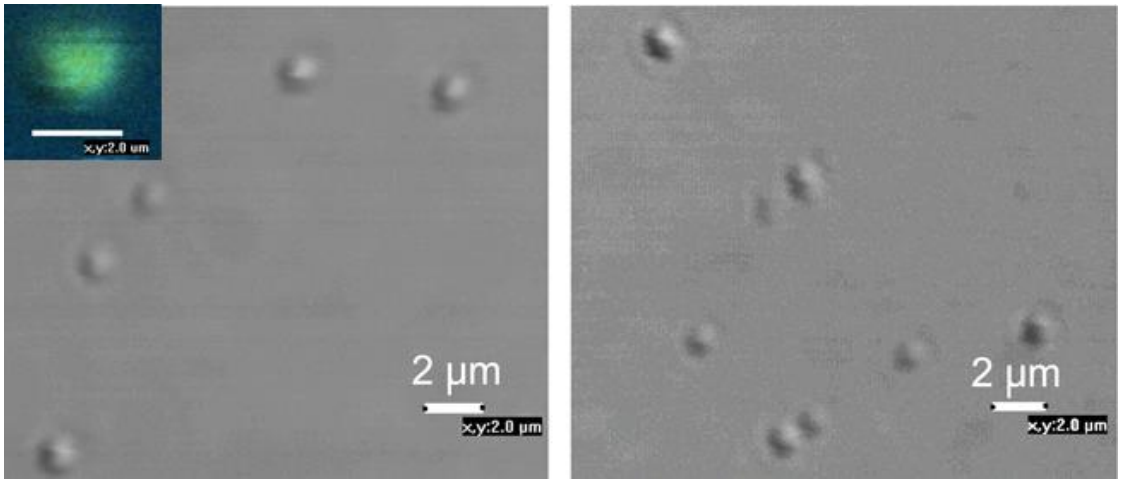

Figure 1. Confocal microscope images in the DIC mode, of the microsphere suspensions of (a) mPEO-CUR-PA and (b) paclitaxel-loaded mPEO-CUR-PA prepared at a paclitaxel: curcumin molar ratio of 0.01:100. Inserts show the fluorescent image of the mPEO-CUR-PA suspension, detected at the emission wavelength of 450-550 nm.

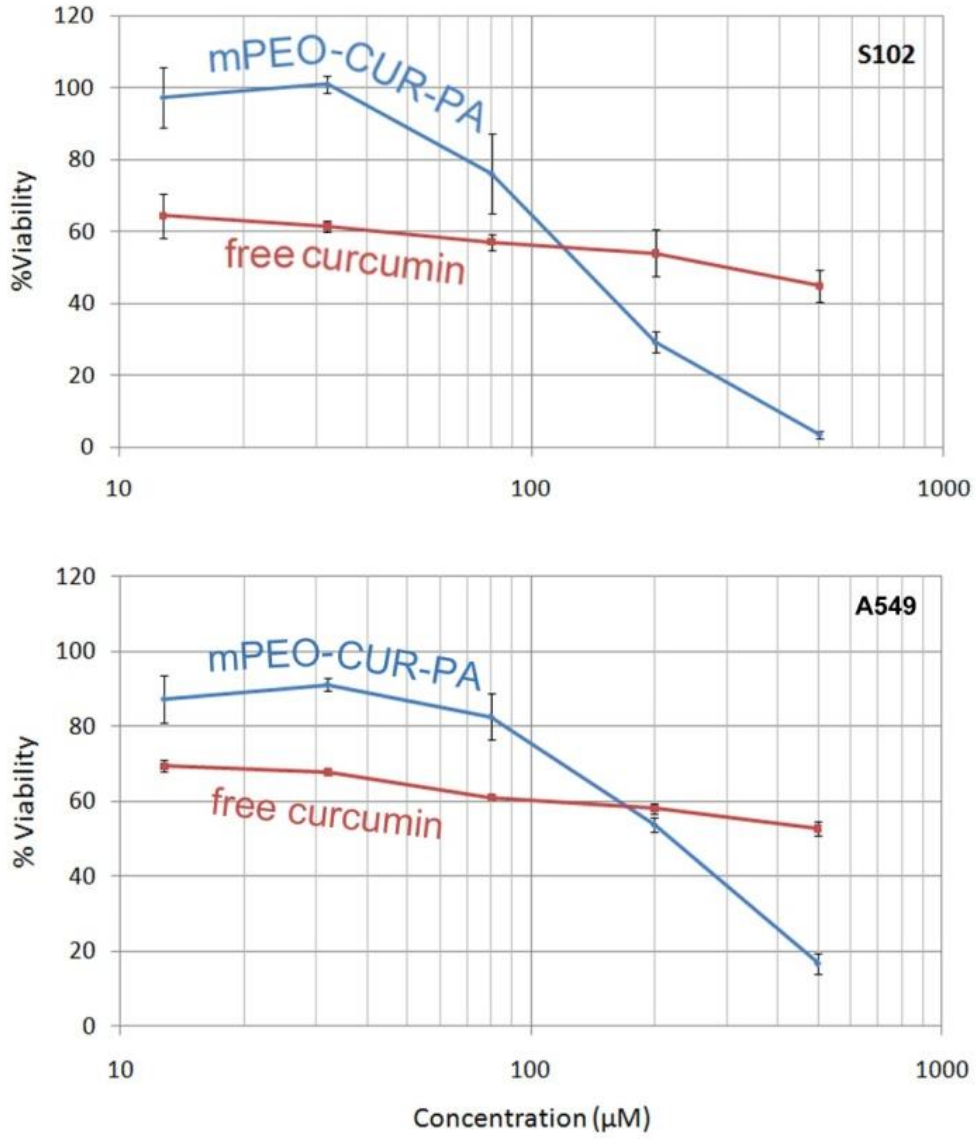

Figure 2. The *in vitro* cytotoxic activity of mPEO-CUR-PA microspheres and free curcumin against (a) HCC-S102 and (b) A549 cancer cells in tissue culture. The % viability was measured after 72 h incubation of the cells with the tested materials.

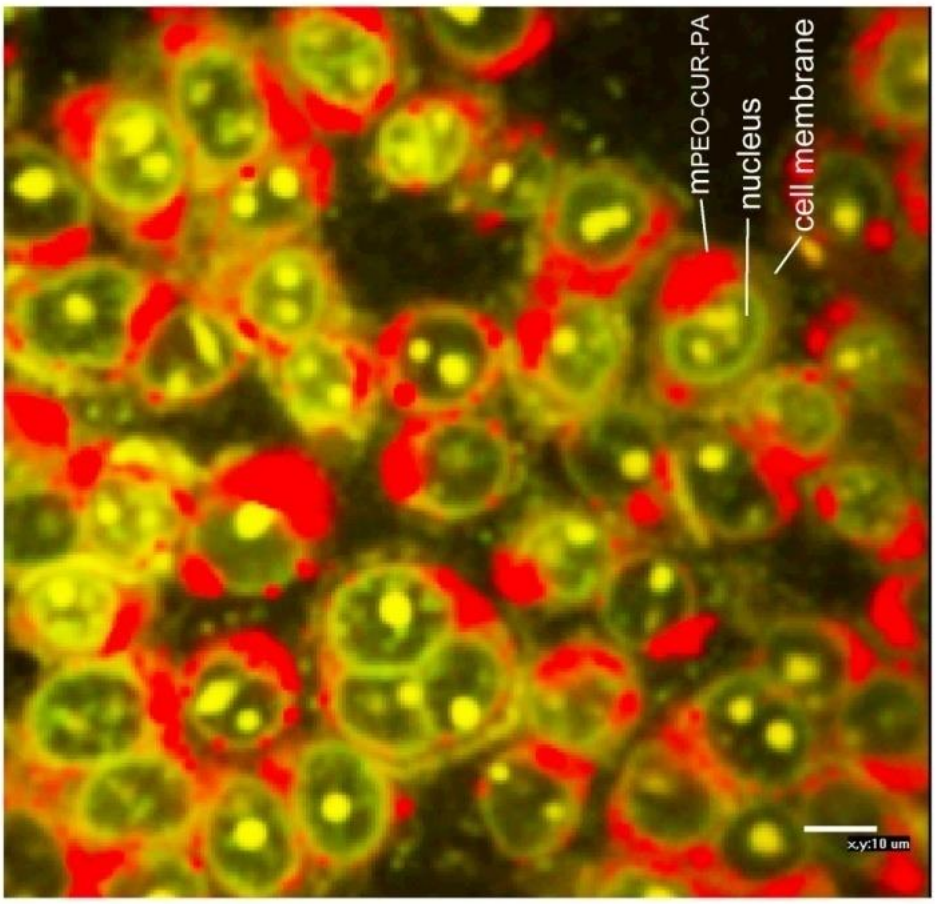

Figure 3. *In vitro* uptake of mPEO-CUR-PA spheres into HEp-2 cells in tissue culture. Cells were incubated with a 100 μM mPEO-CUR-PA suspension for 120 min, washed twice with RPMI 1640 medium, stained with acridine orange, washed, and subjected to laser fluorescent microscopic analysis.

The problem of the low water solubility of paclitaxel is well recognized.[20,21] Even at very low concentrations of paclitaxel (0. 01 – 1 nM), the *in vitro* cytotoxic activity of paclitaxel in water was seen to be approximately 30-40% lower than that in 0.2% (v/v) DMSO against the cell lines in tissue culture. To enable the use of paclitaxel in an aqueous environment, and also to maximize the synergism between curcumin and paclitaxel in cytotoxic activity, paclitaxel was loaded into the mPEO-CUR-PA microspheres by allowing the mPEO-CUR-PA to self-assemble in the presence of paclitaxel under ultrasonication. The rational is that the hydrophobic nature of paclitaxel will drive the molecules to move into the hydrophobic core

of the spheres. Indeed, after ultrasonication, no paclitaxel crystals were observed by confocal light microscopy in the DIC mode, indicating the likely high level of encapsulation of the drug into the mPEO-CUR-PA spheres. Thus, in the confocal images (DIC mode) of the paclitaxel-loaded mPEO-CUR-PA microspheres they showed only the suspended microspherical architectures with a diameter of approximately ~ 1.5 – 2.0 μm and no crystals (Figure 1). This observed size agreed well with the hydrodynamic diameter obtained from the DLS analysis of 1.794 ± 0.197, 2.090 ± 0.299 and 2.621 ± 0.112 μm for the unloaded and paclitaxel-loaded mPEO-CUR-PA spheres prepared at 0.01:100 and 0.10:100 paclitaxel: mPEO-CUR-PA molar ratios, respectively. Thus the hydrodynamic size of the spheres increased with paclitaxel loading levels.

The *in vitro* cytotoxicity of paclitaxel loaded mPEO-CUR-PA microspheres against the HCC-S102 cell line in tissue culture indicated a clear enhancement of the anti-tumor activity. Compared to the use of 0.01 μM paclitaxel in DMSO alone (15% mortality), an ~five-fold higher level of cytotoxic activity (measured as reduced cell viability, in this case ~75% mortality) was observed when the mPEO-CUR-PA carriers were used to deliver 0.01 μM paclitaxel (Figure 4a), and this was significantly higher than that seen for the carrier (~42% mortality) or drug (~15%) alone or their summed total (42 + 15 = 57%), clearly supporting the synergism between the mPEO-CUR-PA and the loaded paclitaxel drug. Indeed, since the cytotoxic activity was higher than that with paclitaxel in DMSO alone or the carrier alone, then the observed enhancement of cytotoxic activity was due to more than just the diminishing of the poor water solubility of paclitaxel. Rather, this is likely to be the result of (i) the effective transportation of both the drug and bioactive carrier (paclitaxel and mPEO-CUR-PA) into the cells *via* endocytosis and (ii) the synergistic effect between paclitaxel and mPEO-CUR-PA in killing the cancer cells.

Curcumin can reverse the drug resistance seen in many cancer cells by blocking the ABC-mediated drug efflux mechanisms in multidrug resistant cancer cells,[6,7] and can improve the anti-cancer activity of paclitaxel by suppressing the activation of NF-κB and Akt survival signals that are otherwise induced by paclitaxel.[8,9] Therefore, paclitaxel loaded mPEO-CUR-PA was tested for *in vitro* cytotoxic activity against the paclitaxel resistant cell line, A549RT-eto, in tissue culture. Paclitaxel-loaded mPEO-CUR-PA was observed to override the drug resistance of the A549RT-eto cells. When 0.01 and 0.1 μM paclitaxel-loaded mPEO-CUR-PA microspheres were administered, a 3.6- to 44- fold increase in the cytotoxic activity (reduced cell viability) was observed compared to that with unencapsulated paclitaxel in DMSO, or a 3.2- to 5.0-fold higher level than that seen with the mPEO-CUR-PA carrier alone, or a 2.1- to 3.1-fold higher than the sum of that seen for the free paclitaxel and free mPEO-CUR-PA, respectively (Figure 4b). The synergism between mPEO-CUR-PA and paclitaxel was likely made possible by the ability to effectively co-deliver both paclitaxel and mPEO-CUR-PA into the same cells at the same time, allowing mPEO-CUR-PA to override the paclitaxel resistance mechanism in the cells actually subjected to paclitaxel exposure, and so is more efficient.

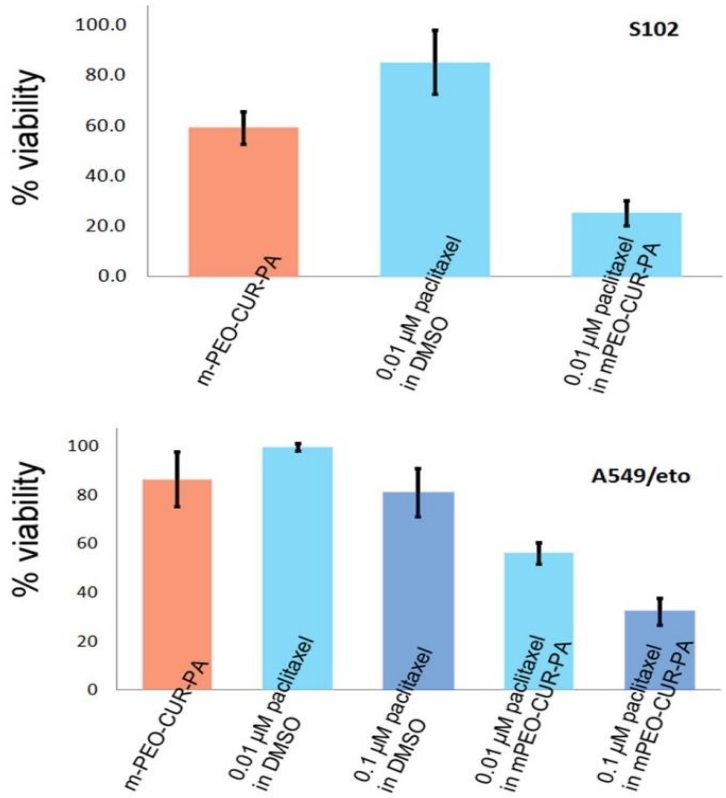

Figure 4. *In vitro* cytotoxicity of paclitaxel loaded mPEO-CUR-PA microspheres against the (A) HCC-S102 and (B) A549RT-eto cell lines, compared to that with free paclitaxel in DMSO and unloaded mPEO-CUR-PA microspheres. Data are shown as the mean $\pm$ 1SD and are derived from at least 3 independent repeats.

Conclusion

We successfully synthesized the amphiphillic mPEO-CUR-PA derivative of cumin that, in an aqueous environment, automatically self-assembled into ~ 1.8 μm sized spheres at concentrations above 20 μM, which is the CMC value of the material. At 100 μM, a concentration well above the CMC, the mPEO-CUR-PA showed a clear ability to be uptaken into cells, likely to be *via* endocytosis, and demonstrated a significantly higher *in vitro* cytotoxicity than the unmodified standard curcumin. Paclitaxel was successfully loaded into the mPEO-CUR-PA microspheres. *In vitro* cytotoxicity assays in tissue culture against

paclitaxel sensitive and resistant cell lines of the paclitaxel-loaded mPEO-CUR-PA microspheres revealed up to an ~44-fold increase in their cytotoxicity compared to that for the free paclitaxel (in DMSO) and an ~5-fold higher level than the sum of that seen for the free paclitaxel and free mPEO-CUR-PA, indicating the likely synergism between paclitaxel and mPEO-CUR-PA. The use of mPEO-CUR-PA as the carrier to deliver paclitaxel into paclitaxel resistant cells resulted in a reverse of the drug resistance of the cells. This demonstration of a bioactive carrier that works synergistically with the loaded drug should open up the possibility to not only use a lower concentration of the drug, and specifically in this case to use a lower concentration of paclitaxel and to reverse the paclitaxel resistance in cancer treatment. Along these principals other combinations of drugs and carriers can now be explored.

REFERENCES

1. Shen, Y.; Jin, E.; Zhang, B.; Murphy, C. J.; Sui, M.; Zhao, J.; Wang, J.; Tang, J.; Fan, M.; Van Kirk, E.; Murdoch, W. J. *Journal of the American Chemical Society* **2010**, *132*, 4259.

2. Anumansirikul, N.; Wittayasuporn, M.; Klinubol, P.; Tachaprutinun, A.; Wanichwecharungruang, S. P. *Nanotechnology* **2008**, 205101, 9 pp.

3. Kidsaneepoiboon, P.; Wanichwecharungruang, S. P.; Chooppawa, T.; Deephum, R.; Panyathanmaporn, T. *Journal of Materials Chemistry* **2011**, *21*, 7922.

4. Sarkar, F. H.; Li, Y. *Cancer Treatment Reviews* **2009**, *35*, 597.

5. Singh, S.; Aggarwal, B. B. *Journal of Biological Chemistry* **1995**, *270*, 30235.

6. Limtrakul, P.; Chearwae, W.; Shukla, S.; Phisalphong, C.; Ambudkar, S. V. *Molecular and cellular biochemistry* **2007**, *296*, 85.

7. Chearwae, W.; Wu, C. P.; Chu, H. Y.; Lee, T. R.; Ambudkar, S. V.; Limtrakul, P. *Cancer chemotherapy and pharmacology.* **2006**, *57*, 376.

8. Bava, S. V.; Puliappadamba, V. T.; Deepti, A.; Nair, A.; Karunagaran, D.; Anto, R. J. *Journal of Biological Chemistry* **2005**, *280*, 6301.

9. Bava, S. V.; Sreekanth, C. N.; Thulasidasan, A. K. T.; Anto, N. P.; Cheriyan, V. T.; Puliyappadamba, V. T.; Menon, S. G.; Ravichandran, S. D.; Anto, R. J. *International Journal of Biochemistry and Cell Biology* **2011**, *43*, 331.

10. Shishodia, S.; Amin, H. M.; Lai, R.; Aggarwal, B. B. *Biochemical Pharmacology* **2005**, *70*, 700.

11. Aggarwal, B. B.; Shishodia, S.; Takada, Y.; Banerjee, S.; Newman, R. A.; Bueso-Ramos, C. E.; Price, J. E. *Clinical Cancer Research* **2005**, *11*, 7490.

12. Siwak, D. R.; Shishodia, S.; Aggarwal, B. B.; Kurzrock, R. *Cancer* **2005**, *104*, 879.

13. Sarkar, F. H.; Li, Y. *Cancer Treatment Reviews* **2009**, *35*, 597.

14. Wang, Y. J.; Pan, M. H.; Cheng, A. L.; Lin, L. I.; Ho, Y. S.; Hsieh, C. Y.; Lin, J. K. *Journal of Pharmaceutical and Biomedical Analysis* **1997**, *15*, 1867.

15. Tonnesen, H. H.; Karlsen, J.; van Henegouwen, G. B. *Zeitschrift fur Lebensmittel-Untersuchung und -Forschung* **1986**, *183*, 116.

16. Anand, P.; Kunnumakkara, A. B.; Newman, R. A.; Aggarwal, B. B. *Molecular Pharmaceutics* **2007**, *4*, 807.

17. Sharma, R. A.; McLelland, H. R.; Hill, K. A.; Ireson, C. R.; Euden, S. A.; Manson, M. M.; Pirmohamed, M.; Marnett, L. J.; Gescher, A. J.; Steward, W. P. *Clin Cancer Res* **2001**, *7*, 1894.

18. Bisht, S.; Maitra, A. *Current Drug Discovery Technologies* **2009**, *6*, 192.

19. Suwannateep, N.; Banlunara, W.; Wanichwecharungruang, S. P.; Chiablaem, K.; Lirdprapamongkol, K.; Svasti, J. *Journal of Controlled Release* **2011**, *151*, 176.

20. Dong, X.; Mattingly, C. A.; Tseng, M.; Cho, M.; Adams, V. R.; Mumper, R. J. *European Journal of Pharmaceutics and Biopharmaceutics* **2009**, *72*, 9.

21. Mugabe, C.; Hadaschik, B. A.; Kainthan, R. K.; Brooks, D. E.; So, A. I.; Gleave, M. E.; Burt, H. M. *BJU International* **2009**, *103*, 978.

22. Laohathai, K.; Bhamarapravati, N. *American Journal of Pathology* **1985**, *118*, 203.

23. Kanintronkul, Y.; Worayuthakarn, R.; Thasana, N.; Winayanuwattikun, R.; Pattanapanyasat, K.; Surarit, R.; Ruchirawat, S.; Svasti, J. *Anticancer Research* **2011**, *31*, 921.

Acknowledgement

This study was performed at School of Materials Sciences, Japan Advanced Institute of Science and Technology (JAIST), Japan. I am particularly very grateful to the Doctoral Dual Degree Program (JAIST-CU) and the Royal Golden Jubilee Ph.D. Program (PHD/0261/2553), Thailand for financial support during my doctoral study.

I would like to express my sincere gratitude to my supervisor, Associate Professor Tatsuo Kaneko of JAIST for his active valuable guidance, helpful suggestions and kindly support during my staying in Japan. All of achievements during my study would not be possible without his creative mind and his enthusiastic guidance.

I also express my specially thank my second supervisor Prof. Masayuki Yamaguchi and my advisor for minor research Associate Professor Kazuaki Matsumura in JAIST for their valuable guidance and creative mind in Japan.

I also thank Research Lecturer Seiji Tateyama, Assistants Professor Kosuke Okeyoshi and Dr. Maiko Okajima to all appreciate comment and suggestions. They made me improve my scientific skill and made me believe that I can be the good scientist.

I would like to grateful acknowledge Dr. Maiko Okajima for her kindness and concern that made it possible for me to complete my study without any difficulties in JAIST, Associate Professor Kazuaki Matsumura for their good discussion and supported me to do cell culture and Dr. Osamu Notoya (JAIST) for observation of SEM image.

I would like to express myappreciation to my referees, Professor Masayuki Yamaguchi, Associate Professor Kazuaki Matsumura, Associate Professor Toshiaki Taniike of JAIST and Associate Professor Supason Wanichwecharungruang of Chulalongkorn University for their assistance to complete my thesis.

I would like to thank all of my lab mates, Ms. Phruetchika Suvannasara, Mr. Kai Kan, Mr. Asif Mohammad, Mr. Katsuaki Yasaki, Mr. Jin Xin, Mr. Hieu Duc Nquyen, Mr. Shin Hojoon, Mr. Masanori Miyasato, Mr. Kawamoto Hirotoshi, Mr. Kohei Goto, Mr. Takahiro Noda, Mr. Hiroshi Shimosegawa, Mr. Ryosuke Mishima, Mr. Yusuke Ibuki, Mr. Saranyoo Sornkamnird, Ms. Sakshi Rawat, Mr. Toru Abe, Mr. Masaki Inagaki, Mr. Asuka Komuro, Ms. Shiho Maetani, Mr. Nag Aniruddha, Ms. Joshi Gargi, Mr. Junya Okuda, Mr. Satoshi Karikome, Ms. Mayumi Tamaki, Mr. Kazuya Taya, Mr. Yosuke Mori and Mr. Naoto Watanabe for help me and sharing happy time.

I would like to express my grateful acknowledge to my advisor in Thailand, Associate Professor Supason Wanichwecharungruang of Faculty of Science, Chulalongkorn University, Thailand for her invaluable guidance, open mind, encouragement during my study in Japan. She made me stronger and stands at this point as well.

Finally, I would like to express my heartfelt appreciation to my parents Mr. Mongkol Amornwachirabodee, Mrs. Wiboonbhan Thammarat, my sister Ms. Natthawan Chindejchartwut and my brother Mr. Dechakorn Amornwachirabodee for thoughtful attention and continuous encouragements. Thank you, all Thai members in JAIST for their love, emotional support and making me feel less lonely.

Kittima Amornwachirabodee

March, 2016

Ishikawa, Japan